CHEMICAL CONSTITUENTS OF *OROXYLUM INDICUM* (L.) VENT., ANTIBACTERIAL AND ANTIOXIDATION PROPERTIES

KULSIRI YOSSATHERA

MASTER OF SCIENCE

IN

APPLIED CHEMISTRY

SCHOOL OF SCIENCE

MAE FAH LUANG UNIVERSITY

2013

CHEMICAL CONSTITUENTS OF *OROXYLUM INDICUM* (L.) VENT., ANTIBACTERIAL AND ANTIOXIDATION PROPERTIES

KULSIRI YOSSATHERA

THIS THESIS IS A PARTIAL FULFILLMENT OF
THE REQUIREMENTS FOR THE DEGREE OF
MASTER OF SCIENCE
IN
APPLIED CHEMISTRY

SCHOOL OF SCIENCE
MAE FAH LUANG UNIVERSITY
2013

CHEMICAL CONSTITUENTS OF *OROXYLUM INDICUM* (L.) VENT., ANTIBACTERIAL AND ANTIOXIDATION PROPERTIES

KULSIRI YOSSATHERA

THIS THESIS HAS BEEN APPROVED
TO BE A PARTIAL FULFILLMENT OF THE REQUIREMENTS
FOR THE DEGREE OF MASTER OF SCIENCE
IN
APPLIED CHEMISTRY
2013

THESIS COMMITTEE

....CHAIRPERSON

(Asst. Prof. Dr. Orasa Pancharoen)

....ADVISOR

(Dr. Suwanna Deachathai)

....CO-ADVISOR

(Asst. Prof. Dr. Siripat Suteerapataranon)

....CO-ADVISOR

(Asst. Prof. Dr. Sarin Sriprang)

....EXAMINER

(Dr. Nisakorn Saewan)

ACKNOWLEDGEMENTS

Thesis Title   Chemical Constituents of *Oroxylum indicum* (L.) Vent.,

Antibacterial and Antioxidation Properties

Author   Kulsiri Yossathera

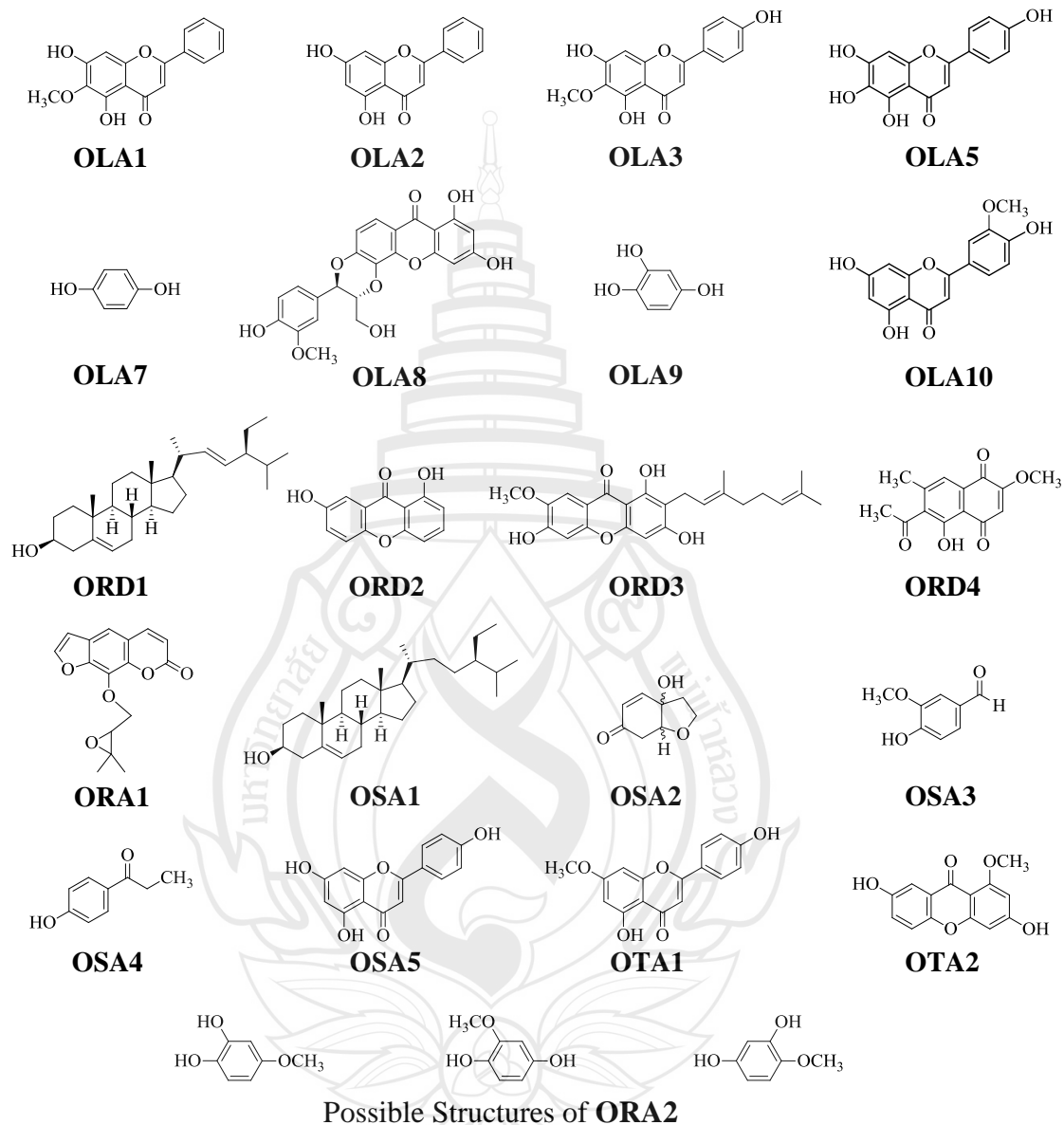**Degree**   Master of Science (Applied Chemistry)

Advisor   Dr. Suwanna Deachathai

Co-Advisor   Asst. Prof. Dr. Siripat Suteerapataranon

Asst. Prof. Dr. Sarin Sriprang

ABSTRACT

The studies of chemical constituents from leaves, roots, stems, and twigs of *Oroxylum indicum* (L.) Vent. using chromatographic seperation led to twenty one compounds; **OLA1** (oroxylin A), **OLA2** (chrysin), **OLA3** (hispidulin), **OLA5** (scutellarein), **OLA7** (hydroquinone), **OLA8** (5'-demethoxycadensin G), **OLA9** (hydroxyquinol), **OLA10** (chrysoeriol), **ORD1** (stigmasterol), **ORD2** (euxanthone), **ORD3** (cowaxanthone), **ORD4** (orientalone), **ORA1** (heraclenin), **OSA1** (β-sitosterol), **OSA2** (rengyolone), **OSA3** (vanillin), **OSA4** (1-(4-hydroxyphenyl) propan-1-one), **OSA5** (apigenin), **OTA1** (genkwanin), **OTA2** (3,7-dihydroxy-1-methoxyxanthone), and three possible structures of **ORA2** (2-methoxy-1,4-benzenediol or 4-methoxy-1,2-benzenediol or 4-methoxy-1,3-benzenediol). Their structures were elucidated by spectroscopic analysis. The acetone extract from the leaves and roots exhibited strong radical scavenging activity with IC_{50} of 8.01 ± 0.29 and 9.81 ± 0.09 µg/mL, respectively. **OLA5** and **OLA10** exhibited strong and moderate antioxidative activity with IC_{50} values of 11.88 ± 0.06 and 33.45 ± 1.45 µM, respectively. In addition, all crude extracts exhibited weak to moderate antibacterial activities against gram-positive and gram-negative bacteria. **OLA3** was found to

possess moderate activity against MRSA SK1 with an MIC value of 32 μg/mL, whereas **OLA8** exhibited strong activity against *B. cereus* with an MIC value of 16 μg/mL.

OLA1 **OLA2** **OLA3** **OLA5**

OLA7 **OLA8** **OLA9** **OLA10**

ORD1 **ORD2** **ORD3** **ORD4**

ORA1 **OSA1** **OSA2** **OSA3**

OSA4 **OSA5** **OTA1** **OTA2**

Possible Structures of **ORA2**

TABLE OF CONTENTS

TABLE OF CONTENTS (continued)

LIST OF TABLES

LIST OF TABLES (continued)

LIST OF FIGURES

LIST OF FIGURES (continued)

ABBREVIATION AND SYMBOLS

Absorbance	Abs
Acetone	Me_2CO
Bacillus cereus	B.C
Broad singlet	*br s*
Carbon Nuclear Magnetic Resonance	^{13}C NMR
Centimeter	cm
Chemical Shift Relative to TMS	δ
Chloroform	$CHCl_3$
Chloroform-*d*$_6$	$CDCl_3$
Colony Forming Unit	CFU
Column Chromatography	CC
Concentration	c
Correlated Spectroscopy	COSY
Coupling Constant	*J*
Degree Celcius	°C
Dichloromethane	CH_2Cl_2
Dimethyl sulfoxide	DMSO
Dimethyl sulfoxide-*d*$_6$	DMSO-*d*$_6$
1,1-Diphenyl-2-picrylhydrazyl	DPPH
Distortionless Enhancement by Polarization Transfer	DEPT
Doublet	*d*
Doublet of doublet	*dd*
Escherichia coli	E.C
Ethyl Acetate	EtOAc
Flow Injection Analysis	FIA
Geranyl Pyrophosphate	GPP
Gram	g

ABBREVIATION AND SYMBOLS (continued)

Heteronuclear Multiple Bond Correlation	HMBC
Heteronuclear Multiple Quantum Correlation	HMQC
Hour	h
Infrared	IR
50% Inhibition Concentration	IC_{50}
Kilogram	kg
Megahertz	MHz
Melting Point	m.p.
Methanol	MeOH
Methicillin resistant *Staphylococcus aureus*	MRSA
Microgram	μg
Microliter	μL
Micromolar	μM
Milligram	mg
Milliliter	mL
Millimeter	mm
Millimolar	mM
Minimum Inhibition Concentrations	MICs
Minute	min
Molar Extinction Coefficient	ε
Mueller Hinton Agar	MHA
Mueller Hinton Broth	MHB
Multiplet	*m*
Nanometer	nm
Non-Communicable Diseases	NCD
Normal Saline Solution	NSS
Not Applicable	N/A

ABBREVIATION AND SYMBOLS (continued)

Nuclear Magnetic Resonance	NMR
One Dimentional Nuclear Magnetic Resonance	1D NMR
Parts per Million	ppm
Percentage	%
Preparative Thin-Layer Chromatography	PLC
Proton Nuclear Magnetic Resonance	^{1}H NMR
Pseudomonas aurenginosa	Ps.A
Quartet	*q*
Quick Column Chromatography	QCC
Reciprocal Centimeter (wave number)	cm $^{-1}$
Revolutions per Minute	rpm
Salmonellae typhimurium	S.T
Singlet	*s*
Staphylococcus aureus	S.A
Tetrachloromethane	CCl_4
Tetramethylsilane	TMS
Thailand Institute of Scientific and Technological Research	TISTR
Thin-Layer Chromatography	TLC
Triplet	*t*
Two Dimentional Nuclear Magnetic Resonance	2D NMR
Ultraviolet	UV
Ultraviolet-Visible	UV-Vis
United States of America	USA
Wavelength at maximum absorption	λ_{max}
World Health Organization	WHO

CHAPTER 1

INTRODUCTION

1.1 Introduction

The World Health Organization (WHO) global status report on non-communicable diseases (NCD) 2010 showed that NCDs are the biggest cause of death worldwide. More than 36 million people died from NCDs in 2008, mainly cardiovascular diseases (48%), cancers (21%), chronic respiratory diseases (12%) and diabetes (3%). More than 9 million of these deaths occurred before the age of 60 and could have largely been prevented (World Health Organization, 2011). Up to the present, WHO considers phytotheraphy in its health programs suggested basic procedures for validation of drugs from plants origin in developing countries (Anushia, Sampathkumar & Ramkumar, 2009), plants have provided a source of inspiration for novel drug compounds, as plant derived medicines have made large contribution to human health and well being (lgbinosa, O. O., Igbinosa, O. E. & Aiyegoro, 2009). Developing countries still depend mainly on medicinal herbs due to their cheaper cost and their effectiveness in the treatment of various infectious diseases with lesser side effects and are widely accepted as sources of antioxidative substances (Joshi, Mishra, Khetwal & Bisht, 2012).

Medicinal plants have been used for centuries as remedies for human diseases as they contain components of therapeutic value (Al-Bakri & Afifi, 2007). Phenolic compounds are the largest group of phytochemicals and accounts for most of the antioxidant activity in plants or plant products (Aliyu et al., 2009). Phenolic substances such as naringin, apigenin, myricetin, coumarins, caffeic acids, and flavonoids are known to posses antioxidant properties which play important roles

in protecting foods, cells and organs from oxidative degeneration (Heim, Tagliaferro & Bobilya, 2002; Osawa, 1999). Flavonoids are a class of secondary plant phenolics occuring in foods primarily as glycosides and polymers that are degraded to variable extents in the digestive tract (Heim et al., 2002). Flavonoids are found in fruits, seeds, stem, flowers, herbs, nuts, as well as tea and red wine, they are usually subdivided according to their substituents into flavonols, anthocyanidins, flavones, flavonones, and chalcones (Middleton, Kandaswami & Theoharides, 2000). Flavonoids have important effects in plant biochemistry and physiology, acting as antioxidants, enzyme inhibitors, precursors of toxic substances, pigments, and light screens (Heim et al., 2002). They have long been recognized to possess anti-inflammatory, antioxidant, antibacterial, antiallergic, hepatoprotective, antiviral, and anticarcinogenic activities (Middleton et al., 2000). Mostly, drug discovery from natural sources is an area perlinent to complementary and alternative medicine, and natural sources provide a basis for the isolation of unique and potentially effective bioactive compounds (Rajkumar, Guha & Kumar, 2012).

Oroxylum indicum was known as an Asian medical plant used in folk medicines. In Thailand, stembark is used for arthritis and old seed is used for laxative and relief of cough expectorants (Laupattarakasem, Houghton, Hoult & Itharat, 2003). According to these data, *O. indicum* has been investigated for the chemical constituents and biological activities. It is a part of the basic research on the utilization of Thai medicinal plants. In the last few years, a number of studies have been reported; most of the chemical constituents of *O. indicum* are flavonoids and the interesting biological activities of *O. indicum* have been reported such as antimicrobial, antioxidant, anti-inflamatory, and cytotoxicity activities (Nair & Joshi, 1979; Chen, Games & Jones, 2003; Uddin et al., 2003; Babu et al., 2010; Yan et al., 2011).

With gradually increasing cases of human diseases, all around microbes have also increased to a great extent. Although pharmacological industries have produced a number of new antibiotics in the last three decades, the resistance to these drugs by microorganisms has increased (Das & Choudhury, 2010). In recent times the critical area of primary health concern is the usual causative agents that are responsible for the incidence of new and re-emerging infectious diseases which pathogenic bacteria

are frequently exposed to infection, for example gram-positive (*Staphylococcus aureus*) and gram-negative (*Escherichia coli*, *Salmonella typhimurium*) (Joshi et al., 2012). The synthetic drugs, antimicrobials of plant origin are not associated with many side effects and an enormous therapeutic potential could heal many infectious diseases (Iwu Duncan & Okunji, 1999). There is need to develop alternative microbial drugs which plants are also known to contain enumerable biological active compounds which possess antibacterial properties (Anushia et al., 2009). The most widely used testing methods include broth microdilution, rapid automated instrument, disk diffusion and gradient diffusion methods. The microdilution is a type broth microdilution using small, disposable, plastic microdilution trays. The advantages of the microdilution procedure include the generation of minimum inhibitory concentration (MICs), the reproducibility and convenience of having prepared panels, and the economy of reagents and space that occurs due to the miniaturization of the test (Jorgensen & Ferraro, 2009).

Many of flavonoids as well as flavonoid glycosides, most commonly known for their antioxidaive activity *in vitro*, were recognized as major compounds of *O. indicum.* Antioxidant compounds can scavenge free radicals such as peroxide, hydroperoxide or lipid peroxyl and thus inhibit the oxidative mechanisms that lead to degenerative diseases (Scartezzini & Speroni, 2000). Several methods have been published to determine the antioxidant activity such as the thiobarbituric acid reactive substances (TBARS) assay, trolox equivalent antioxidant capacity (TEAC) assay, 2,2′-azinobis-(3-ethylbenzothiazoline-6-sulphonic acid) (ABTS$^{\bullet+}$) assay, total radical-trapping antioxidant parameter (TRAP) assay and 2,2-diphenyl-1-picrylhydrazyl radical (DPPH) assay. TBARS assay is commonly used for the detection of lipid peroxidation. TEAC assay is one widely used *in vitro* assay for the determination of antioxidant activity. ABTS$^{\bullet+}$ assay is generated by oxidation of ABTS with potassium persulfate and is reduced in the presence of such hydrogen-donating antioxidants. TRAP assay determines the overall ability of an antioxidant to trap free radicals (Dris & Jain, 2004; Magalhães, Santos, Segundo, Reis & Lima, 2009). The DPPH assay antioxidant activity test is more widely used than the other techniques. This is because this stable free radical is the most widely used radical for determining free radical scavenging properties of potential antioxidants and the available DPPH radical

scavenging tests are described as simple and useful in the screening of large numbers of compounds/extracts, and are convenient (Ukeda, Adachi & Sawamura, 2002). A new method for determine antioxidation properties using DPPH assay has been reported (Mrazek, Watla-iad, Deachathai & Suteerapataranon et al., 2012). The developed flow-injection system for determination of the antioxidation activity provided good reproducibility, rapid analysis and cost-effective method, which can achieve real-time, online and automatic analysis of samples.

Therefore, to obtain good reproducibility and the automation degree, this work will employ the flow-injection system for determination of antioxidation activity using DPPH assay. The isolation of chemical constituents and evaluation of biological activities of this plant is of great interest and importance because of their role in drug development and in management of many chronic diseases.

1.2 Research Objectives

This research involved isolation, purification, structural determination of the chemical constituents from leaves, roots, stems and twigs of *O. indicum* and evaluation of the antibacterial and antioxidative activities of crude extracts and pure compounds.

CHAPTER 2

LITERATURE REVIEWS

2.1 General Characteristics of *Oroxylum indicum* (L.) Vent.

Oroxylum indicum (L.) Vent., a plant belonging to Bignoniaceae family, local common names Phe-kaa, Ma-lid-mai, Lin-fah in Thailand, Midnight horror in England and Sorizayanoki in Japan.

O. indicum (figure 1) is an evergreen or semi-deciduous tree. Young trees have a single main stem with the leaves clustered at the top. Barks are pale creamy brown or pale grey, smooth or finely cracked with large leaf scars on younger trees. Leaves, pinnately compound are up to 150 cm in length, giving the whole leaf a triangular appearance. Flowers, 8 to 12 cm, reddish-brown outside, greyish-white inside, are clustered near top of an upright, fleshy stem at end of twigs. Fruits, 30 to 120 cm, are dark brown, flattened, slightly curved at base with a fine ridge on each side, woody, splitting into two sections lengthways. Seeds, 4 to 8 cm, are flat with a broad, semi-transparent wing (Gardner, Sidisunthorn & Anusarnsunthorn, 2000).
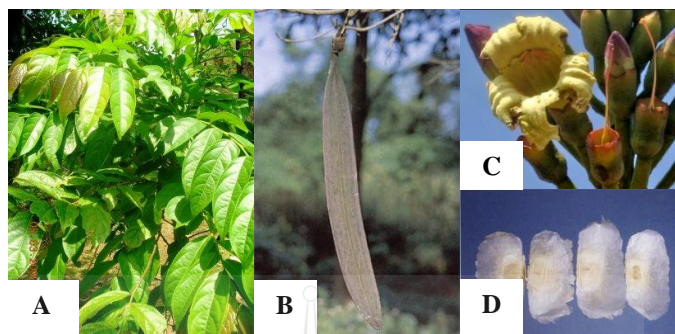
Source A: Vrajesh (2009)

         B: Dharmananda (2006a)

         C: Garg (2010)

         D: Dharmananda (2006b)

Figure 2.1 *Oroxylum indicum* (L.) Vent.

A: Leaves, B: Fruits, C: Flowers, D: Seeds

2.2 Chemical Constituents from *Oroxylum indicum* (L.) Vent.

According to Napalert database, Sciencedirect and SciFinder Scholar, no more than 50 chemical constituents and some biological activities have been reported for *O. indicum*. It was found that most of the chemical constituents of *O. indicum* are flavonoids (Nair & Joshi, 1979; Chen et al., 2003; Uddin et al., 2003; Babu et al., 2010; Yan et al., 2011) and anthraquinones (Dey, Mukherjee, Das & Chatterjee, 1979). The chemical constituents isolated from *O. indicum* are shown in table 2.1.

Table 2.1 Chemical Constiuents Isolated from *Oroxylum indicum* (L.) Vent.

Part	Compound (Structure, Type)	Reference
Bark	oroxylin A (1e)	Bose & Battacharya, 1938
	p-coumaric acid (2i)	Gaitonde & Sapre, 1989
Fruit	cleroindicin B (3d)	Teshima et al., 1996
	cleroindicin C (4d)	
	cornoside (5f)	
	hydroxytyrosol-1-*O*-glucoside (6f)	
	rengyol (7d)	
	salidroside (8f)	
Heart wood	apigenin (9e)	Nguyen, M. T. T.,
	balanophonin (10i)	Nguyen, N. T., Nguyen,
	ficusal (11i)	H. X., Huynh & Min,
	hispidulin (12e)	2012
	p-hydroxybenzoic acid (13i)	
	2-(1-hydroxymethylethyl)-4*H*,9*H*-naphtho[2,3-b] furan-4,9-dione (14c)	
	β-hydroxypropiovanillon (15i)	
	isovanillin (16i)	
	oroxylin A (1e)	
	oroxyloside (17e)	
	protocatechuic acid (18i)	
	salicylic acid (19i)	
Leaf	aloe-emodin (20b)	Dey et al., 1979
	baicalein (21e)	Yuan, Hou, Tang, Luo,
	baicalin (2e)	Chen, Guan &
	baicalein-7-*O*-glucoside (23e)	Sutherland, 2008
	chrysin (24e)	
	chrysin-diglucoside (25e)	
	chrysin-7-*O*-glucuronide (26e)	Yuan et al., 2008
	oroxin B (27e)	

Table 2.1 (continued)

Part	Compound (Structure, Type)	Reference
Root	ellagic acid (28i)	Vasanth, Natarajan, Sundaresan, Rao & Kundu, 1991
	lapachol (29c)	Ali, Houghton, Raman & Hoult, 1998
	oroxylin A (1e)	
	β-sitosterol (30g)	
	baicalein (21e)	Yadav, Manika, Bagchi & Gupta, 2012
	chrysin (24e)	
	hispidulin (12e)	
	oroxylin A (1e)	
Root bark	oroxylin A (1e)	Shah, Mehta & Wheeler, 1935
	2-acetylfuro-1,4-naphthoquinone (31c)	Kizu, Habe, Ishida & Tomimori, 1994
	catalponol (32c)	
	catalponone (33c)	
	dehydro-iso-*α*-lapachone (34c)	
	2,5-dihydroxy-6,7-dimethoxyflavone (35e)	Uddin et al., 2003
	3,7,3',5'-tetramethoxy-4'-hydroxyflavone (36e)	
	oroxylin B (37e)	Sastry, S. V. A., Sastry, G., Mallikarjun & Srinivas, 2011
Seed	oroxindin (38e)	Nair & Joshi, 1979
	apigenin (9e)	Tomimori, Imoto, Ishida, Kizu & Namba, 1988
	baicalin (22e)	
	hispidulin (12e)	
	hydroxy-6,7-dimethoxyflavone (39e)	
	oroxin B (27e)	

Table 2.1 (continued)

Part	Compound (Structure, Type)	Reference
Seed	oroxylin A (1e)	Tomimori et al.,
	scutellarin (40e)	1988
	scutellarein (41e)	
	baicalein (21e)	Chen et al., 2003
	baicalin (22e)	
	baicalein-7-*O*-glucoside (23e)	
	chrysin (24e)	
	oroxin B (27e)	
	adenosine (42i)	Yan et al., 2011
	baicalein (21e)	
	baicalin (22e)	
	baicalein-7-*O*-glucoside (23e)	
	baicalein-7-*O*-*β*-D-glucuronopyranosyl-(1→3)-[*β*-D-glucopyranosyl-(1→6)]-*β*-D-glucopyranoside (43e)	
	chrysin (24e)	
	chrysin-7-*O*-gentiobioside (44e)	
	chrysin-7-*O*-glucuronide (26e)	
	chrysin-6-*C*-*β*-D-glucopyranosyl-8-*C*-*α*-L-arabinopyranoside (45e)	
	chrysin-6-*C*-*β*-D-glucopyr-anosyl-8-*O*-*β*-D-glucuronopyranoside (46e)	
	dimethyl sulfone (47i)	
	echinulin (48a)	
	2*α*-hydroxyllupeol (49h)	
	lupeol (50h)	
	2-methyl-6-phenyl-4*H*-pyran-4-one (51i)	
	oroxylin A (1e)	
	oroxin B (27e)	
	pinobanksin (52e)	

Table 2.1 (continued)

Part	Compound (Structure, Type)	Reference
Seed	pinocembrin (53e)	Yan et al., 2011
	β-sitosterol (30g)	
	scutellarein-7-*O*-glucopyranoside (54e)	
	scutellarein-7-*O*-β-D-glucopyranosyl-(1→6)-β-D-glucopyranoside (55e)	
	baicalein (21e)	Krüger & Ganzera, 2012
	baicalein-7-*O*-glucoside (23e)	
	baicalein-7-*O*-glucuronide (22e)	
	chrysin (24e)	
	chrysin-7-*O*-gentiobioside (44e)	
	chrysin-7-*O*-glucuronide (26e)	
	oroxin B (27e)	
	oroxylin A (1e)	
Stem bark	baicalein (21e)	Ali et al., 1998
	chrysin (24e)	
	lapachol (29c)	
	dehydro-iso-α-lapachone (34c)	
	baicalein (21e)	Dinda, Mohanta,
	baicalein-7-*O*-glucoside (23e)	Arima, Sato &
	8,8''-bisbaicalein (56e)	Harigaya, 2007
	bisbaicalein-7-*O*-caffeate (57e)	
	chrysin (24e)	
	6-hydroxyluteolin (58e)	
	6-methoxyluteolin (59e)	
	scutellarein (41e)	
	β-sitosterol (30g)	
	baicalein (21e)	Babu et al., 2010
	chrysin (24e)	

Table 2.1 (continued)

Part	Compound (Structure, Type)	Reference
Stem bark	dehydro-iso-α-lapachone (34c)	Babu et al., 2010
	dihydro-oroxylin A (60e)	
	dihydro-oroxylin A-7-*O*-methyl glucuronide (61e)	
	5-hydroxy-7,4'-dimethoxyflavone (62e)	
	5-hydroxyl-7-methoxy-2-(2-methoxy-6-(3,4,5-trihydroxy-6-(hydroxymethyl)tetrahydro-2*H*-pyran-2-yoloxy)phenyl)-4*H*-chromen-4-one (63e)	
	7-*O*-methylchrysin (64e)	
	oroxylin A (1e)	
	kaempferol (65e)	Islam, Eti & Chowdhury, 2010
	baicalein (21e)	Luitel et al., 2010
	oroxylin A (1e)	
	pinostrobin (66e)	
	stigmast-7-en-3-ol (67g)	
	apigenin (9e)	Maungjunburee &
	chrysin (24e)	Mahabusarakam,
	5,7-dihydroxy-3methoxyflavone (68e)	2010
	kaempferol (65e)	
	3,5,7-trihydroxyflavone (69e)	
	5,7,4'-trihydroxy-3-methoxyflavone (70e)	

Note. a : Alkaloid b : Anthraquinone c : Naphthoquinones d : Cyclohexylethanoids
e : Flavonoids f : Phenylethanoids g : Steroids h : Triterpenoids
i : Miscellanous

a : Alkaloid
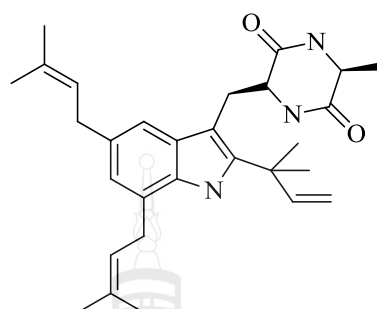
48 echinulin

b : Anthraquinone
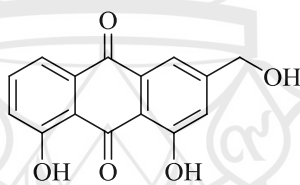
20 aloe-emodin

c : Naphthoquinones
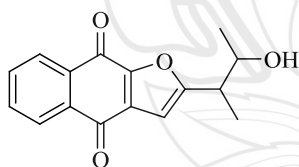
14 2-(1-hydroxymethylethyl)-4*H*,9*H*-
naphtho[2,3-b]furan-4,9-dione
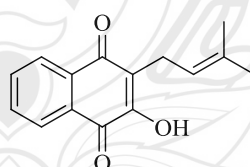
29 lapachol
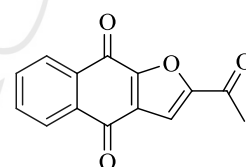
31 2-acetylfuro-
1,4-naphthoquinone
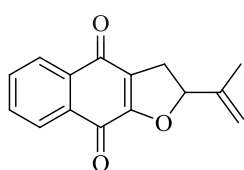
32 dehydro-iso-α-lapachone
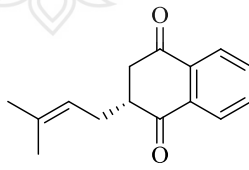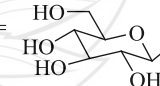
33 catalponone
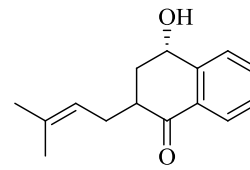
34 catalponol

Figure 2.2 Structure of Compounds Isolated from *Oroxylum indicum* (L.) Vent.

d : Cyclohexylethanoids
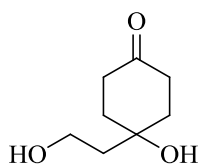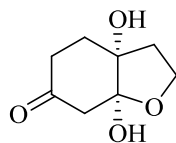
3 cleroindicin B   **4** cleroindicin C   **7** rengyol
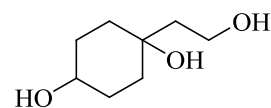
e : Flavonoids
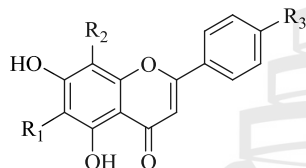
1 R_1 = OCH$_3$, R_2 = H, R_3 = H : oroxylin A

9 R_1 = H, R_2 = H, R_3 = OH : apigenin

12 R_1 = OCH$_3$, R_2 = H, R_3 = OH : hispidulin

21 R_1 = OH, R_2 = H, R_3 = H : baicalein

24 R_1 = H, R_2 = H, R_3 = H : chrysin

37 R_1 = H, R_2 = OH, R_3 = OCH$_3$: oroxylin B

41 R_1 = OH, R_2 = H, R_3 = OH : scutellarein

17 R_1 = OCH$_3$, R_2 = H, R_3 = H : oroxyloside

22 R_1 = OH, R_2 = H, R_3 = H : baicalin

26 R_1 = H, R_2 = H, R_3 = H : chrysin-7-*O*-glucuronide

38 R_1 = H, R_2 = OCH$_3$, R_3 = H : oroxindin

40 R_1 = OH, R_2 = H, R_3 = OH : scutellarin

46 R_1 = (sugar), R_2 = H, R_3 = H : chrysin-6-*C*-β-D-glucopyranosyl-8-*O*-β-D-glucuronopyranoside
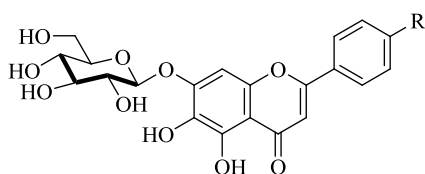
23 R = H : baicalein-7-*O*-glucoside

54 R = OH : scutellarein-7-*O*-glucopyranoside

Figure 2.2 (continued)

e : Flavonoids (continued)

27 $R_1 = OH$, $R_2 = H$: oroxin B

44 $R_1 = R_2 = H$: chrysin-7-*O*-gentiobioside

55 $R_1 = R_2 = OH$: scutellarein-7-*O*-β-D-glucopyranosyl-(1→6)-β-D-glucopyranoside

35 $R_1 = OCH_3$, $R_2 = OH$: 2,5-dihydroxy-6,7-dimethoxyflavone

66 $R_1 = H$, $R_2 = H$: pinostrobin

39 $R_1 = OCH_3$, $R_2 = H$: hydroxy-6,7-dimethoxyflavone

62 $R_1 = H$, $R_2 = OCH_3$: 5-hydroxy-7,4'-dimethoxyflavone

64 $R_1 = H$, $R_2 = H$: 7-*O*-methylchrysin

53 $R_1 = H$, $R_2 = H$: pinocembrin

60 $R_1 = OCH_3$, $R_2 = H$: dihydro-oroxylin A

61 $R_1 = OCH_3$, $R_2 = $: dihydro-oroxylin A-7-*O*-methyl glucuronide

58 $R = OH$: 6-hydroxyluteolin

59 $R = OCH_3$: 6-methoxyluteolin

65 $R_1 = OH$, $R_2 = OH$: kaempferol

68 $R_1 = H$, $R_2 = OCH_3$: 5,7-dihydroxy-3-methoxyflavone

69 $R_1 = H$, $R_2 = OH$: 3,5,7-trihydroxyflavone

70 $R_1 = OH$, $R_2 = OCH_3$: 5,7,4'-trihydroxy-3-methoxyflavone

Figure 2.2 (continued)

e : Flavonoids (continued)

36 3,7,3',5'-tetramethoxy-
4'-hydroxyflavone
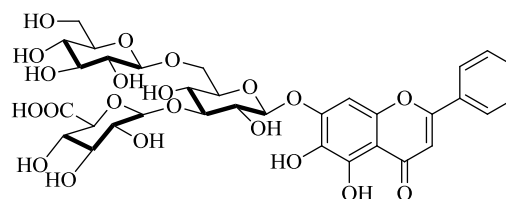
43 baicalein-7-*O*-*β*-D-glucuronopyranosyl-(1→3)-
[*β*-D-glucopyranosyl-(1→6)]-*β*-D-glucopyranoside
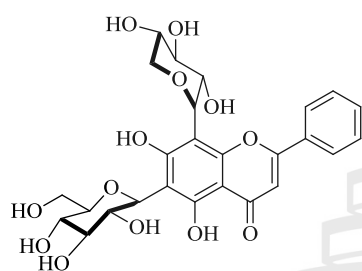
45 chrysin-6-*C*-*β*-D-glucopyranosyl-
8-*C*-*α*-L-arabinopyranoside
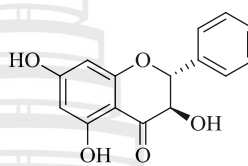
52 pinobanksin
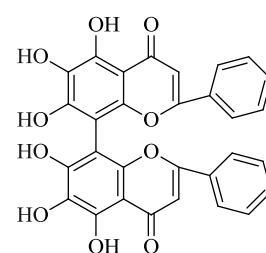
56 8,8''-bisbaicalein
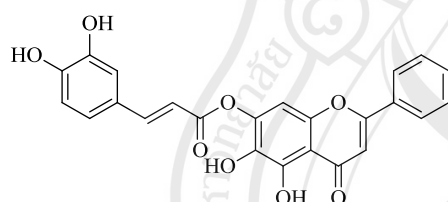
57 bisbaicalein-7-*O*-caffeate
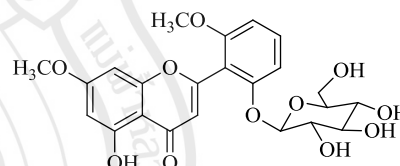
63 5-hydroxyl-7-methoxy-2-(2-methoxy-6-
(3,4,5-trihydroxy-6-(hydroxymethyl)tetrahydro-
2*H*-pyran-2-yoloxy)phenyl)-4*H*-chromen-4-one

f : Phenylethanoids
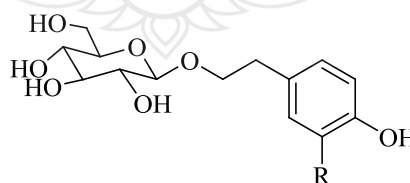
6 R = OH : hydroxytyrosol-1-*O*-glucoside

8 R = H : salidroside

Figure 2.2 (continued)

g : Steroids
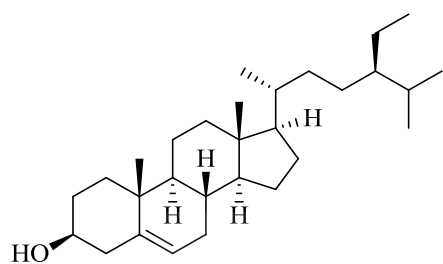
30 β-sitosterol
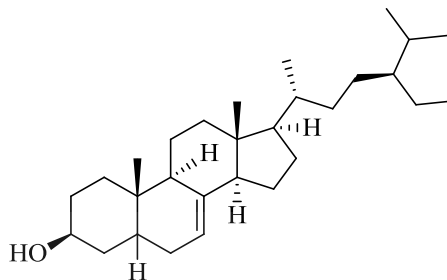
67 stigmast-7-en-3-ol

h : Triterpenoids
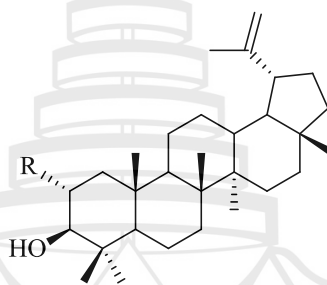
49 R = OH : 2α-hydroxyllupeol

50 R = H : lupeol

i : Miscellanous
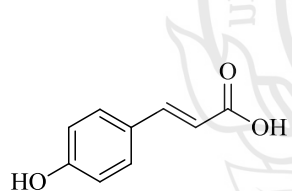
2 *p*-coumaric acid
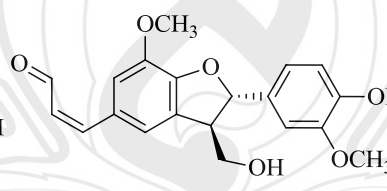
10 balanophonin
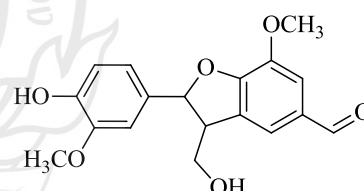
11 ficusal
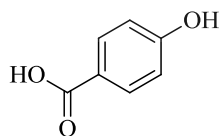
13 *p*-hydroxybenzoic acid
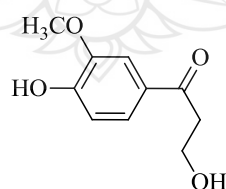
15 β-hydroxypropiovanillon
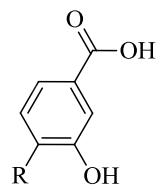
16 R = OCH$_3$: isovanillin

18 R = OH : protocatechuic acid

Figure 2.2 (continued)

i : Miscellanous (continued)

19 salicylic acid   **28** ellagic acid

42 adenosine   **47** dimethyl sulfone   **51** 2-methyl-6-phenyl-4*H*-pyran-4-one
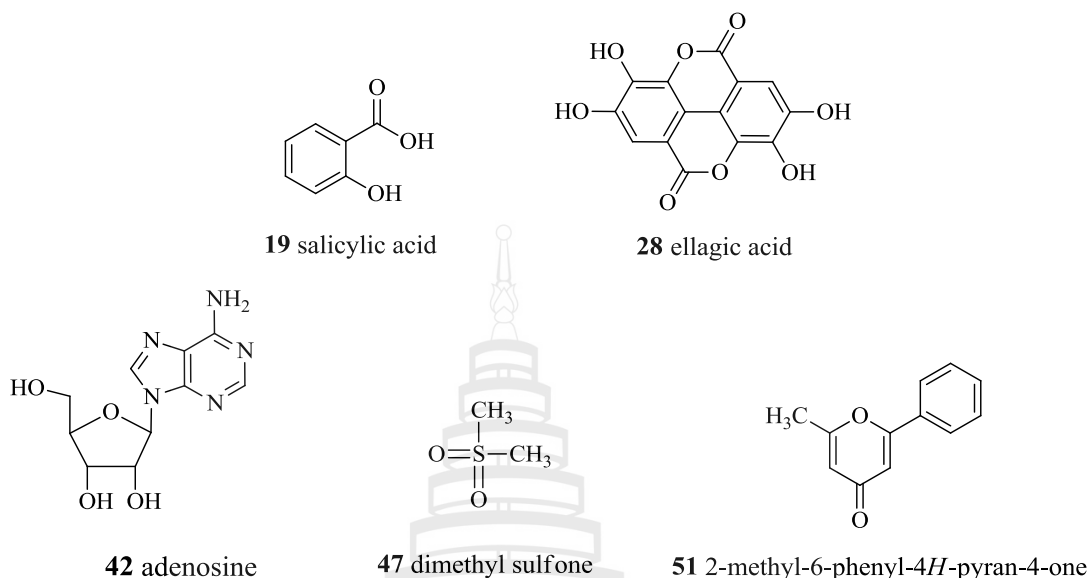
Figure 2.2 (continued)

2.3 Biological Activities of *Oroxylum indicum* (L.) Vent.

Plants are the largest reservoir of secondary metabolites which contribute in combating different diseases from ancient times (Merina, Chandra & Jibon, 2012). Several known metabolites possessing biological properties such as alkaloids, anthraquinones, flavonoids, triterpenoids were isolated from natural sources (Kumar, N. R. D., George, Suresh & Kumar, A. R., 2012). A number of studies have been reported, most of the chemical constituents of *O. indicum* are flavonoids. They exhibited different biochemical activities such as antimicrobial (Ali et al., 1998; Uddin et al., 2003; Vinod & Kamlesh, 2009; Das & Choudhury, 2010; Islam et al., 2010), antioxidant (Upaganlawar & Tenpe; 2007; Gupta, Sharma, V., Sharma, N., Kumar & Singh, 2008; Kalaivani & Mathew, 2009; Kumar, Rajkumar, Guha & Mathew, 2010; Siriwatanametanon, Fiebich, Efferth, Prieto & Heinrich, 2010; Yan et al., 2011; Rajkumar et al., 2012), anti-inflamatory (Laupattarakasem et al., 2003; Le & Nguyen, 2005; Harminder & Chaudhary, 2009), cytotoxicity (Tepsuwan, Furihata, Rojanapo & Matsushima, 1992; Nakahara, Onishi-Kameyama, Ono, Yoshida & Trakoontivakorn, 2001; Costa-Lotufo et al., 2005; Roy et al., 2007; Kumar et al.,

2010; Brahma, Prasad, Verma & Rosangkima, 2011; Kumar et al., 2012; Rajkumar et al., 2012), gastroprotective (Khandhar, Shah, Santani & Jain, 2006; Babu et al., 2010), hepatoprotective (Tenpe, Aman, Sushil & Yeole, 2009) and immunstimulant (Zaveri, Gohil & Jain, 2006) activities.

2.3.1 Antimicrobial Activities of *O. indicum*

It was recently found that dichloromethane extracts of stembark and root of *O. indicum* were found to have antimicrobial activities against gram-positive bacteria (*Bacillus subtilis* and *Stephylococcus aureus*), gram-negative bacteria (*Escherichia coli* and *Pseudomonae aeruginosa*) and a yeast (*Candida albicans*) (Ali et al., 1998). In 2003, the crude petroleum ether, ethyl acetate and methanol extracts, 2,5-dihydroxy-6,7-dimethoxyflavone and 3,7,3',5'-tetramethoxy-4'-hydroxyflavone of root bark showed mild to moderate activity against bacteria and fungi (Uddin et al., 2003). The ethanolic and aqueous extracts of root bark against bacteria (*E. coli*, *Shigella dysenteriae*, *S. aureus*, *Streptococcus mutant*) and fungi (*Aspergillus niger*, *C. albicans*) were studied by using disc diffusion method (Vinod & Kamlesh, 2009). The methanolic extract of stem bark was found to show antimicrobial activities towards the gram-positive and gram-negative bacteria and some fungi (Islam et al., 2010). Moreover, the activity of 100% ethanol extract against *B. subtilis* and 70% ethanol extract against *E. coli* were better than those of the standard Ampicillin (Das & Choudhury, 2010).

2.3.2 Antioxidant Activities of *O. indicum*

The ethanolic extract of leaves possessed significant antioxidant activity with an IC_{50} value of 24.22 μg/mL in scavenging nitric oxide (NO) radical (Upaganlawar & Tenpe, 2007). Ascorbic acid which was used as a standard showed an IC_{50} of 24 μg/mL, whereas, the crude ethyl acetate, methanolic and water extracts showed antioxidant activity with IC_{50} values of 49.0, 55.0, and 42.5, respectively at 100 μg/mL concentration (Gupta et al., 2008). The order of total antioxidant activity of the various extracts of stembark can be seen as chloroform > ethanol > benzene > water > petroleum ether. The scavenging activity of ethanol and chloroform extracts showed high potency compared to the other extracts (Kalaivani & Mathew, 2009). In 2010,

the ethyl acetate extract of *O. indicum* stembark showed the most promising NF-KB inhibitory effects with the lowest IC_{50} value of 47.45 μg/mL and a high level of antioxidant activity by inhibiting lipid-peroxidation with IC_{50} value of 0.08 μg/mL (Siriwatanametanon et al., 2010). The methanolic and aqueous extracts of stembark exhibited considerable free radical scavenging and ferric reducing abilities. Both extracts exhibited moderate levels of DNA protection against oxidative stress (Kumar et al., 2010). Moreover, the isolated metabolites from the methanolic extract of *O. indicum* stembark showed good antioxidant property by DPPH radical scavenging assay (Rajkumar et al., 2012). Furthermore, antioxidant activity of some isolated compounds from the seeds was studied in DPPH and ORAC assays (Yan et al., 2011), as shown in table 2.2.

Table 2.2 Antioxidant Capacity of Isolated Compounds from the Seeds of *O. indicum*

Compound	DPPH ± SD (IC_{50}, μg/mL)	ORAC ± SD (μM)
baicalein	51.64 ± 0.02	2.15 ± 0.19
baicalein-7-*O*-diglucoside	139.62 ± 0.02	0.75 ± 0.13
baicalein-7-*O*-glucoside	101.32 ± 0.01	1.34 ± 0.03
baicalin	114.35 ± 0.07	2.08 ± 0.15
chrysin	-	0.51 ± 0.04
chrysin-7-*O*-gentiobioside	-	1.07 ± 0.16
chrysin-6-*C*-*β*-D-glucopyranosyl-8-*C*-*α*-L-arabinopyranoside	-	0.88 ± 0.07
chrysin-7-*O*-glucuronide	-	1.14 ± 0.11
oroxylin A	-	2.00 ± 0.17
pinobanksin	-	2.90 ± 0.15
pinocembrin	-	3.51 ± 0.47
scutellarein-7-*O*-glucopyranoside	112.95 ± 0.40	7.55 ± 1.32
scutellarein-7-*O*-*β*-D-glucopyranosyl-(1→6)-*β*-D-glucopyranoside	136.59 ± 1.60	6.77 ± 0.28
queroetin	27.59 ± 0.38	3.06 ± 0.65
Trolox	44.76±1.23	-

2.3.3 Anti-inflammatory Activities of *O. indicum*

The study of the aqueous extracts of *O. indicum* displayed no relevant activity except for significantly reduced myeloperoxide (MPO) release (64%) and this may indicate that a reduction in inflammation *in vivo* may occur if an aqueous extract is applied topically or taken internally. It is unlikely that significant amounts of the lapachol compound are present in the aqueous extract (Laupattarakasem et al., 2003). In *vivo*, flavonoids from *O. indicum* had anti-inflammatory effects in dextran-induced edema of mouse paw. When they were combined with α-chymotrypsin, their anti-inflammatory activity was increased (Le & Nguyen, 2005). The aqueous extract of leaves exhibited significant anti-inflammatory activity at a dose of 150 mg/kg body weight and 300 mg/kg body weight. The extract at a dose of 300 mg/kg body showed maximum anti-inflammatory activity (Harminder et al., 2009).

2.3.4 Cytotoxicity Activities of *O. indicum*

In the present study, the nitrosated *O. indicum* fraction exhibited *in vivo* genotoxic and cell proliferative activities in stomach mucosa of male F344 rats by *in vivo* short-term methods (Tepsuwan et al., 1992). A methanolic extract of *O. indicum* strongly inhibited the mutagenicity of Trp-P-1 in an Ames test. The major antimutagenic constituent was identified as baicalein with an IC_{50} value of 2.78 ± 0.15 μM (Nakahara et al., 2001). Administration of the ethanolic extract of *O. indicum* stembark was tested for cytotoxicity using the brine shrimp lethality assay, sea urchin eggs assay, hemolysis assay and MTT assay using tumor cell lines (Costa-Lotufo et al., 2005), as shown in table 2.3.

Table 2.3 Cytotoxicity Activities of the Ethanolic Extract of *O. indicum*

Assay	Result
Brine shrimp lethality	N/A
Sea urchin eggs	The extract inhibited the progression of cell cycle since the first cleavage ($IC_{50} = 13.5$ μg/mL)

Table 2.3 (continued)

Assay	Result
Hemolysis	The extract was tested on mouse erythrocyte ($ED_{50} > 2500$ µg/mL)
MTT	The extract showed the highest toxicity on tumor cell lines with IC_{50}:
	CEM (19.6 µg/mL)
	HL-60 (14.2 µg/mL)
	B-16 (17.2 µg/mL)
	HCT-8 (32.5 µg/mL)

Moreover, baicalein showed apoptosis in the HL-60 cell line which, posses a 50% inhibition of HL-60 cells at concentrations of 25–30 µM (Roy et al., 2007). The methanolic and aqueous extracts of *O. indicum* bark demonstrated extensive cytotoxicity in both tested cell lines (MDA-MB-435S and Hep 3B), with the methanolic extract showing greater cytotoxic potential (Kumar et al., 2010). In addition, *in vitro* cytotoxicity assay with the MTT test it revealed an IC_{50} value at 63.2 µg/ml for the methanol crude extract of *O. indicum* while for standard drug of cisplatin under the same conditions it was 44.4 µg/ml. Therefore, the methanol crude extract of *O. indicum* is effective against Dalton's lymphoma both *in vitro* and *in vivo* (Brahma et al., 2011). On the other hand, the chemopreventive properties of the hot and cold non-polar extracts of *O. indicum* (petroleum ether and chloroform) were investigated with MDA-MB-231 (cancer cells) and WRL-68 (non-tumor cells) by XTT assay. All the extracts, particularly the petroleum ether hot extract (PHO), exhibited significantly (P<0.05) higher cytotoxicity in MDA-MB-231 when compared to WRL-68 cells. PHO was then tested for apoptosis induction in estrogen receptor (ER)-negative (MDA-MB-231) and ER-positive (MCF-7) breast cancer cells by cellular DNA fragmentation ELISA, where it proved more efficient in the MDA-MB-231 cells (Kumar et al., 2012). In addition, the isolated metabolites from the methanolic extract of *O. indicum* stembark exhibited cytotoxic potential on cancer cells (MDA-MB-435S) 1.5 times higher than in normal cells (WRL-68) by the XTT assay (Rajkumar et al., 2012).

2.3.4 Gastroprotective Activities of *O. indicum*

The current study was undertaken to investigate the effect of the root bark of *O. indicum* against gastric ulcers. The petroleum ether (96%) and *n*-butanol (99%) fractions showed maximum inhibition of gastric lesions against ethanol-induced gastric mucosal damage (Khandhar et al., 2006). In addition, the activity for gastric ulceration models in rat, at two random dosage of 100 mg and 250 mg/kg body weights, hexane and acetone extract exhibited mild to moderate gastroprotective activity. Acetone extract displayed better activity than hexanes extract (Babu et al., 2010).

2.3.5 Hepatoprotective Activities of *O. indicum*

Hepatoprotective activity of different extracts (petroleum ether (PEE), ethanol (EE), water (WTE) and chloroform (CE) extracts) of *O. indicum* leaves in different system was induced by CCl_4 which leads to significant increased in the level of serum glutamate oxaloacetate transaminase (SGOT), serum glutamate pyruvate transaminase (SGPT), alkaline phosphatase (ALP) and total bilirubin whereas there were significant decrease in the activity of total protein. Administration of different extracts of *O. indicum* (300 mg/kg) leads to significant alteration in biochemical parameters towards normal (Tenpe et al., 2009).

2.3.6 Immunostimulant Activities of *O. indicum*

The study of the action of the *n*-butanol fraction (100 mg/kg body weight, per os) of the root bark of *O. indicum* was evaluated in rats. In response to red blood cells (SRBC haemagglutinating antibody (HA) titer), treatment with the *n*-butanol fraction caused significant rise in circulating HA titers during secondary antibody responses, indicating a potentiation of certain aspects of the human response (Zaveri et al., 2006).

CHAPTER 3

RESEARCH METHODOLOGY

3.1 General Methods

Melting points were determined by BÜCHI model B-540 melting point apparatus at Switzerland. It was recorded in celsius (°C). Ultraviolet spectra (UV) were recorded using UV-Vis spectrometer (Perkin Elmer Lambda, United States of America (USA)). Principle bands (λ_{max}) were recorded as wavelengths (nm) and log ε in methanol solution. Infrared spectra (IR) were recorded on Perkin-Elmer FTSFT IR/Spectum spectrometer at United States of America. Major bands (ν_{max}) were recorded in wavenumber (cm^{-1}). 1D and 2D NMR spectra were performed on a Brüker FTNMR Ultra Shield 300 MHz at Germany (Prince of Songkla University, Songkhla), Brüker FTNMR Ultra Shield 400 MHz at Germany (Naresuan University, Phitsanulok), and Brüker AVANCE 300 MHz at Germany (Silpakorn University, Nakhon Pathom). Spectra were recorded in acetone-d_6 solution and recorded as chemical shift (δ) value in ppm down field from TMS (internal standard δ 0.00). Pre-coated thin layer chromatography (TLC) aluminum sheets of silica gel 60 F$_{254}$ (20x20 cm, layer thickness 0.2 mm, Merck, Germany) were used for analytical purposes and the compounds were visualized under ultraviolet light or anisaldehyde-sulfuric acid and vanillic acid spraying reagents. Preparative thin layer chromatography (PLC) was carried out on glass plate coated with silica gel 60 F$_{254}$ (20x20 cm, layer thickness 1.0 mm, Merck, Germany). Bands were detected by exposure to short wavelength UV light. Column chromatography (CC) and quick column chromatography (QCC) were performed on silica gel 100 (0.063-0.200 mm, Merck, Germany) and silica gel 60 (0.063-0.230 mm, Merck, Germany), respectively. Organic solvents for extraction and

chromatography distilled at their boiling point ranges prior to use. Solvents for UV and IR were analytical grade reagents. The analytical grade of absolute ethanol, 1,1-diphenyl-2-picrylhydrazyl free radical (DPPH•, Fluka, USA), and ascorbic acid (Fluka, USA) were used for antioxidative activity testing and the absorption of the test solution were measured with flow injection analysis (FIA), which its system consisting of a peristaltic pump (REGLO Anlalog MS-2/6, Ismatec, Switzerland), a 6-port injection valve (V-450, UpChurch Scientific, Washington, USA) with a 50-ll sample loop, one reaction coil (PFA tubings, 0.030 in i.d.), and a spectrophotometer (SpectraSystem UV1000, Thermo Separation Products, USA) using a Suprazil® quartz flow-through cell (pathlength 10 mm, chamber volume 390 ll, Hellma®, Germany). A PC with Clarity Lite software (Thermo Separation Products, USA) was used to collect the real-time absorbance data from the spectrophotometer. The dimethyl sulfoxide (DMSO) and nutrient broth were used for antibacterial activity testing against 6 strains of microorganism; *Bacillus cereus* TISTR 687, *Escherichia coli* TISTR 780, *Pseudomonas aeruginosa* TISTR 781, *Salmonella typhimurium* TISTR 292, *Staphylococcus aureus* TISTR 1466, and methicillin resistant *Staphylococcus aureus* SK1. Vancomycin and gentamicin were used as standard maker of antibacterial activity.

3.2 Plant Materials and Microorganism Culture Materials

Leaves, roots, stems, and twigs of *O. indicum* which were collected from Lamphun province, Thailand in April 2011. Five microorganism cultures including *B. cereus* TISTR 687, *E. coli* TISTR 780, *P. aurenginosa* TISTR 781, *S. typhimurium* TISTR 292, and *S. aureus* TISTR 1466 were derived from the Microbiological Resources Center of the Thailand Institute of Scientific and Technological Research, Mae Fah Luang University whereas MRSA-SK1 was supported by Department of Microbiology, Faculty of Science, Prince of Songkla University.

3.3 Chemical Investigation of the *Oroxylum indicum* Leaves

3.3.1 Extraction, Isolation, and Purification

The dried leaves of *O. indicum* (3.521 kg) were chopped and immersed at room temperature in hexanes (10 L, 7 days), CH_2Cl_2 (10 L, 7 days), Me_2CO (10 L, 7 days) and MeOH (10 L, 7 days), respectively. After evaporation, the viscous crude hexanes (crude LH, 44.290 g), crude CH_2Cl_2 (crude LD, 26.450 g), crude acetone (crude LA, 12.220 g), and crude MeOH (crude LM, 22.090 g) extracts were obtained as shown in figure 3.1.
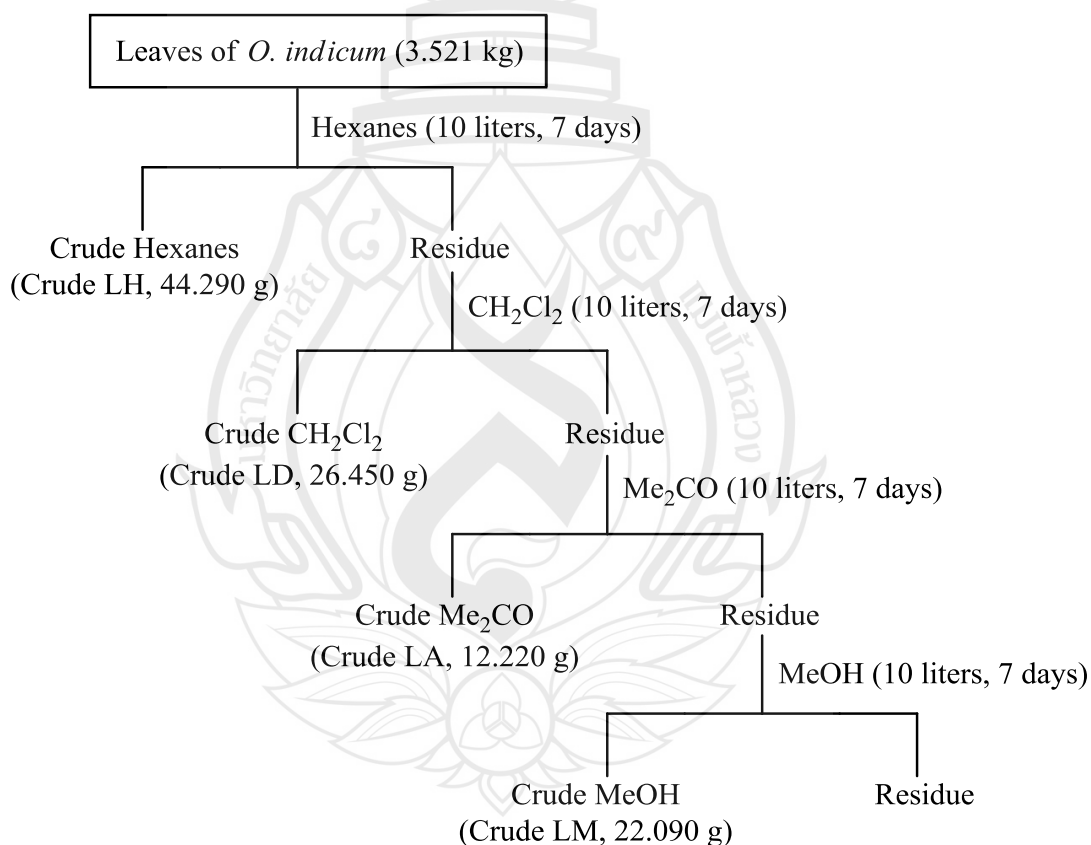
Figure 3.1 Extraction of Crudes LH, LD, LA, and LM from the Leaves of *O. indicum*

Crude LA (12.220 g) was subjected to QCC over silica gel and gradiently eluted with hexanes, hexanes-CH_2Cl_2, CH_2Cl_2-Me_2CO, and Me_2CO-MeOH. The collected fractions were combined according to the characteristic on TLC and evaporated to give seventeen fractions (LA1-LA17), as shown in table 3.1. The selected fractions were further purified as shown in figure 3.2.

Table 3.1 Physical Characteristic and Weight of Fractions obtained from Crude LA

Fraction	Weight (g)	Physical Characteristic
LA1	0.025	Yellow solid
LA2	0.031	Yellow solid
LA3	0.254	Brown solid
LA4	0.659	Brown solid
LA5	0.131	Yellow solid
LA6	0.564	Green viscous liquid
LA7	5.195	Green viscous liquid
LA8	6.314	Green viscous liquid
LA 9	0.028	Green viscous liquid
LA10	3.473	Green viscous liquid
LA11	4.168	Green viscous liquid
LA12	3.101	Green viscous liquid
LA13	1.895	Green viscous liquid
LA14	5.248	Green viscous liquid
LA15	6.428	Green viscous liquid
LA16	0.036	Green viscous liquid
LA17	5.035	Green viscous liquid

Crude LA (12.220 g)

QCC (hexanes, hexanes-CH$_2$Cl$_2$, CH$_2$Cl$_2$-Me$_2$CO, and Me$_2$CO-MeOH)

LA1 ....LA3-LA4   LA5   LA6   LA7-LA8   LA9

| CC | CC | TLC | | Cryst. |

OLA1 (897.0 mg)   **OLA1** (120.3 mg)   **OLA1**   CC   **OLA3** (10.5 mg)

LA7-8.1   LA7-8.2   LA7-8.3 .... LA7-8.6   LA7-8.7   LA7-8.8   LA7-8.9   LA7-8.10   LA7-8.11

TLC   TLC   CC   CC   CC   PLC   PLC   TLC

OLA1   **OLA1**   LA7-8.3.1 LA7-8.3.2   LA7-8.6.1 LA7-8.6.2 LA7-8.6.3   **OLA5** (8.1 mg)   LA7-8.10.1 LA7-8.10.2 LA7-8.10.3   **OLA5**

TLC   TLC

OLA1 + OLA2   **OLA2** (1.5 mg)   **OLA3** (2.0 mg)   **OLA3 + OLA5**

OLA3 (1.2 mg)   **OLA5** (0.8 mg)   **OLA9** (1.2 mg)

CC

LA7-8.7.1 LA7-8.7.2 LA7-8.7.3 LA7-8.7.4 LA7-8.7.5 LA7-8.7.6 LA7-8.7.7 LA7-8.7.8 LA7-8.7.9   LA7-8.8.1 LA7-8.8.2 LA7-8.8.3 LA7-8.8.4 LA7-8.8.5 LA7-8.8.6   LA7-8.8.7

TLC   TLC   TLC   PLC   PLC   TLC   CC   CC   TLC   CC   CC

OLA3 + OLA5   **OLA3 + OLA5**   **OLA3** (14.4 mg)   **OLA3 + OLA5**   **OLA3** (1.0 mg)   **OLA3 + OLA5**   **OLA3** (42.2 mg)   **OLA5** (25.5 mg)   **OLA3** (1.0 mg)   **OLA3 + OLA5**   **OLA5** (9.1 mg)

LA7-8.7.7.1 LA7-8.7.7.2   LA7-8.7.9.1 LA7-8.7.9.2   LA7-8.8.6.1 LA7-8.8.6.2 LA7-8.8.6.3   LA7-8.8.6.4 LA7-8.8.6.5 LA7-8.8.6.6   LA7-8.8.7.1 LA7-8.8.7.2 .... LA7-8.8.7.4

TLC   TLC   TLC   CC   TLC   TLC

OLA3 (1.0 mg)   **OLA7** (1.3 mg)   **OLA3** (1.7 mg)   **OLA3 + OLA5**   **OLA1** (7.2 mg)   **OLA3** (5.1 mg)   **OLA1**   **OLA8** (1.2 mg)

CC

LA7-8.8.6.4-5.1 LA7-8.8.6.4-5.2 LA7-8.8.6.4-5.3 LA7-8.8.6.4-5.4

TLC   TLC   TLC

OLA5 (8.8 mg)   **OLA3 + OLA5**   **OLA8**   **OLA5 + OLA8**

Figure 3.2 Isolation of Pure Compounds from Crude LA of *O. indicum*

Crude LA (12.220 g)

QCC (hexanes, hexanes-CH$_2$Cl$_2$, CH$_2$Cl$_2$-Me$_2$CO, and Me$_2$CO-MeOH)

LA10
Cryst.

LA11-LA15
CC

LA16
Cryst.

OLA3
+
OLA5

LA17
TLC

OLA5

LA11-15.1

LA11-15.2
TLC

LA11-15.3
TLC

LA11-15.4

LA11-15.5
TLC

LA11-15.6

LA11-15.7

LA11-15.8
PLC

LA11-15.9

OLA1
(118.4 mg)

OLA1
+
OLA2

OLA1
+
OLA2
+
OLA3
+
OLA7

OLA2
(44.4 mg)

OLA3
+
OLA5

LA10.1
TLC

LA10.2
TLC

LA10.3
Cryst.

LA10.4

LA10.5
Cryst.

OLA1
+
OLA2

OLA2
+
OLA3

OLA5
(8.4 mg)

LA10.3.1
TLC

LA10.3.2
TLC

LA10.3.3

LA10.5.1
TLC

LA10.5.2

OLA1
+
OLA2

OLA1
+
OLA2
+
OLA3
+
OLA5

OLA3
(30.0 mg)

OLA1
+
OLA2
+
OLA3
+
OLA5

OLA5
(79.5 mg)

CC

LA11-15.6.1-.3

LA11-15.6.4
TLC

LA11-15.6.5

LA11-15.6.6
TLC

OLA5
(32.8 mg)

OLA5
+
OLA8

OLA8
(1.3 mg)

OLA8

LA11-15.8.1
TLC

LA11-15.8.2
PLC

OLA3
+
OLA5

OLA9
(2.0 mg)

LA11-15.9.1
PLC

LA11-15.9.2

LA11-15.9.3

OLA5
(48.3 mg)

band1

band2
TLC

OLA5
(0.8 mg)

OLA5
+
OLA9

CC

LA11-15.7.2

LA11-15.7.2
TLC

LA11-15.7.3
TLC

LA11-15.7.4
TLC

LA11-15.7.5
TLC

LA11-15.7.6
TLC

LA11-15.7.7

LA11-15.7.8
CC

LA11-15.7.9
CC

LA11-15.7.10
CC

OLA1
(5.0 mg)

OLA2

OLA2
+
OLA3

OLA3
+
OLA5

OLA3
+
OLA5
+
OLA9

OLA5
(13.4 mg)

LA11-15.7.8.1

LA11-15.7.8.2
TLC

LA11-15.7.8.3

LA11-15.7.8.4

LA11-15.7.8.5

LA11-15.7.8.6
TLC

OLA10
(2.6 mg)

OLA5
+
OLA8

OLA8
(2.0 mg)

OLA10
(12.7 mg)

OLA8
(1.7 mg)

OLA8
+
OLA9

LA11-15.7.9.1

LA11-15.7.9.2

LA11-15.7.9.3

LA11-15.7.9.4
TLC

OLA10
(24.3 mg)

OLA8
(1.5 mg)

OLA10
(8.0 mg)

OLA3
+
OLA8

LA11-15.7.10.1

LA11-15.7.10.2
TLC

OLA8
(5.4 mg)

OLA8
+
OLA9

Figure 3.2 (continued)

Fractions LA3 and LA4 were combined (0.912 g) and purified by CC using 50% CH_2Cl_2-hexanes to give **OLA1** (897.0 mg) as a yellow solid.

Fraction LA5 (0.088 g) was purified by CC using 50% CH_2Cl_2-hexanes, CH_2Cl_2, and 100% Me_2CO to give **OLA1** (120.3 mg) as a yellow solid.

Fraction LA6 (0.564 g) was shown to be a major spot of **OLA1** as a purple spot on TLC in 100% CH_2Cl_2 mobile phase.

Fractions LA7 and LA8 were combined (11.509 g) and subjected to CC using 10% EtOAc-hexanes and 100% EtOAc to give eleven fractions (LA7-8.1-LA7-8.11). Selected subfractions were further purified by CC or PLC technique as shown in table 3.2.

Table 3.2 Purification of the Subfractions from LA7 and LA8

Subfraction	Technique	Result
LA7-8.1	TLC (30% EtOAc-hexanes)	**OLA1**
LA7-8.2	TLC (30% EtOAc-hexanes)	**OLA1**
LA7-8.3	CC (100% CH_2Cl_2 and 50% Me_2CO-CH_2Cl_2)	Two subfractions (LA7-8.3.1- LA7-8.3.2)
LA7-8.3.1	TLC (100% CH_2Cl_2)	**OLA1** and **OLA2**
LA7-8.3.2	-	**OLA2** (yellow solid, 1.5 mg)
LA7-8.6	CC (5% Me_2CO-hexanes)	Three subfractions (LA7-8.6.1- LA7-8.6.3)
LA7-8.6.1	-	**OLA3** (yellow solid, 2.0 mg)
LA7-8.6.2	TLC (20% EtOAc-hexanes)	**OLA3** and **LOA5**
LA7-8.7	CC (20% EtOAc-benzene and 100% EtOAc)	Nine subfractions (LA7-8.7.1-LA7-8.7.9)
LA7-8.7.2	TLC (30% EtOAc-hexanes)	**OLA3** and **OLA5**
LA7-8.7.3	TLC (30% EtOAc-hexanes)	**OLA3** and **OLA5**
LA7-8.7.4	-	**OLA3** (yellow solid, 14.4 mg)
LA7-8.7.5	TLC (30% EtOAc-hexanes)	**OLA3** and **OLA5**
LA7-8.7.6	PLC (30% EtOAc-benzene)	**OLA3** (yellow solid, 1.0 mg)
LA7-8.7.7	PLC (30% EtOAc-benzene)	**OLA3** (yellow solid, 1.0 mg) **OLA7** (yellow solid, 1.3 mg)

Table 3.2 (continued)

Subfraction	Technique	Result
LA7-8.7.8	TLC (30% EtOAc-hexanes)	**OLA3** and **OLA5**
LA7-8.7.9	CC (10% EtOAc-benzene, EtOAc and 20% Me$_2$CO-EtOAc)	Two subfractions (LA7-8.7.9.1- LA7-8.7.9.2)
LA7-8.7.9.1	-	**OLA3** (yellow solid, 1.7 mg)
LA7-8.7.9.2	TLC (30% EtOAc-hexanes)	**OLA3** and **OLA5**
LA7-8.8	CC (15% EtOAc-hexanes and 100% EtOAc)	Seven subfractions (LA7-8.8.1-LA7-8.8.7)
LA7-8.8.1	-	**OLA3** (yellow solid, 42.2 mg)
LA7-8.8.2	-	**OLA5** (orange solid, 25.5 mg)
LA7-8.8.3	CC (15% EtOAc-benzene and 100% EtOAc)	**OLA3** (yellow solid, 1.0 mg)
LA7-8.8.4	TLC (30% EtOAc-benzene)	**OLA3** and **OLA5**
LA7-8.8.5	-	**OLA5** (orange solid, 9.1 mg)
LA7-8.8.6	CC (15% EtOAc-benzene and 100% EtOAc)	**OLA5** (orange solid, 8.8 mg)
LA7-8.8.6.2	TLC (100% CH$_2$Cl$_2$)	**OLA1**
LA7-8.8.6.3	TLC (30% EtOAc-benzene)	**OLA3**
LA7-8.8.6.4-5.2	TLC (30% EtOAc-benzene)	**OLA3** and **OLA5**
LA7-8.8.6.4-5.3	TLC (35% EtOAc-benzene)	**OLA8**
LA7-8.8.6.4-5.4	TLC (35% EtOAc-benzene)	**OLA5** and **OLA8**
LA7-8.8.7	CC (100% benzene-100% EtOAc)	Three subfractions (LA7-8.8.7.1- LA7-8.8.7.3)
LA7-8.8.7.2	TLC (20% EtOAc-benzene)	**OLA1**
LA7-8.8.7.3	-	**OLA8** (yellow solid, 1.2 mg)
LA7-8.9	PLC (30% EtOAc-benzene)	**OLA5** (orange solid, 8.1 mg)
LA7-8.10	PLC (30% EtOAc-benzene)	**OLA3** (yellow solid, 1.2 mg)
		OLA5 (orange solid, 0.8 mg)
		OLA9 (yellow solid, 1.2 mg)
LA7-8.11	TLC (30% Me$_2$CO-hexanes)	**OLA5**

Fraction LA9 (0.028 g) was crystallized from 50% $Me_2CO-CH_2Cl_2$ to give **OLA3** (10.5 mg) as a yellow solid.

Fraction LA10 (3.473 g) was crystallized from 100% CH_2Cl_2 to give five fractions (LA10.1-LA10.5). Fraction LA10.1 was shown to be a mixture of **OLA1** and **OLA2** on TLC (100% CH_2Cl_2). Fraction LA10.2 was shown to be a mixture of **OLA2** and **OLA3** on TLC (20% Me_2CO-hexanes). Fraction LA10.3 was recrystallized from 100% CH_2Cl_2 to give three subfractions (LA10.3.1-LA10.3.3). Subfraction LA10.3.1 was shown to be a mixture of **OLA1** and **OLA2** on TLC (100% CH_2Cl_2). Subfraction LA10.3.2 was shown to be a mixture of **OLA1**, **OLA2**, **OLA3**, and **OLA5** on TLC (30% EtOAc-hexanes). Subfraction LA10.3.3 yielded **OLA3** (30.0 mg) as a yellow solid. Subfraction LA10.4 afforded **OLA5** (8.4 mg) as an orange solid. Subfraction LA10.5 was recrystallized from 100% CH_2Cl_2 to give two subfractions. The first subfraction was shown to be a mixture of **OLA1**, **OLA2**, **OLA3**, and **OLA5** on TLC (30% EtOAc-hexanes). The second subfraction yielded **OLA5** (79.5 mg) as an orange solid.

Fractions LA11, LA12, LA13, LA14, and LA15 were combined (20.840 g) and purified by CC using 100% hexanes, EtOAc-hexanes, 100% EtOAc, and 30% Me_2CO-EtOAc in a polarity gradient manner to give nine subfractions (LA11-15.1-LA11-15.9). Selected subfractions were further purified by CC or PLC technique as shown in table 3.3.

Table 3.3 Purification of the Subfractions from LA11, LA12, LA13, LA14, and LA15

Subfraction	Technique	Result
LA11-15.1	-	**OLA1** (yellow solid, 118.4 mg)
LA11-15.2	TLC (100% CH_2Cl_2)	**OLA1** and **OLA2**
LA11-15.3	TLC (30% EtOAc-benzene)	**OLA1**, **OLA2**, **OLA3**, and **OLA7**
LA11-15.4	-	**OLA2** (yellow solid, 44.4 mg)
LA11-15.5	TLC (30% EtOAc-hexanes)	**OLA3** and **OLA5**
LA11-15.6	CC (10% EtOAc-CH_2Cl_2 and 100% EtOAc)	Six subfractions (LA11-15.6.1- LA11-15.6.6)
LA11-15.6.1-3	-	**OLA5** (orange solid, 32.8 mg)

Table 3.3 (continued)

Subfraction	Technique	Result
LA11-15.6.4	TLC (35% EtOAc-hexanes)	**OLA5** and **OLA8**
LA11-15.6.5	-	**OLA8** (yellow solid, 1.3 mg)
LA11-15.6.6	TLC (35% EtOAc-benzene)	**OLA8**
LA11-15.7	CC (15% EtOAc-benzene and 100% EtOAc)	Ten subfractions (LA11-15.7.1- LA11-15.7.10)
LA11-15.7.2	-	**OLA1** (yellow solid, 5.0 mg)
LA11-15.7.3	TLC (100% CH_2Cl_2)	**OLA2**
LA11-15.7.4	TLC (30% EtOAc-benzene)	**OLA2** and **OLA3**
LA11-15.7.5	TLC (30% EtOAc-benzene)	**OLA3** and **OLA5**
LA11-15.7.6	TLC (35% EtOAc-benzene)	**OLA3**, **OLA5**, and **OLA9**
LA11-15.7.7	-	**OLA5** (orange solid, 13.4 mg)
LA11-15.7.8	CC (10% EtOAc-benzene and 100% EtOAc)	Six subfractions (LA11-15.7.8.1- LA11-15.7.8.6)
LA11-15.7.8.1	-	**OLA10** (yellow solid, 2.6 mg)
LA11-15.7.8.2	TLC (40% EtOAc-CH_2Cl_2)	**OLA5** and **OLA8**
LA11-15.7.8.3	-	**OLA8** (yellow solid, 2.0 mg)
LA11-15.7.8.4	-	**OLA10** (yellow solid, 12.7 mg)
LA11-15.7.8.5	-	**OLA8** (yellow solid, 1.7 mg)
LA11-15.7.8.6	TLC (40% EtOAc-benzene)	**OLA8** and **OLA9**
LA11-15.7.9	CC (10% EtOAc-CH_2Cl_2 and 100% EtOAc)	Four subfractions (LA11-15.7.9.1- LA11-15.7.9.4)
LA11-15.7.9.1	-	**OLA10** (yellow solid, 24.3 mg)
LA11-15.7.9.2	-	**OLA8** (yellow solid, 1.5 mg)
LA11-15.7.9.3	-	**OLA10** (yellow solid, 8.0 mg)
LA11-15.7.9.4	TLC (35% EtOAc-hexanes)	**OLA3** and **OLA8**
LA11-15.7.10	CC (100% CH_2Cl_2, EtOAc-CH_2Cl_2 and 10% EtOAc)	Two subfractions (LA11-15.7.10.1- LA11-15.7.10.2)
LA11-15.7.10.1	TLC (40% EtOAc-hexanes)	**OLA8** (yellow solid, 5.4 mg)
LA11-15.7.10.2		**OLA8** and **OLA9**
LA11-15.8	PLC (30% EtOAc-benzene)	**OLA3** and **OLA5** **OLA9** (yellow solid, 2.0 mg)

Table 3.3 (continued)

Subfraction	Technique	Result
LA11-15.9	CC (15% EtOAc-hexanes and 100% EtOAc)	Three subfractions (LA11-15.9.1- LA11-15.9.3)
LA11-15.9.1	PLC (30% EtOAc-benzene)	**OLA5** (orange solid, 0.8 mg)
LA11-15.9.2	TLC (30% EtOAc-benzene)	**OLA5** and **OLA9**
LA11-15.9.2	-	**OLA5** (orange solid, 48.3 mg)

Fraction LA16 (0.0356 g) was crystallized from 100% CH_2Cl_2 to give a yellow solid, which was a mixture of **OLA3** and **OLA5**.

Fraction LA17 (5.0350 g) was shown to be a major spot of **OLA5** as a green viscous liquid.

3.4 Chemical Investigation of the *Oroxylum indicum* Roots

3.4.1 Extraction, Isolation, and Purification

The dried roots of *O. indicum* (3.460 kg) were chopped and immersed at room temperature in CH_2Cl_2 (10.5 L, 7 days) and Me_2CO (17 L, 7 days), respectively, to give, after evaporation, the CH_2Cl_2 extract (crude RD, 22.110 g) and acetone extract (crude RA, 21.060 g). The process of extraction was shown in figure 3.3.
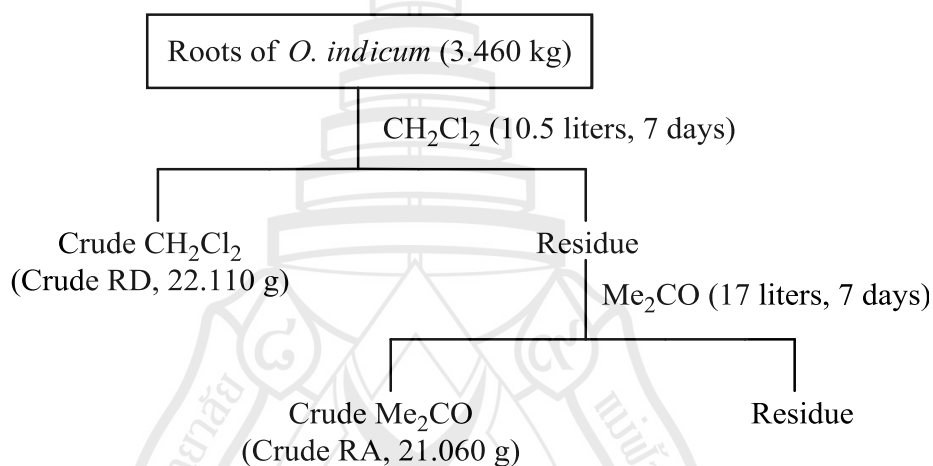
Figure 3.3 Extraction of Crudes RD and RA from the Roots of *O. indicum*

Crude RD (22.110 g) was subjected to QCC over silica gel and gradiently eluted with hexanes, hexanes-CH_2Cl_2, CH_2Cl_2 and 20% Me_2CO-CH_2Cl_2. The collected fractions were combined according to the characteristic on TLC and evaporated to give fifteen fractions (RD1-RD15), as shown in table 3.4. The selected fractions were further purified as shown in figure 3.4.

Table 3.4 Physical Characteristic and Weight of Fractions obtained from Crude RD

Fraction	Weight (g)	Physical Characteristic
RD1	0.345	Green viscous liquid
RD2	0.294	Yellow viscous liquid
RD3	0.506	Orange viscous liquid
RD4	0.291	Yellow solid
RD5	0.757	Yellow viscous liquid
RD6	1.426	Green viscous liquid
RD7	0.392	Yellow solid
RD8	0.276	Yellow solid
RD9	1.479	Yellow solid
RD10	6.161	Yellow solid
RD11	1.171	Yellow solid
RD12	0.462	Yellow solid
RD13	0.110	Yellow solid
RD14	0.631	Orange solid
RD15	1.318	Brown viscous liquid

Crude RD (22.110 g)

QCC (hexanes, hexanes-CH$_2$Cl$_2$, CH$_2$Cl$_2$ and 20% Me$_2$CO- CH$_2$Cl$_2$)

RD1 .... RD4 .... RD6 | RD7 | RD8 | RD9 | RD10 | RD11 | RD12 | RD13 | RD14 | RD15

- RD1 ... RD4 ... RD6 → CC → **ORD1** (23.5 mg)
- RD6 → TLC → SOI2
- RD7 → Crys. → **OLA1** (20.7 mg)
- RD8 → Crys. → **OLA1** (50.1 mg)
- RD9 → Crys. → RD9.1, RD9.2
  - RD9.1 → TLC → **OLA1 + OLA2**
- RD10 → Crys. → RD10.1, RD10.2
  - RD10.1 → TLC → **OLA1 + OLA2**
  - RD10.2 → TLC → **OLA1 + OLA2 + OLA3**
- RD11 → Crys. → RD11.1, RD11.2
  - RD11.1 → TLC → **OLA1 + OLA2**
- RD12 → Crys. → RD12.1, RD12.2
  - RD12.1 → TLC → **OLA1 + OLA2**
  - RD12.2 → TLC → **OLA1 + OLA2 + OLA3 + OLA8 + ORD2 + ORD3**
- RD13 → Crys. → RD13.1, RD13.2
  - RD13.1 → TLC → **OLA1 + OLA2 + OLA3**
- RD14 → Crys. → RD14.1, RD14.2
  - RD14.1 → TLC → **OLA3 + OLA5**
  - RD14.2 → CC → RD14.2.1, RD14.2.2
- RD15 → TLC → **OLA5 + OLA8 + OLA9**

RD9.2 → CC → RD9.2.1, RD9.2.2, RD9.2.3, RD9.2.4, RD9.2.5
- RD9.2.1 → TLC → **OLA1**
- RD9.2.2 → TLC → **OLA1** (23.8 mg)
- RD9.2.3 → PLC → **ORD4** (4.6 mg)
- RD9.2.4 → TLC → **OLA1 + OLA3**
- RD9.2.5 → TLC → **OLA1 + OLA1**

RD11.2 → CC → RD11.2.1, RD11.2.2, RD11.2.3, RD11.2.4, RD11.2.5, RD11.2.6, RD11.2.7
- RD11.2.1 → TLC → **ORD2** (1.0 mg)
- RD11.2.2 → TLC → **ORD2 + ORD3 + OLA1**
- RD11.2.3 → TLC → **OLA1 + OLA2**
- RD11.2.4 → TLC → **OLA1 + OLA3 + OLA8**
- RD11.2.5 → TLC → **OLA1 + OLA8**
- RD11.2.6 → TLC → **OLA1 + OLA8**
- RD11.2.7 → **OLA8** (1.9 mg)

RD13.2 → CC → RD13.2.1, RD13.2.2, RD13.2.3, RD13.2.4, RD13.2.5, RD13.2.6, RD13.2.7, RD13.2.8, RD13.2.9, RD13.2.10
- RD13.2.2 → **ORD2** (1.9 mg)
- RD13.2.3 → TLC → **OLA1**
- RD13.2.4 → TLC → **OLA1**
- RD13.2.5 → TLC → **OLA1 + OLA2**
- RD13.2.6 → TLC → **OLA3 + OLA7**
- RD13.2.7 → TLC → **OLA5 + OLA7**
- RD13.2.8, RD13.2.9 → PLC → RD13.2.8-9.1, RD13.2.8-9.2, RD13.2.8-9.3
  - RD13.2.8-9.1 → TLC → **OLA3 + OLA5**
  - RD13.2.8-9.2 → **OLA5** (1.8 mg)

RD14.2.2 → CC → RD14.2.2.1, RD14.2.2.2, RD14.2.2.3, RD14.2.2.4
- RD14.2.1 → TLC → **OLA1 + OLA2 + OLA3 + OLA5**
- RD14.2.2.3 → TLC → **OLA1 + OLA5 + OLA9**
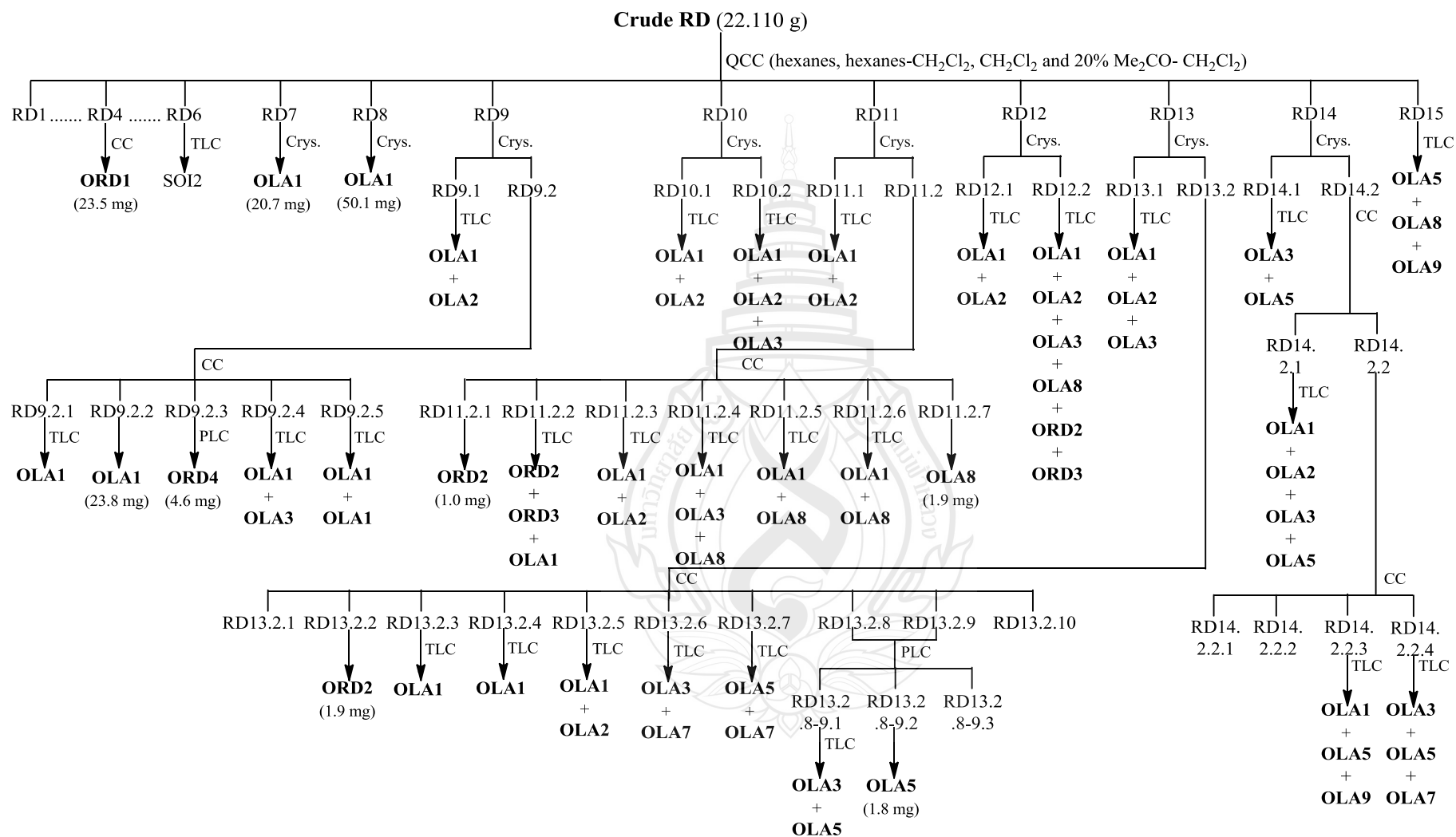- RD14.2.2.4 → TLC → **OLA3 + OLA5 + OLA7**

Figure 3.4 Isolation of Pure Compounds from Crude RD of *O. indicum*

36

Fraction RD4 (0.291 g) was subjected to CC and gradiently eluted with hexanes, hexanes-CH_2Cl_2 and CH_2Cl_2 to give three subfractions (RD4.1-RD4.3). Subfraction RD4.2 yielded **ORD1** (23.5 mg) as a white solid.

Fraction RD6 (1.426 g) was shown to be a major spot of **OLA2** on TLC (100% CH_2Cl_2).

Fractions RD7 (0.392 g) and RD8 (0.276 g) were crystallized from 40% CH_2Cl_2-hexanes to give a yellow solid of **OLA1** (20.7 mg and 50.1 mg, respectively).

Fraction RD9 (1.479 g) was crystallized from 40% CH_2Cl_2-hexanes to give a solid (RD9.1) and a filtrate (RD9.2). Selected subfractions were further purified by CC and PLC techniques as shown in table 3.5.

Table 3.5 Purification of the Subfractions from RD9

Subfraction	Technique	Result
RD9.1	TLC (100% CH_2Cl_2)	**OLA1** and **OLA2**
RD9.2	CC (10% EtOAc-benzene and 100% EtOAc)	Five subfractions (RD9.2.1-RD9.2.5)
RD9.2.1	TLC (100% CH_2Cl_2)	**OLA1**
RD9.2.2	-	**OLA1** (yellow solid, 23.8 mg)
RD9.2.3	PLC (30% EtOAc-benzene)	**ORD4** (yellow viscous liquid, 4.6 mg)
RD9.2.4	TLC (15% EtOAc-benzene)	**OLA1** and **OLA3**
RD9.2.5	TLC (15% EtOAc-benzene)	**OLA1** and **OLA3**

Fraction RD10 (6.161 g) was crystallized from 20% Me_2CO-CH_2Cl_2 to yield a yellow solid (RD10.1) which was shown to be a charateristic of **OLA1** and **OLA2** on TLC (100% CH_2Cl_2). The filtrate (RD10.2) was shown to be a mixture of **OLA1**, **OLA2**, and **OLA3** on TLC (15% Me_2CO-hexanes).

Fraction RD11 (1.171 g) was crystallized from 20% Me_2CO-CH_2Cl_2 to give a solid (RD11.1) and a filtrate (RD11.2). The filtrate was purified by CC using 10% EtOAc-benzene and 100% EtOAc in a polarity gradient manner to give seven subfractions (RD11.2.1-RD11.2.7), as shown in table 3.6.

Table 3.6 Purification of the Subfractions from RD11

Subfraction	Technique	Result
RD11.2.1	-	**ORD2** (yellow solid, 1.0 mg)
RD11.2.2	TLC (100% CH_2Cl_2)	**ORD2**, **ORD3**, and **OLA1**
RD11.2.3	TLC (100% CH_2Cl_2)	**OLA1** and **OLA2**
RD11.2.4	TLC (30% EtOAc-benzene)	**OLA1**, **OLA3**, and **OLA8**
RD11.2.5	TLC (30% EtOAc-benzene)	**OLA1** and **OLA8**
RD11.2.6	TLC (30% EtOAc-benzene)	**OLA1** and **OLA8**
RD11.2.7	-	**OLA8** (yellow solid, 1.9 mg)

Fraction RD12 (0.462 g) was crystallized from 30% $Me_2CO-CH_2Cl_2$ to afford a mixture of a solid (RD12.1) of **OLA1** and **OLA2** on TLC (100% CH_2Cl_2). The filtrate (RD12.2) was shown to be a mixture of **OLA1**, **OLA2**, **OLA3**, **OLA8**, **ORD2**, and **ORD3** on TLC (15% EtOAc-benzene).

Fraction RD13 (0.110 g) was crystallized from 30% $Me_2CO-CH_2Cl_2$ to give a solid (RD13.1) and a filtrate (RD13.2). Selected subfractions were further purified by CC and PLC techniques as shown in table 3.7

Table 3.7 Purification of the Subfractions from RD13

Subfraction	Technique	Result
RD13.1	10% $Me_2CO-CH_2Cl_2$	**OLA1**, **OLA2**, and **OLA3**
RD13.2	CC (10% EtOAc-benzene and 100% EtOAc)	Ten subfractions (RD13.2.1-RD13.2.10)
RD13.2.2	PLC (30% EtOAc-benzene)	**ORD2** (yellow solid, 1.9 mg)
RD13.2.3	TLC (100% CH_2Cl_2)	**OLA1**
RD13.2.4	TLC (100% CH_2Cl_2)	**OLA1**
RD13.2.5	TLC (100% CH_2Cl_2)	**OLA1** and **OLA2**
RD13.2.6	TLC (30% EtOAc-hexanes)	**OLA3** and **OLA7**
RD13.2.7	TLC (30% EtOAc-hexanes)	**OLA5** and **OLA7**

Table 3.7 (continued)

Subfraction	Technique	Result
RD13.2.8-9	PLC (30% EtOAc-benzene)	**SOI3** and **LOA5**
		OLA5 (orange solid, 1.8 mg)

Fraction RD14 (0.631 g) was crystallized from 40% $Me_2CO-CH_2Cl_2$ to afford a solid (RD14.1) and a filtrate (RD14.2). The filtrate was purified by CC and gradiently eluted with 15% Me_2CO-hexanes and 100% Me_2CO to give two subfractions (RD14.2.1 and RD14.2.2). Selected subfractions were further purified by CC and PLC techniques as shown in table 3.8

Table 3.8 Purification of the Subfractions from RD14

Subfraction	Technique	Result
RD14.1	TLC (20% $Me_2CO-CH_2Cl_2$)	**OLA3** and **OLA5**
RD14.2.1	TLC (20% EtOAc-benzene)	**OLA1**, **OLA2**, **OLA3**, and **OLA5**
RD14.2.2	CC (15% EtOAc-benzene and 100% EtOAc)	Four subfractions (RD14.2.2.1-RD14.2.2.4)
RD14.2.2.3	TLC (30% EtOAc-benzene)	**OLA3**, **OLA5**, and **OLA9**
RD14.2.2.4	TLC (30% EtOAc-benzene)	**OLA3**, **OLA5**, and **OLA7**

Fraction RD15 (1.318 g) was displayed to be a characteristic of **OLA5**, **OLA8**, and **OLA9** on TLC (35% EtOAc-hexanes).

Crude RA (20.000 g) was subjected to CC using hexanes, hexanes-EtOAc, and EtOAc in a polarity gradient manner. The collected fractions were combined according to the characteristic on TLC and evaporated to give sixteen fractions (RA1-RA16) as shown in table 3.9. The selected fractions were further purified as shown in figure 3.5.

Table 3.9 Physical Characteristic and Weight of Fractions obtained from Crude RA

| Fraction	Weight (g)	Physical characteristic
RA1	0.010	Green viscous liquid
RA2	0.041	Yellow viscous liquid
RA3	0.167	Orange viscous liquid
RA4	0.151	Yellow solid
RA5	0.103	Yellow viscous liquid
RA6	0.053	Green viscous liquid
RA7	0.276	Yellow solid
RA8	0.102	Yellow solid
RA9	0.076	Yellow solid
RA10	0.036	Yellow solid
RA11	0.031	Yellow solid
RA12	0.016	Yellow solid
RA13	0.302	Yellow solid
RA14	0.024	Orange solid
RA15	1.655	Brown viscous liquid
RA16	2.591	Brown viscous liquid
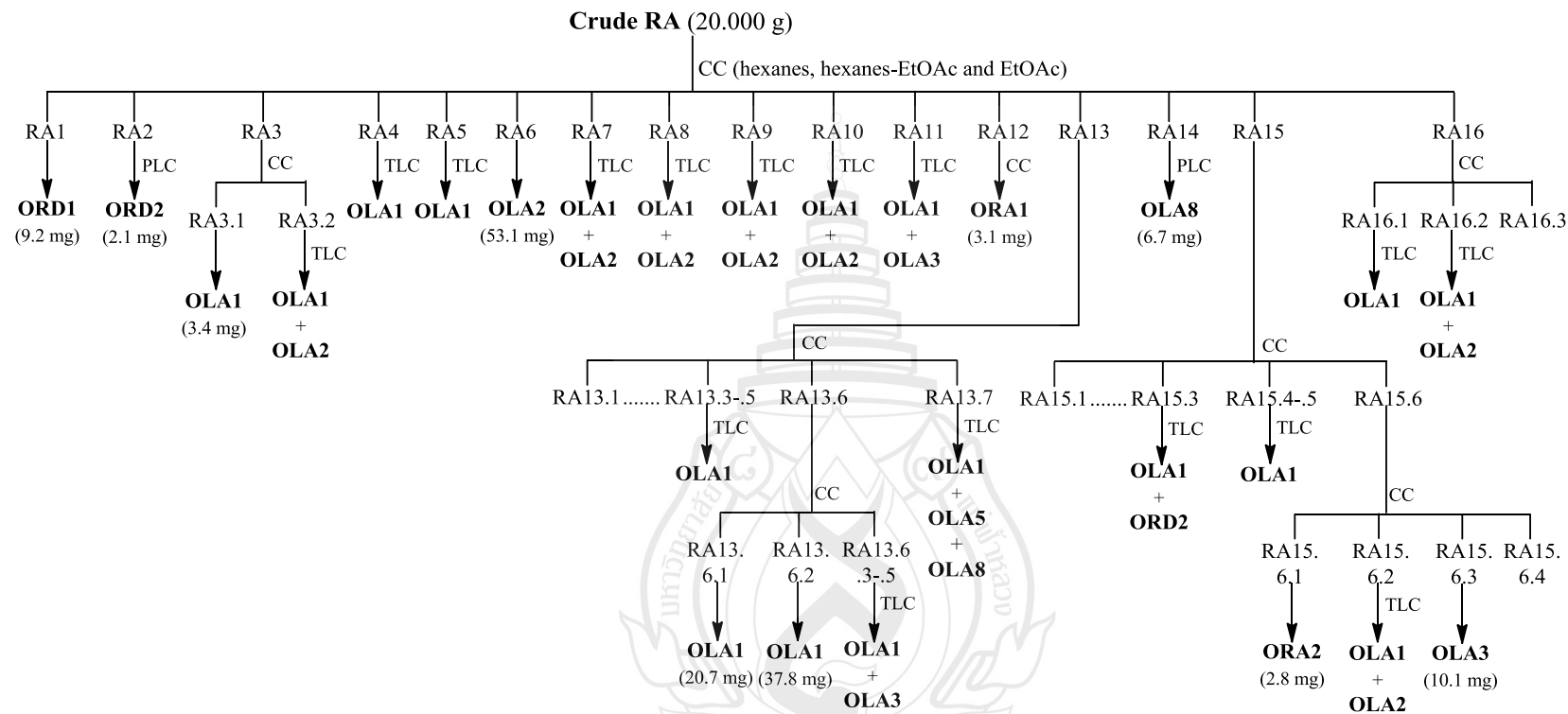
Figure 3.5 Isolation of Pure Compounds from Crude RA of *O. indicum*

Fraction RA1 (0.010 g) yielded **ORD1** (9.2 mg) as a white solid.

Fraction RA2 (0.041 g) was separated by PLC using 30% EtOAc-benzene as the developing solvent to give **ORD2** (2.1 mg) as a yellow solid.

Fraction RA3 (0.1673 g) was purified by CC and gradiently eluted with 100% CH_2Cl_2 up to 50% EtOAc-CH_2Cl_2 to give two subfractions (RA3.1 and RA3.2). The first subfraction yielded **OLA1** (3.4 mg) as a yellow solid. The second subfraction was shown to be a mixture of **OLA1** and **OLA2** on TLC (100% CH_2Cl_2).

Fractions RA4 (0.151 g) and RA5 (0.103 g) were shown to be a major spot of **OLA1** on TLC (100% CH_2CL_2).

Fraction RA6 (0.0531 g) afforded **OLA2** as a yellow solid.

Fractions RA7 (0.276 g), RA8 (0.102 g), RA9 (0.076 g), and RA10 (0.036 g) were displayed to be a mixture of **OLA1** and **OLA2** on TLC (100% CH_2Cl_2).

Fraction RA11 (0.0312 g) was displayed to be a characteristic of **OLA1** and **OLA3** on TLC (20% EtOAc-CH_2CL_2).

Fraction RA12 (0.016 g) was purified by CC using 5% EtOAc-hexanes and 100% EtOAc as the developing solvent to give **ORA1** (3.1 mg) as a yellow solid.

Fraction RA13 (0.302 g) was purified by CC and gradiently eluted with 15% EtOAc-benzene and 100% EtOAc to give seven subfractions (RA13.1-RA13.7), as shown in table 3.10.

Table 3.10 Purification of the Subfractions from RA13

Subfraction	Technique	Result
RA13.3-5	TLC (100% CH_2Cl_2)	**OLA1**
RA13.6	CC (10% EtOAc-hexanes)	Five subfractions (RA13.6.1-RA13.6.5)
RA13.6.1	-	**OLA1** (yellow solid, 20.7 mg)
RA13.6.2	-	**OLA1** (yellow solid, 37.8 mg)
RA13.6.3-5	TLC (20% EtOAc-CH_2Cl_2)	**OLA1** and **OLA3**
RA13.7	TLC (35% EtOAc-benzene)	**OLA1**, **OLA5**, and **OLA8**

Fraction RA14 (0.024 g) was separated by PLC using 10% Me_2CO-CH_2Cl_2 as the developing solvent to yield **OLA8** (6.7 mg) as a yellow solid.

Fraction RA15 (1.655 g) was purified by CC with gradiently eluted with 15% EtOAc-benzene and 100% EtOAc to give six subfractions (RA15.1-RA15.6), as shown in table 3.11.

Table 3.11 Purification of the Subfractions from RA15

Subfraction	Technique	Result
RA15.3	TLC (100% CH_2Cl_2)	**OLA1** and **ORD2**
RA15.4	TLC (100% CH_2Cl_2)	**OLA1**
RA15.5	TLC (100% CH_2Cl_2)	**OLA1**
RA15.6	CC (15% EtOAc-hexanes)	Four subfractions (RA15.6.1-RA15.6.4)
RA15.6.1	-	**ORA2** (yellow solid, 2.8 mg)
RA15.6.2	TLC (100% CH_2Cl_2)	**OLA1** and **OLA2**
RA15.6.3	-	**OLA3** (orange solid, 10.1 mg)

Fraction RA16 (2.591 g) was separated by CC and gradiently eluted with 5% EtOAc-benzene up to 100% EtOAc to give three subfractions (RA16.1-RA16.3). Fraction RA16.1 was shown to be a major spot of **OLA1** on TLC (100% CH_2Cl_2). Fraction RA16.2 was displayed to be a mixture of **OLA1** and **OLA2** on TLC (100% CH_2Cl_2).

3.5 Chemical Investigation of the *Oroxylum indicum* Stems

3.5.1 Extraction, Isolation, and Purification

The stems of *O. indicum* (11.870 kg) were dried, chopped and extracted with Me_2CO (20 L, 7 days) and MeOH (20 L, 7 days) at room temperature, respectively. Removal of the solvents from each extract under reduced pressure to give the acetone extract (crude SA, 44.540 g) and methanolic extract (crude SM, 615.280 g), as shown in figure 3.6.
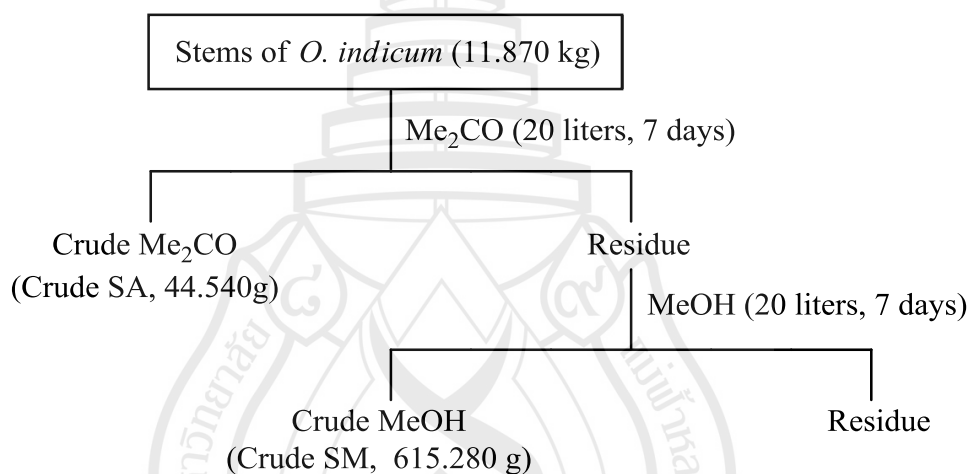
Figure 3.6 Extraction of Crudes SA and SM from the Stems of *O. indicum*

Crude SA (10.100 g) was separated by QCC using hexanes-CH_2Cl_2, CH_2Cl_2 CH_2Cl_2-Me_2CO, and Me_2CO in a polarity gradient manner. The collected fractions were combined according to the characteristic on TLC and evaporated to give twelve fractions (SA1-SA12) as shown in table 3.12. The selected fractions were further purified as shown in figure 3.7.

Table 3.12 Physical Characteristic and Weight of Fractions obtained from Crude SA

Fraction	Weight (g)	Physical characteristic
SA1	0.895	Orange viscous liquid
SA2	0.520	Yellow solid
SA3	0.700	Yellow solid
SA4	0.930	Brown viscous liquid
SA5	0.290	Brown viscous liquid
SA6	1.500	Green viscous liquid
SA7	0.250	Green viscous liquid
SA8	0.140	Green viscous liquid
SA9	0.196	Brown viscous liquid
SA10	0.032	Brown viscous liquid
SA11	0.070	Yellow solid
SA12	1.950	Brown viscous liquid

Crude SA (10.100 g)

QCC (hexanes-CH$_2$Cl$_2$, CH$_2$Cl$_2$-Me$_2$CO and Me$_2$CO)

SA1 — CC

SA2 — CC

SA3 — CC

SA4 — CC

SA5 — TLC

SA6 — CC

OLA1 + OLA2 (from SA5)

SA1.1 SA1.2 — CC SA1.3 — TLC SA1.4 SA1.5 — TLC SA1.6

OSA1 (10.0 mg)
OSA1 + ORD3
OLA1 (13.7 mg)
OLA1 + OLA2
OLA2 (15.8 mg)

SA2.1 — TLC SA2.2

OLA1 + OLA2
OLA1 (20.2 mg)

SA3.1 — TLC SA3.2 SA3.3 — TLC SA3.4 — TLC SA3.5 SA3.6 — TLC SA3.7 — TLC SA3.8

OLA1
OLA1 (96.6 mg)
OLA1 + OLA2
OLA1 + OLA2
OLA1 (28.7 mg)
OLA2
OLA2
OLA2 (7.3 mg)

SA4.1 — TLC SA4.2 SA4.3 — Crys.

OLA1
OLA1 (81.9 mg)

SA4.3.1 SA4.3.2 — TLC

OLA1
OLA1 (73.4 mg)

SA6.1 — CC

SA6.2 — TLC

SA6.3 — CC

SA6.4

OLA1 + OLA3 (from SA6.2)

SA6.1.1 — TLC SA6.1.2 — CC SA6.1.3 — TLC SA6.1.4 — PLC SA6.1.5 — Crys. SA6.1.6 — CC SA6.1.7 SA6.1.8 — TLC SA6.1.9 — CC

OLA1
OLA1 (25.0 mg)
OLA1 + OLA2 (7.0 mg)
OLA1
OLA1 + OLA2

SA6.1.6.1
OLA2 (25.1 mg)

SA6.1.6.2 — CC

OLA2 (95.7 mg)
OLA1 + OLA2

SA6.1.9.1 SA6.1.9.2 SA6.1.9.3 SA6.1.9.4 — PLC

OLA1 (56.8 mg) **OLA1** (6.0 mg)

SA6.1.9.5 — CC SA6.1.9.6 SA6.1.9.7

SA6.3.1 SA6.3.2 — TLC SA6.3.3 SA6.3.3

OLA1 (6.3 mg)
OLA1 + OLA2
OLA2 (2.4 mg)
OSA3 (2.6 mg)

SA6.1.6.2.1 — TLC SA6.1.6.2.2 — TLC

OLA3 + OLA5
OLA2

PLC

SA6.1.9.2.1 SA6.1.9.2.2 — TLC SA6.1.9.2.3 — TLC SA6.1.9.2.4

OLA1 (2.3 mg)
OLA1 + OLA3
OLA1 + OLA5
OLA5 (1.5 mg)

SA6.1.9.5.1 — CC

OLA1 (6.0 mg)
OLA5 (45.4 mg)
OLA8 (5.3 mg)
OLA9 (1.1 mg)

SA6.1.9.5.2 — PLC

OLA1 (3.2 mg)
OLA5 (7.1 mg)
OLA7 (6.5 mg)

SA6.1.9.5.3 — PLC

SA6.1.9.5.3.1 SA6.1.9.5.3.2 — TLC SA6.1.9.5.3.3 SA6.1.9.5.3.4 — TLC

OLA1 (13.6 mg)
OLA1 + OLA5
OLA8 (1.2 mg)
OLA8 + OLA9

Figure 3.7 Isolation of Pure Compounds from Crude SA of *O. indicum*

46

Crude SA (10.100 g)

QCC (hexanes-CH$_2$Cl$_2$, CH$_2$Cl$_2$-Me$_2$CO and Me$_2$CO)

SA7 — CC
SA8 — CC
SA9 — CC
SA10 — Crys. CC
SA11 — CCx2
SA12

SA7.1 — PLC
SA7.2 — Crys.
SA7.3
SA7.4 — TLC
SA8.1 — CC Crys.
SA8.2
SA9.1 SA9.2 SA9.3 SA9.4-5 SA9.6
SA10.2.1 — TLC
SA10.2.2 — PLC
SA11.1 — CC
SA11.2 — CC TLC

SA7.1.1 — PLC
SA7.1.2
filtrate
OLA3 (5.5 mg)
OLA3 + **OLA5**
OLA3 (2.4 mg)
OLA3 (5.4 mg)
OLA8 (3.2 mg)
OLA3 + **OLA5**
OSA2 (3.9 mg)
OSA5 (5.0 mg)
OLA3 + **OLA5**

OSA2 (0.9 mg)
OLA3 (47.2 mg)
OLA3 (1.4 mg)
OLA3 + **OLA5** (TLC)

PLC
PLC
PLC

SA8.2.1 SA8.2.2 — TLC SA8.2.3
SA9.3.1 — TLC SA9.3.2
SA9.4-.5.1 SA9.4-.5.2 SA9.4-.5.3 — TLC SA9.4-.5.4 — TLC SA9.4-.5.5 — TLC

OLA1 (3.1 mg)
OLA1 + **OLA2**
OLA3 + **OLA5**
OLA7 (1.7 mg)
OSA2 (1.5 mg)
OSA4 (2.6 mg)
OLA5 + **OLA8**
OLA8
OLA8

Figure 3.7 (continued)

47

Fraction SA1 (0.895 g) was purified by CC and gradiently eluted with 50% CH$_2$Cl$_2$-hexanes, CH$_2$Cl$_2$, 80% Me$_2$CO-CH$_2$Cl$_2$ to give six subfractions (SA1.1-SA1.6). Fraction SA1.2 was purified by CC and eluted with 100% hexanes to give **OSA1** (10.0 mg) as a white solid. Fraction SA1.3 was shown to be a mixture of **OSA1** and **ORD3** on TLC (100% hexanes). Fraction SA1.4 yielded **OLA1** (13.7 mg) as a yellow solid. Fraction SA1.5 was shown to be a mixture of **OLA1** and **OLA2** on TLC (100% CH$_2$Cl$_2$). Fraction SA1.6 afforded **OLA2** (15.8 mg) as a yellow solid.

Fraction SA2 (0.520 g) was subjected to CC using 50% CH$_2$Cl$_2$-hexanes, CH$_2$Cl$_2$, and 100% Me$_2$CO in a polarity gradient manner to afford two subfractions (SA2.1-SA2.2). Fraction SA2.1 was shown to be a mixture spot of **OLA1** and **OLA2** on TLC (100% CH$_2$Cl$_2$). Fraction SA2.2 yielded **OLA1** (20.2 mg) as a yellow solid.

Fraction SA3 (0.700 g) was purified by CC using 50% CH$_2$Cl$_2$-hexanes, CH$_2$Cl$_2$, and 100% Me$_2$CO as an eluent to give eight subfractions (SA3.1-SA3.8). Fraction SA3.1 was shown to be a major spot of **OLA1** on TLC (100% CH$_2$Cl$_2$). Fraction SA3.2 afforded **OLA1** (96.6 mg) as yellow solid. Fractions SA3.3 and SA3.4 were displayed to be a characteristic of **OLA1** and **OLA2** on TLC (100% CH$_2$Cl$_2$). Fraction SA3.5 yielded **OLA1** (28.7 mg) as a yellow solid. Fractions SA3.6 and SA3.7 were shown to be a major spot of **OLA2** on TLC (100% CH$_2$Cl$_2$). Fraction SA3.8 yielded **OLA2** (7.3 mg) as a yellow solid.

Fraction SA4 (0.930 g) was purified by CC and gradiently eluted with 50% CH$_2$Cl$_2$-hexanes, CH$_2$Cl$_2$, Me$_2$CO-CH$_2$Cl$_2$ and 100% Me$_2$CO to give three fractions (SA4.1-SA4.3). Fraction SA4.1 was shown to be a major spot of **OLA1** on TLC (100% CH$_2$Cl$_2$). Fraction SA4.2 yielded **OLA1** (81.9 mg) as a yellow solid. Fraction SA4.3 was crystallized from 50% Me$_2$CO-CH$_2$Cl$_2$ to give a solid (SA4.3.1) which yielded **OLA1** (73.4 mg) as a yellow solid. The filtrate (SA4.3.2) was displayed to be a major spot of **OLA1** on TLC (100% CH$_2$Cl$_2$).

Fraction SA5 (0.290 g) was displayed to be a mixture of **OLA1** and **OLA2** on TLC (100% CH$_2$Cl$_2$).

Fraction SA6 (1.500 g) was subjected to CC with 50% CH$_2$Cl$_2$-hexanes, CH$_2$Cl$_2$, 100% Me$_2$CO to give four fractions (SA6.1-SA6.4). Selected subfractions were further purified by CC and PLC techniques as shown in table 3.13.

Table 3.13 Purification of the Subfractions from SA6

Subfraction	Technique	Result
SA6.1	CC (CH$_2$Cl$_2$-hexanes, CH$_2$Cl$_2$, Me$_2$CO-CH$_2$Cl$_2$, and 100% Me$_2$CO)	Nine fractions (SA6.1.1-SA6.1.9)
SA6.1.1	100% CH$_2$Cl$_2$	**OLA1**
SA6.1.2	CC (30% EtOAc-benzene)	**OLA1** (yellow solid, 25.0 mg)
SA6.1.3	TLC (100% CH$_2$Cl$_2$)	**OLA1** and **OLA2**
SA6.1.4	PLC (30% EtOAc-benzene)	**OLA1** (yellow solid, 7.0 mg)
SA6.1.5	TLC (100% CH$_2$Cl$_2$)	**OLA1** and **OLA2**
SA6.1.6	CC (CH$_2$Cl$_2$, CH$_2$Cl$_2$-Me$_2$CO, and Me$_2$CO)	Two subfractions (SA6.1.6.1 and SA6.1.6.2)
SA6.1.6.1	-	**OLA2** (yellow solid, 25.1 mg)
SA6.1.6.2	CC (hexanes, hexanes-EtOAc, and EtOAc)	Two subfractions (SA6.1.6.2.1 and SA6.1.6.2.2)
SA6.1.6.2.1	TLC (30% EtOAc-hexanes)	**OLA3** and **OLA5**
SA6.1.6.2.2	TLC (100% CH$_2$Cl$_2$)	**OLA2**
SA6.1.7	-	**OLA2** (yellow solid, 95.7 mg)
SA6.1.8	TLC (100% CH$_2$Cl$_2$)	**OLA1** and **OLA2**
SA6.1.9	CC (10% EtOAc-benzene and 100% EtOAc)	Seven subfractions (SA6.1.9.1-SA6.1.9.7)
SA6.1.9.2	PLC (30% EtOAc-benzene)	**OLA1** (yellow solid, 2.3 mg)
		OLA1 and **OLA3**
		OLA1 and **OLA5**
		OLA5 (orange solid, 1.5 mg)
SA6.1.9.3	-	**OLA1** (yellow solid, 56.8 mg)
SA6.1.9.4	PLC (30% EtOAc-benzene)	**OLA1** (yellow solid, 6.0 mg)
SA6.1.9.5	CC (15% EtOAc-benzene and 100% EtOAc)	Three subfractions (SA6.1.9.5.1-SA6.1.9.5.3)
SA6.1.9.5.1	CC (10% EtOAc-benzene and 100% EtOAc)	**OLA1** (yellow solid, 30.3 mg)
		OLA5 (orange solid, 45.4 mg)
		OLA8 (yellow solid, 5.3 mg)
		OLA9 (yellow solid, 1.1 mg)

Table 3.13 (continued)

Subfraction	Technique	Result
SA6.1.9.5.2	PLC (30% EtOAc-benzene)	**OLA1** (yellow solid, 3.2 mg)
		OLA5 (orange solid, 7.1 mg)
		OLA7 (yellow solid, 6.5 mg)
SA6.1.9.5.3	PLC (30% EtOAc-benzene)	Four subfractions
		(SA6.1.9.5.3.1-SA6.1.9.5.3.4)
SA6.1.9.5.3.1	-	**OLA1** (yellow solid, 13.6 mg)
SA6.1.9.5.3.2	TLC (20% EtOAc-benzene)	**OLA1** and **OLA5**
SA6.1.9.5.3.3	-	**OLA8** (yellow solid, 1.2 mg)
SA6.1.9.5.3.4	TLC (40% EtOAc-benzene)	**OLA8** and **OLA9**
SA6.2	TLC (20% EtOAc-hexanes)	**OLA1**, **OLA2**, and **OLA3**
SA6.3	PLC (30% EtOAc-benzene)	Four fractions
		(SA6.3.1-SA6.3.4)
SA6.3.1	-	**OLA1** (yellow solid, 6.3 mg)
SA6.3.2	TLC (100% CH_2Cl_2)	**OLA1** and **OLA2**
SA6.3.3	-	**OSA3** (yellow solid, 2.6 mg)

Fraction SA7 (0.250 g) was purified by CC using 50% CH_2Cl_2-hexanes to 100% Me_2CO in a polarity gradient manner to give four subfractions (SA7.1-SA7.4). Fraction SA7.1 was purified by PLC to give two subfractions (SA7.1.1 and SA7.1.2). Fraction SA7.1.1 was reseparated by PLC using 30% EtOAc-benzene as the developing solvent to give **OSA2** (0.9 mg) as a yellow solid. Fraction SA7.1.2 yielded **OLA3** (47.2 mg) as a yellow solid. Fraction SA7.2 was crystallized from 100% Me_2CO to give a yellow solid of **OLA3** (1.4 mg) and the filtrate was shown to be a mixture of **OLA3** and **OLA5** on TLC (30% EtOAc-benzene). Fraction SA7.3 yielded **OLA3** (5.5 mg) as a yellow solid. Fraction SA7.4 was shown to be a mixture of **OLA3** and **OLA5** on TLC (30% EtOAc-benzene).

Fraction SA8 (0.140 g) was purified by CC and gradiently eluted with 50% CH_2Cl_2-hexanes and 100% Me_2CO to give two fractions (SA8.1 and SA8.2). Fraction SA8.1 was purified by CC with 100% CH_2Cl_2 and CH_2Cl_2-Me_2CO in a polarity gradient manner to give two subfractions. The first subfraction was crystallized from

100% Me$_2$CO to afford **OLA3** (2.4 mg) as a yellow solid. Fraction SA8.2 was purified by PLC using 30% EtOAc-benzene to give three fractions (SA8.2.1-SA8.2.3). Fraction SA8.2.1 yielded **OLA1** (3.1 mg) as a yellow solid. Fraction SA8.2.2 was shown to be a mixture of **OLA1** and **OLA2** on TLC (10% EtOAc-hexanes).

Fraction SA9 (0.196 g) was subjected to CC and gradiently eluted with 15% EtOAc-benzene and 100% EtOAc to give six fractions (SA9.1-SA9.6). Selected subfractions were further purified by CC and PLC techniques as shown in table 3.14.

Table 3.14 Purification of the Subfractions from SA9

Subfraction	Technique	Result
SA9.2	-	**OLA1** (yellow solid, 5.4 mg)
SA9.3	PLC (30% EtOAc-benzene)	**OLA3** and **OLA5**
		OLA7 (yellow solid, 1.8 mg)
SA9.4-5	PLC (30% EtOAc-benzene)	**OSA2** (yellow solid, 1.5 mg)
		OSA4 (yellow solid, 2.6 mg)
SA9.4-5.3	TLC (30% EtOAc-benzene)	**OLA5** and **OLA8**
SA9.4-5.4	TLC (30% EtOAc-benzene)	**OLA8**
SA9.4-5.5	TLC (30% EtOAc-benzene)	**OLA8**
SA9.6	-	**OLA8** (yellow solid, 3.2 mg)

Fraction SA10 (0.032 g) was crystallized from 100% Me$_2$CO and rechromatographed on CC and gradiently eluted with 50% CH$_2$Cl$_2$-hexanes and 100% Me$_2$CO to give two fractions (SA10.2.1 and SA10.2.2). Fraction SA10.2.1 was shown to be a mixture of **OLA3** and **OLA5** on TLC (20% EtOAc-hexanes). Fraction SA10.2.2 was reseparated by PLC using 30% EtOAc-benzene as the mobile phase to afford **OSA2** (3.9 mg) as a yellow solid.

Fraction SA11 (0.070 g) was purified by CC using CH$_2$Cl$_2$, CH$_2$Cl$_2$-Me$_2$CO, Me$_2$CO in a polarity gradient manner to give two fractions. The second fraction was purified by CC and gradiently eluted with 100% CH$_2$Cl$_2$, CH$_2$Cl$_2$-Me$_2$CO, and 100% Me$_2$CO to give two subfractions (SA11.1 and SA11.2). Subfraction SA11.1 was

rechromatographed on CC and gradiently eluted with 100% hexanes, EtOAc-hexanes, and 100% EtOAc to give **OSA5** (5.0 mg) as a yellow solid. Subfraction SA11.2 was purified by CC using 20% EtOAc-hexanes and 100% EtOAc as an eluent to give a yellow solid, which was shown to be a mixture of **OLA3** and **OLA5** on TLC (30% EtOAc-hexanes).

3.6 Chemical Investigation of the *Oroxylum indicum* Twigs

3.6.1 Extraction, Isolation, and Purification

The dried twigs of *O. indicum* (393.320 g) were chopped and extracted with CH_2Cl_2 (10 L, 7 days), Me_2CO (10 L, 7 days), and MeOH (18.5 L, 7 days) at room temperature, respectively, to give, after evaporation, the CH_2Cl_2 (crude TD, 88.670 g), acetone (crude TA, 8.180 g) and methanolic (crude TM, 89.770 g) extracts, as shown in figure 3.8.
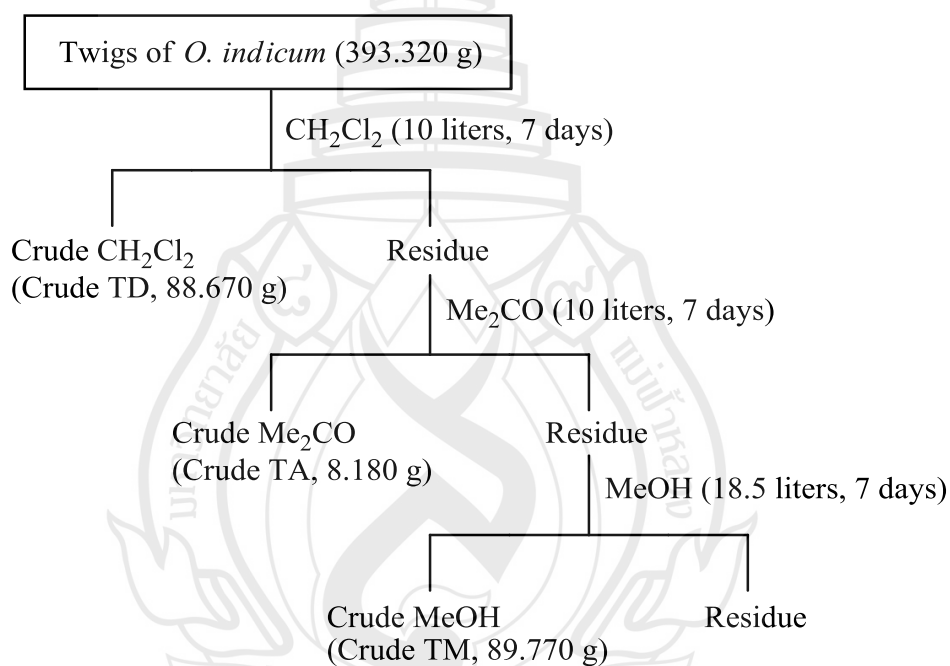
Figure 3.8 Extraction of Crudes TD, TA and SM from the Twigs of *O. indicum*

Crude TA (3.150 g) was subjected by QCC over silica gel using hexanes, hexanes-CH_2Cl_2, CH_2Cl_2-Me_2CO and Me_2CO-MeOH in a polarity gradient manner. The collected fractions were combined according to the characteristic on TLC and evaporated to give nineteen fractions (TA1-TA19) as shown in table 3.15. The selected fractions were further purified as shown in figure 3.9.

Table 3.15 Physical Characteristic and Weight of Fractions obtained from Crude TA

Fraction	Weight (g)	Physical characteristic
TA1	0.007	Yellow solid
TA2	0.001	Yellow solid
TA3	0.006	Brown solid
TA4	0.063	Brown solid
TA5	0.016	Yellow solid
TA6	0.237	Green viscous liquid
TA7	1.531	Green viscous liquid
TA8	0.113	Green viscous liquid
TA 9	0.098	Green viscous liquid
TA10	0.075	Green viscous liquid
TA11	0.060	Green viscous liquid
TA12	0.050	Green viscous liquid
TA13	0.093	Green viscous liquid
TA14	0.025	Green viscous liquid
TA15	0.101	Green viscous liquid
TA16	0.384	Green viscous liquid
TA17	0.336	Green viscous liquid
TA18	0.284	Brown viscous liquid
TA19	0.821	Brown viscous liquid

Crude TA (3.150 g)

| QCC (hexanes, hexanes-CH$_2$Cl$_2$, CH$_2$Cl$_2$-Me$_2$CO and Me$_2$CO-MeOH)

TA1 .... TA4   TA5   TA6   TA7   TA8-TA11   TA12-TA14   TA15   TA16   TA17 TA18 TA19

| CC | CC | PLC | CC | TLC | TLC | CC

ORD3   TA4.1 TA4.2 TA4.3   **OTA1**   TA6.1 TA6.2 TA6.3   **OLA1**   **OLA1**   TA17.1 TA17.2 TA17.3 TA17.4 TA17.5

(1.3 mg)   (2.1 mg) | TLC | TLC   +   + | PLC

| CC | CC | CC | CC |

ORD1   **OLA3**   **ORD2** **OLA1** **OLA1**   **OLA2**   **OLA2**   **OLA7**   **OTA2**

(16.5 mg)   (1.1 mg)   (1.5 mg)   +   +   +   (2.1 mg)   (4.9 mg)

OLA2   **OLA3**   **OLA3**   **OLA8**

                              +   +   (2.5 mg)

                              OLA5   **OLA5**

| CC | CC | CC

TA7.1   TA7.2   TA7.3-.6   TA7.7   TA8-11.1 TA8-11.2 TA8-11.3   TA16.1 TA16.2 TA16.3 TA16.4   TA16.5 TA16.6

| | | TLC | | | TLC | TLC | TLC | TLC

OLA1 **OLA1** **OLA1**   **OLA2**   **OLA1** **OLA1**   **OLA1** **OLA1** **OLA1**

(128.3 mg) (235.4 mg) +   (60.0 mg) (10.4 mg)   +   +

OLA2   **OLA2**   **OLA2**

Figure 3.9 Isolation of Pure Compounds from Crude TA of *O. indicum*

Fraction TA1 (0.007 mg) was purified by CC and gradiently eluted with 100% CH_2Cl_2 and 60% Me_2CO-CH_2Cl_2 to give two fractions. The first fraction TA1.1 was rechromatographed by CC and gradiently eluted with 100% CH_2Cl_2 and 60% Me_2CO-CH_2Cl_2 to yield **ORD3** (1.3 mg) as a yellow solid.

Fraction TA4 (0.063 mg) was subjected to CC and gradiently eluted with 50% CH_2Cl_2-hexanes and 100% CH_2Cl_2 to give fractions TA4.1 and TA4.3 which yielded **ORD1** (16.5 mg) and **OLA3** (1.1 mg), respectively.

Fraction TA5 (0.005 g) was separated by PLC using 30% EtOAc-benzene as the developing solvent to yield **OTA1** (2.1 mg) as a yellow solid.

Fraction TA6 (0.232 g) was purified by CC and gradiently eluted with 50% CH_2Cl_2-hexanes, CH_2Cl_2, 7% Me_2CO-CH_2Cl_2 to give three fractions (TA6.1-TA6.3). Fraction TA6.1 yielded **ORD2** (1.5 mg) as a yellow solid. Fraction TA6.2 was shown to be a major spot of **OLA1** on TLC (100% CH_2Cl_2). Fraction TA6.3 was shown to be a mixture of **OLA1** and **OLA2** on TLC (100% CH_2Cl_2).

Fraction TA7 (1.531 g) was purified by CC and gradiently eluted with 50% CH_2Cl_2-hexanes, CH_2Cl_2 and 50% Me_2CO-CH_2Cl_2 to give seven subfractions (TA7.1-TA7.7). Fractions TA7.1 and TA7.2 yielded yellow solids **OLA1** (128.3 and 235.4 mg, respectively). Fractions TA7.3-TA7.6 were combined (1.056 g) and shown to be a mixture of **OLA1** and **OLA2** on TLC (100% CH_2Cl_2). Fraction TA7.7 afforded **OLA2** (60.0 mg) as a yellow solid.

Fractions TA8, TA9, TA10, and TA11 were combined (0.346 g) and purified by CC and gradiently eluted with 100% CH_2Cl_2 and 80% Me_2CO-CH_2Cl_2 to give three subfractions (TA8-TA11.1–TA8-TA11.3). Fraction TA8-TA11.1 yielded **OLA1** (10.4 mg) as a yellow solid. Fraction TA8-TA11.2 were shown to be a mixture of **OLA1** and **OLA2** on TLC (100% CH_2Cl_2).

Fractions TA12, TA13, and TA14 were combined (0.168 g) and shown to be a mixture of **OLA1**, **OLA2**, **OLA3,** and **OLA5** on TLC (30% EtOAc-hexanes).

Fraction TA15 was displayed to be a mixture of **OLA1**, **OLA2**, **OLA3**, and **OLA5** on TLC (30% EtOAc-hexanes).

Fraction TA16 (0.384 g) was subjected to CC using 15% EtOAc-hexanes and 100% EtOAc in a polarity gradient manner to give six fractions (TA16.1-TA16.6). Fractions TA16.2 and TA16.3 were shown to be a major spot of **OLA1** on TLC

(100% CH$_2$Cl$_2$). Fraction TA16.4 was displayed to be a mixture of **OLA1** and **OLA2** on TLC (100% CH$_2$Cl$_2$).

Fraction TA17 (0.3357 g) was purified by CC and gradiently eluted with 15% EtOAc-hexanes and 100% EtOAc to give five subfractions (TA17.1-TA17.5). Fraction TA17.3 yielded **OLA7** (2.1 mg). Fraction TA17.5 was purified by PLC using 15% EtOAc-benzene as the developing solvent to yield **OTA2** (4.9 mg) and **OLA8** (2.5 mg).

3.7 Antibacterial Activity Assays

Antibacterial activity using broth microdilution method (Clinical and Laboratory Standards Institute, 2002) was used for screening and determining of minimum inhibition concentration (MICs) of crude extracts and isolated compounds.

3.7.1 Screening of Crude Extracts and Isolated Compounds

Test samples were dissolved in DMSO and mixed with melted Mueller Hinton Broth (MHB) in microtiter plates, 50 µL of inoculum suspensions was added in each well (final concentration of 1×10^4 CFU/well). Final concentration of crude extracts and isolated compounds were 1,000 and 200 µg/mL, respectively. The inoculated plate were incubated at 35-37 ºC for 16-18 h, 0.18% resazurin 10 µL was dropped in microtiter plate and incubated in 35-37 ºC for 2-3 h. The blue color indicated that the sample can inhibit bacterial growth whereas the pink color indicated that the sample can not inhibit bacterial growth. Each sample was tested in triplicate. Vancomycin and gentamicin were used as positive control drugs.

3.7.2 Determination of Minimum Inhibiton Concentrations (MICs) of Crude Extracts and Isolated Compounds

Test samples were dissolved in DMSO. Serial 2-fold dilutions of the test samples were mixed with melted MHB in microtiter plates. Final concentration of crude extract and isolated compound in broth ranged from 2.5-1,280 µg/mL and 0.25-128 µg/mL, respectively. Add 50 µL of inoculum suspensions in each well (final concentration of 1×10^4 CFU/well). The inoculated plates were incubated at 35-37 ºC for 16-18 h, 0.18% resazurin 10 µL was dropped in microtiter plate and incubated in 35-37 ºC for 2-3 h. The blue color indicated that the sample can inhibit bacterial growth, while the pink color indicated that the samples can not inhibit bacterial growth. MICs were recorded by reading the lowest concentration that inhibited visible growth. The tests were performed at least in triplicate. Vancomycin and gentamicin were used as positive control drugs.

3.8 Antioxidation Activity Assays

Evaluation of antioxidation activitie of the crude extracts and pure compounds isolated from *O. indicum* (LH, LD, LA, LM, RD, RA, SA, SM, TD, TA, and TM) were assessed on the basis of scavenging activity of the stable (DPPH) free radical by flow injection analysis (FIA) method. The following assay procedure was modified from those described in the previous report (Mrazek et al., 2012). The DPPH 0.075 mM was flowed though the reaction coil (200 cm) with a flow rate of 1.0 mL/min. The absorbance (Abs) was measured at 520 nm. The sample (50 μL) was dispersed and reacted with DPPH streams, and the solution was flowed though the detector and the signal generated to FIA gram as shown in figure 3.10. The measurements were performed at least in triplicate. The results expressed as percentage inhibition. The concentration needed to decrease %inhibition of DPPH solution to 50 (IC_{50}) was obtained by dose-response curve.
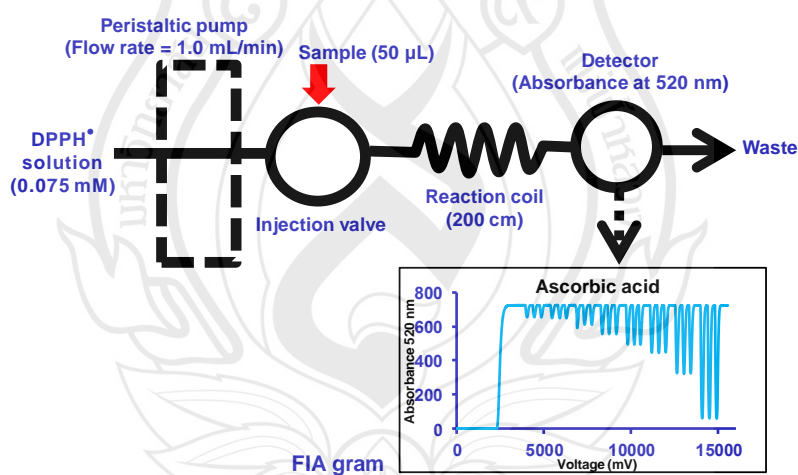
Figure 3.10 Diagram of Flow Injection-Spectrophotometric System

3.8.1 Screening on the Free Radical Scavenging Activity of the Crude Extracts and Isolated Compounds

Crude extracts and isolated compounds were dissolved in absolute ethanol to prepare the solutions with concentrations of 6.1 mg/mL and 3.05 mM, respectively. The solution of each sample (50 μL) was mixed with 0.075 mM DPPH. The trapping effect was assessed by measuring the absorbance change of the solution at 520 nm against 0.075 mM DPPH ethanolic solution in reaction coil. Ascorbic acid was used as a positive control. The measurements were performed at least in triplicate. The degree of loss of color implied the activity. The result expressed as percentage inhibition.

3.8.2 Determination of 50% Inhibition Concentration (IC_{50}) of Crude Extracts and Isolated Compounds

The solution of 0.075 mM DPPH was mixed with the sample at various concentrations of a crude extract in mg/mL and a pure compound in mM. The absorbances were measured at 520 nm. The concentration needed to decrease % inhibition of DPPH solution to 50% inhibition (IC_{50}) was obtained by dose-response curve. The measurements were performed at least in triplicate.

CHAPTER 4

RESULTS AND DISCUSSION

4.1 Structural Elucidation of Isolated Compounds from *Oroxylumindicum*

The studies of chemical constituents from leaves, roots, stems and twigs of *Oroxylum indicum* led to the isolation of twenty-one compounds. Eight compounds (**OLA1**, **OLA2**, **OLA3**, **OLA5**, **OLA7**, **OLA8**, **OLA9**, and **OLA10**) were obtained from acetone extracts of the leaves. Four compounds (**ORD1**, **ORD2**, **ORD3**, and **ORD4**) and two compounds (**ORA1** and **ORA2**) were obtained from the roots dichloromethane and acetone extracts, respectively. Five compounds (**OSA1**, **OSA2**, **OSA3**, **OSA4**, and **OSA5**) were obtained from the stem and two compounds (**OTA1** and **OTA2**) were obtained from acetone extracts of the stems and twigs, respectively. Their structures were elucidated by spectroscopic analysis.
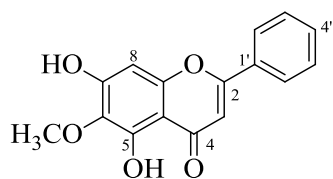
OLA1

5,7-dihydroxy-6-methoxyflavone

(oroxylin A)
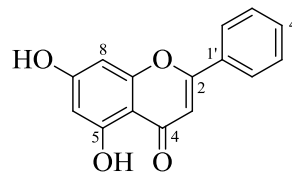
OLA2

5,7-dihydroxyflavone

(chrysin)
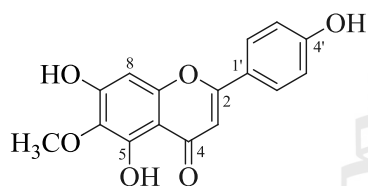
OLA3

5,7,4'-trihydroxy-6-methoxyflavone

(hispidulin)
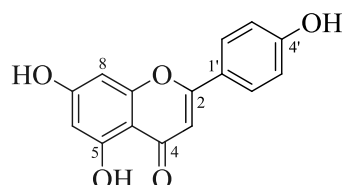
OSA5

5,7,4'-trihydroxyflavone

(apigenin)
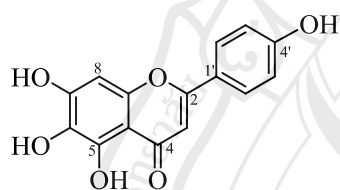
OLA5

5,6,7,4′-tetrahydroxyflavone

(scutellarein)
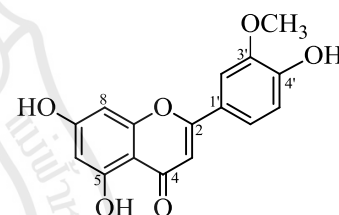
OLA10

5,7,4′-trihydroxy-3′-methoxyflavone

(chrysoeriol)
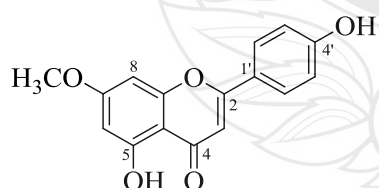
OTA1

5,4′-dihydroxy-7-methoxyflavone

(genkwanin)

Figure 4.1 Structural Determination of Compounds **OLA1**, **OLA2**, **OLA3**,

OLA5, **OLA10**, **OSA5**, and **OTA1**

OLA1 was obtained as a yellow solid, m.p. 218 °C (219 °C, Mouffok et al., 2012).The UV spectrum in MeOH showed maxima absorption (log ε) at 214 (4.48), 271 (4.38), and 318 (4.11) nm, which was characteristic of flavones. The IR (KBr) spectrum showed major absorption bands of O-H stretching at 3003 cm^{-1} and C=O stretching at 1655 cm^{-1}. The ^{1}H NMR spectral data (table 4.1) revealed the presence of a characteristic signal of flavone H-3 (δ 6.79, *s*). A chelated hydroxy group 5-OH (δ 13.12, *s*) and an isolated aromatic proton H-8 (δ 6.67, *s*) were displayed. Two substituents were attached to a flavone nucleus, as indicated by a free hydroxy group 7-OH (δ 9.25, *br s*) and a methoxy group 6-OCH$_3$ (δ 3.88, *s*). The remaining signals are the signals of aromatic protons H-2',6' (δ 8.08, 2H, *m*), H-3',5' (δ 7.59, 2H, *m*), and H-4' (δ 7.61, 1H, *m*) in B-ring. The resulting structure was corresponded with ^{13}C NMR spectral data (table 4.3) and confirmed by HMBC correlations (table 4.5). According to these data **OLA1** was identified as 5,7-dihydroxy-6-methoxyflavone or oroxylin A (Mouffok et al., 2012).

OLA2 was obtained as a yellow solid, m.p. 210 °C (206 °C, Mouffok et al., 2012). The UV spectrum in MeOH exhibited maximum absorption bands (log ε) at 211 (4.75), 268 (4.67), and 313 (4.25) nm. The IR spectrum (KBr) showed absorption bands at 3369 cm^{-1} (O-H stretching) and 1647 cm^{-1} (C=O stretching). The ^{1}H NMR spectral data (table 4.1) exhibited characteristic signals of a flavone proton at δ 6.80 (*s*, H-3), a chelated hydroxy group at δ 12.91 (*s*, 5-OH), and a free hydroxy group at δ 9.74 (*br s*, 7-OH). The signals of a *meta*-coupling at δ 6.28 (*d*, *J* = 2.0 Hz) and δ 6.58 (*d*, *J* = 2.0 Hz), were assigned for H-6 and H-8, respectively. An unsubstituted B-ring displayed the signals of H-2',6' at δ 8.07 (2H, *m*); H-3',5' at δ 7.60 (2H, *m*), and H-4' at δ 7.61 (1H, *m*). The ^{13}C NMR spectral data indicated the presence of a carbonyl carbon, six quaternary carbons and eight methine carbons as shown in table 4.3. The locations of all aromatic protons were confirmed by HMBC correlations shown in table 4.5. The structure of **OLA2** was then identified as 5,7-dihydroxyflavone, which was known as chrysin (Mouffok et al., 2012).

OLA3 was isolated as a yellow solid, m.p. 289-292 °C (289-291 °C, Oliveira, Nakashima, Filho & Frehse, 2001). The strong absorptions (log ε) at 215 (4.53), 274 (4.24), and 334 (4.39) nm were detected in the UV spectrum in MeOH. The presence of O-H stretching (3418 cm^{-1}) and C=O stretching (1644 cm^{-1}) were shown in the IR spectrum (KBr). The ^{1}H NMR spectral data (table 4.1) showed five *singlet* signals of a flavone characteristic H-3 at δ 6.65, a chelated hydroxy group 5-OH at δ 13.23, a methoxy group 6-OCH$_3$ at δ 3.88, an isolated aromatic proton H-8 at δ 6.63, and a free hydroxy group 4'-OH at δ 9.49, which were confirmed by the HMBC correlations (table 4.5): H-3 to C-2, C-4, C-4a, C-1';5-OH to C-4a, C-5, C-6; 6-OCH$_3$ to C-6; H-8 to C-4a, C-6, C-7, C-8a; 4'-OH to C-3', C-5', respectively. A series of AA'BB' system were displayed at δ 7.95 (2H, *d*, *J* = 8.8 Hz) and δ 7.03 (2H, *d*, *J* = 8.8 Hz*)* which were assigned to be H-2',6' and H-3',5', respectively. The ^{13}C NMR spectrum (table 4.3) showed fourteen carbons. **OLA3** was assigned to be 5,7,4'-trihydroxy-6-methoxyflavone or hispidulin (Yadav et al., 2012).

OSA5 was isolated as a yellow solid, m.p. 346-351 °C (345-350 °C, Muthumani et al., 2010). The UV spectrum in MeOH showed maximum absorption bands (log ε) at 206 (4.34), 267 (4.08), and 333 (4.11) nm. The IR spectrum (KBr) exhibited absorption bands of O-H stretching at 3429 cm^{-1} and C=O stretching at 1630 cm^{-1}. The ^{1}H NMR spectral data (table 4.1) revealed a signal of a flavone derivative (H-3) at δ 6.50 (*s*) and a chelated hydroxy group (5-OH) at δ 12.88. Two *doublet* signals of *meta* protons H-6 and H-8 with a coupling constant of 2.1 Hz were existed at δ 6.12 and 6.41, respectively. The AA'BB' system were observed at δ 7.81 (2H, *d*, *J* = 9.0 Hz, H-2',6') and 6.90 (2H, *d*, *J* = 9.0 Hz, H-3',5'). The ^{13}C NMR spectral data (table 4.3) and HMBC correlations (table 4.5) supported the assignment. Thus, **OSA5** was identified to be 5,7,4'-trihydroxyflavone or apigenin (Jeong, G.-S., Lee, Jeong, S.-N., Kim, Y.-C. & Kim, E.-C. 2009).

OLA5 was obtained as an orange solid, m.p. 285-289 °C (285-290 °C, Chen et al., 2012). The UV spectrum in MeOH showed maximum absorption bands (log ε) at 215 (4.08), 275 (3.93), and 323 (3.70) nm. The IR spectrum (KBr) exhibited absorption bands of O-H stretching at 3204 cm^{-1} and C=O stretching at 1662 cm^{-1}. The ^{1}H NMR spectral data (table 4.2) showed a *singlet* of a flavone type vinylic proton H-3 (δ 6.55), a *singlet* of a chelated hydroxyl group 5-OH (δ 12.58), and an isolated aromatic proton H-8 (δ 6.53, *s*). The remaining signals were a free hydroxy 4'-OH (δ 9.10) and an AA′BB′ pattern at δ 7.79 (2H, *d*, J = 7.2 Hz, H-2′,6′) and 7.44 (2H, *d*, J = 7.2 Hz, H-3′,5′). The ^{13}C NMR signals (table 4.4) indicated the presence of a conjugated ketone at δ 182.6 (C-4), six oxygenated sp^2 quaternary carbons at δ 165.0 (C-2), 146.9 (C-5), 150.7 (C-6), 163.7 (C-7), 131.5 (C-8a), and 152.8 (C-4′), two sp^2 quaternary carbons at δ 105.1 (C-4a) and 126.1 (C-1′), and six sp^2 methine carbons at δ 128.9 (C-2′,6′), 115.0 (C-3′,5′), 104.8 (C-3), and 94.1 (C-8). **OLA5** was finally identified to be 5,6,7,4′-tetrahydroxyflavone which was known as scutellarein (Chen et al., 2012).

OLA10 was obtained as a yellow solid, m.p. 325-327 °C (327-328 °C, Lin & Krong, 2006). The UV spectrum in MeOH exhibited maximum absorption bands (log ε) at 209 (4.67), 253 (4.35), 269 (4.32), and 348 (4.43) nm. The IR spectrum (KBr) exhibited absorption bands of O-H stretching at 3405 cm^{-1} and C=O stretching at 1660 cm^{-1}. The ^{1}H NMR spectral data (table 4.2) showed the characteristic resonances of a flavone proton H-3 at δ 6.60, a hydrogen-bonded hydroxyl proton 5-OH (δ 13.00), and a *meta* coupled protons H-6 and H-8 at δ 6.25 (1H, *d*, J = 2.0 Hz) and 6.52 (1H, *d*, J = 2.0 Hz), respectively. The remaining signals are the signals of ABX pattern of H-2′ (δ 7.47, *dd*, J = 8.0, 2.4 Hz), H-5′ (δ 6.99, *d*, J = 8.0 Hz), H-6′ (δ 7.50, *d*, J = 2.4 Hz), and a methoxy group 3′-OCH$_3$ at δ 3.87 (3H, *s*). The ^{13}C NMR spectral data (table 4.4) and HMBC correlations (table 4.6) supported the assignment. Therefore, **OLA10** was identified to be 5,7,4′-trihydroxy-3′-methoxyflavone or chrysoeriol (Lin & Krong, 2006).

OTA1 was obtained as a yellow solid. The UV spectrum in MeOH exhibited UV absorption bands (log ε) at 212 (4.03), 269 (3.74), and 334 (3.82) nm. The IR spectrum (KBr) exhibited absorption bands at 3366 cm^{-1} (a hydroxyl group) and 1657 cm^{-1} (a carbonyl group). The ^{1}H NMR spectral data (table 4.2) exhibited the resonances of a hydrogen bonded hydroxy proton 5-OH (δ 13.02, *s*), a characteristic flavone H-3 (δ 6.64, *s*), and a methoxy group 7-OCH$_3$ (δ 3.87, *s*). Two *doublet* resonances (J = 2.4 Hz) at δ 6.26 (1H) and 6.54 (1H) were in agreement with the *meta*-coupling of aromatic protons H-6 and H-8, respectively. The remaining signals in B-ring were the resonances of an AA′BB′ pattern at δ 7.95 (2H, *d*, J = 8.8 Hz) and 7.03 (2H, *d*, J = 8.8 Hz) implied the presence of H-2′,6′ and H-3′,5′, respectively. The ^{13}C NMR spectral data (table 4.4) and HMBC correlations (table 4.6) supported the assignment. According to these data **OTA1** was identified as 5,4′-dihydroxy-7-methoxyflavone or known as genkwanin (Ayatolloahi, Shojaii, Kobarfard, Mohammadzadeh, & Choudhary, 2009).

Table 4.1 ^{1}H NMR spectral data of compounds **OLA1**, **OLA2**, **OLA3**, and **OSA5**
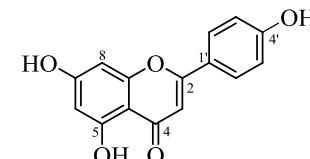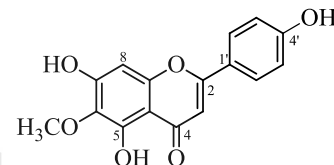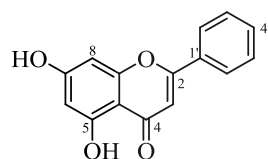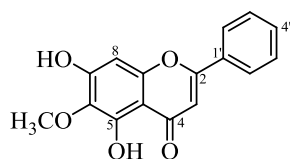

Position	OLA1 (400 MHz, Acetone-d_6)	OLA2 (400 MHz, Acetone-d_6)	OLA3 (400 MHz, Acetone-d_6)	OSA5 (300 MHz, Acetone-d_6)
3	6.79 (1H, *s*)	6.80 (1H, *s*)	6.65 (1H, *s*)	6.50 (1H, *s*)
6	-	6.28 (1H, *d*, *J* = 2.0 Hz)	-	6.12 (1H, *d*, *J* = 2.1 Hz)
8	6.67 (1H, *s*)	6.58 (1H, *d*, *J* = 2.0 Hz)	6.63 (1H, *s*)	6.41 (1H, *d*, *J* = 2.1 Hz)
2',6'	8.08 (2H, *m*)	8.07 (2H, *m*)	7.95 (2H, *d*, *J* = 8.8 Hz)	7.81 (2H, *d*, *J* = 9.0 Hz)
3',5'	7.59 (2H, *m*)	7.60 (2H, *m*)	7.03 (2H, *d*, *J* = 8.8 Hz)	6.90 (2H, *d*, *J* = 9.0 Hz)
4'	7.61 (1H, *m*)	7.61 (1H, *m*)	-	-
5-OH	13.12 (1H, *s*)	12.91 (1H, *s*)	13.23 (1H, *s*)	12.88 (1H, *s*)
6-OCH₃	3.88 (3H, *s*)	-	3.88 (3H, *s*)	-
7-OH	9.25 (1H, *br s*)	9.74 (1H, *br s*)	9.36 (1H, *br s*)	-
4'-OH	-	-	9.49 (1H, *br s*)	-

Table 4.2 ^{1}H NMR spectral data of compound **OLA5**, **OLA10**, and **OTA1**
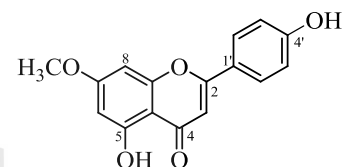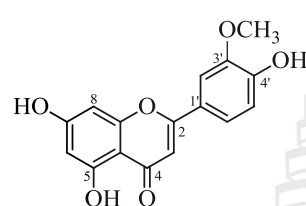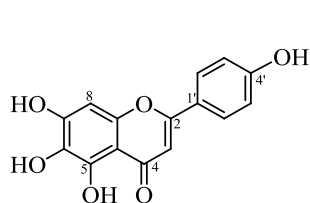
Position	OLA5 (400 MHz, Acetone-d_6)	OLA10 (400 MHz, Acetone-d_6)	OTA1 (400 MHz, Acetone-d_6)
3	6.55 (1H, *s*)	6.60 (1H, *s*)	6.64 (1H, *s*)
6	-	6.25 (1H, *d*, *J* = 2.0 Hz)	6.26 (1H, *d*, *J* = 2.4 Hz)
8	6.53 (1H, *s*)	6.52 (1H, *d*, *J* = 2.0 Hz)	6.54 (1H, *d*, *J* = 2.4 Hz)
2'	7.79 (1H, *d*, *J* = 7.2 Hz)	7.47 (1H, *dd*, *J* = 8.0, 2.4 Hz)	7.95 (1H, *d*, *J* = 8.8 Hz)
3'	7.44 (1H, *d*, *J* = 7.2 Hz)	-	7.03 (1H, *d*, *J* = 8.8 Hz)
5'	7.44 (1H, *d*, *J* = 7.2 Hz)	6.99 (1H, *d*, *J* = 8.0 Hz)	7.03 (1H, *d*, *J* = 8.8 Hz)
6'	7.79 (1H, *d*, *J* = 7.2 Hz)	7.50 (1H, *d*, *J* = 2.4 Hz)	7.95 (1H, *d*, *J* = 8.8 Hz)
5-OH	12.58 (1H, *s*)	13.01 (1H, *br s*)	13.02 (1H, *s*)
4'-OH	9.10 (1H, *br s*)	-	-
5'-OCH$_3$	-	3.87 (3H, *s*)	-
7'-OCH$_3$	-	-	3.87 (3H, *s*)

Table 4.3 ^{13}C NMR spectral data of compounds **OLA1**, **OLA2**, **OLA3**, and **OSA5**

Position	OLA1 (100 MHz, Acetone-d_6)	OLA2 (100 MHz, Acetone-d_6)	OLA3 (100 MHz, Acetone-d_6)	OSA5 (75 MHz, Acetone-d_6)
2	165.1 (C)	165.0 (C)	165.0 (C)	165.1 (C)
3	105.9 (CH)	106.5 (CH)	102.6 (CH)	104.1 (CH)
4	184.0 (C)	183.5 (C)	182.7 (C)	183.1 (C)
4a	106.2 (C)	105.9 (C)	105.0 (C)	105.5 (C)
5	154.4 (C)	163.7 (C)	153.2 (C)	163.4 (C)
6	132.6 (C)	100.3 (CH)	131.5 (C)	99.7 (CH)
7	154.4 (C)	165.6 (C)	165.0 (C)	165.0 (C)
8	95.3 (CH)	95.2 (CH)	93.9 (CH)	94.7 (CH)
8a	158.3 (C)	159.3 (C)	157.0 (C)	158.8 (C)
1'	133.6 (C)	132.6 (C)	122.0 (C)	123.3 (C)
2',6'	127.6 (CH)	127.6 (CH)	128.4 (CH)	129.2 (CH)
3',5'	130.4 (CH)	130.4 (CH)	116.0 (CH)	116.9 (CH)
4'	133.1 (CH)	133.1 (CH)	161.2 (C)	161.9 (C)
6-OCH$_3$	61.0 (CH$_3$)	-	59.8 (CH$_3$)	-

Table 4.4 ^{13}C NMR spectral data of compounds **OLA5**, **OLA10**, and **OTA1**
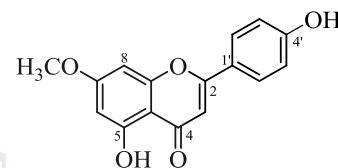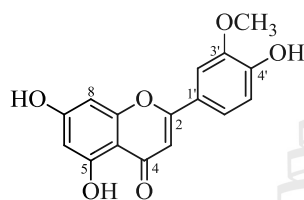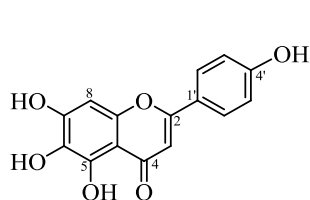
Position	OLA5 (100 MHz, Acetone-d_6)	OLA10 (100 MHz, Acetone-d_6)	OTA1 (100 MHz, Acetone-d_6)
2	165.0	165.2	165.4
3	104.8	104.3	104.3
4	182.6	183.6	183.4
4a	105.1	105.6	105.7
5	146.9	158.9	164.5
6	150.7	99.8	99.8
7	163.7	164.9	163.9
8	94.1	94.8	94.9
8a	131.5	157.5	159.0
1'	126.1	123.9	123.5
2'	128.9	120.2	129.4
3'	115.0	150.1	117.0
4'	152.8	146.5	162.2
5'	115.0	114.2	117.0
6'	128.9	105.8	129.4
3'-OCH$_3$	-	60.7	-
7'-OCH$_3$	-	-	60.8

Table 4.5 HMBC spectral data of compounds **OLA1**, **OLA2**, **OLA3**, and **OSA5**
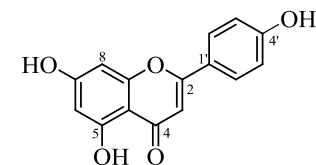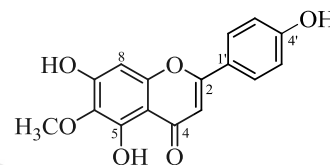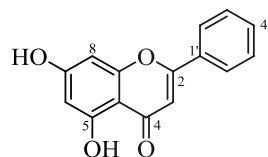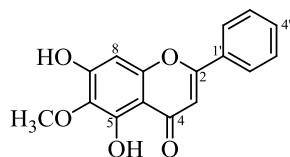
Position	OLA1	OLA2	OLA3	OSA5
3	C-2, C-4, C-4a, C-1'	C-2, C-4, C-4a, C-1'	C-2, C-4, C-4a, C-1'	C-2, C-4, C-4a, C-1'
6	-	C-4a, C-5, C-7, C-8	-	C-4a, C-5, C-7, C-8
8	C-4, C-4a, C-6, C-7, C-8a	C-4, C-4a, C-7, C-8a	C-4a, C-6, C-7, C-8a	C-4a, C-6, C-7, C-8a
2',6'	C-2, C-1', C-2',6', C-3', C-4'	C-4'	C-2, C-3'	C-2, C-2',6', C-4'
3',5'	C-1', C-4', C-2',6', C-3',5'	C-2', C-4', C-5'	C-4', C-5'	C-1', C-3',5', C-4'
4'	C-1', C-6'	C-6'	-	-
5-OH	C-4a, C-5, C-6	C-4a, C-5, C-6	C-4a, C-5, C-6	C-4a, C-5, C-6
6-OCH$_3$	C-6	-	C-6	-
4'-OH	-	-	C-3', C-5'	-

Table 4.6 HMBC spectral data of compounds **OLA10** and**OTA1**
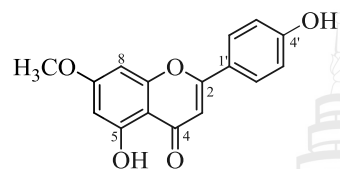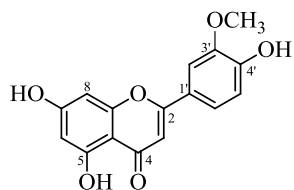
Position	OLA10	OTA1
3	C-4a, C-6'	C-2, C-4, C-4a, C-1'
6	C-4, C-4a, C-7, C-8	C-4a, C-5, C-8
8	C-4, C-4a, C-5, C-6, C-7, C-8a	C-4a, C-6, C-7, C-8a
2'	C-2, C-3', C-4', C-5'	C-2, C-4', C-6'
3'	-	C-1', C-4', C-5'
5'	C-2, C-1', C-4', C-5'	C-1', C-3', C-4'
6'	C-2, C-1', C-2', C-4'	C-2, C-2', C-4'
3'-OCH$_3$	C-3'	-
7'-OCH$_3$	-	C-7
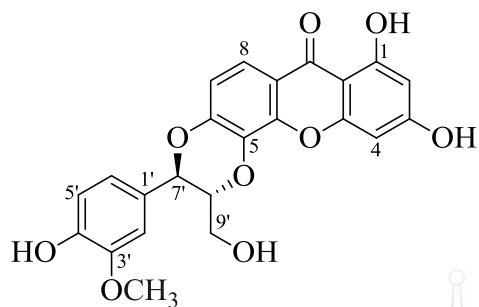
OLA8

5′-demethoxycadensin G
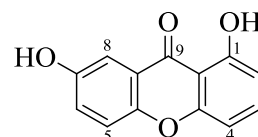
ORD2

1,7-dihydroxyxanthone

(euxanthone)
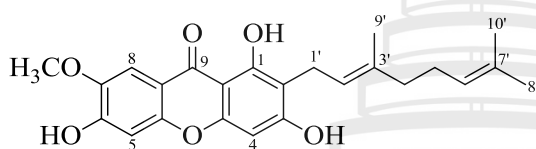
ORD3

1,3,6-trihydroxy-7-methoxy-2-(3,7-dimethyl-

2,6-octadienyl)xanthone

(cowaxanthone)
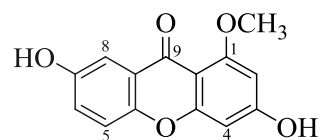
OTA2

3,7-dihydroxy-1-methoxyxanthone

Figure 4.2 Structural Determination of Compounds **OLA8**, **ORD2**, **ORD3**, and **OTA2**

   OLA8 was obtained as a pale yellow solid. The UV spectrum (in MeOH) exhibited maximum absorption bands (log ε) at 203 (3.53), 249 (3.53), 281 (2.83), and 319 (3.06) nm. The IR (KBr) spectrum showed the stretching of hydroxyl (3419 cm^{-1}) and carbonyl (1652 cm^{-1}) functional groups. The ^{1}H NMR spectral data (table 7) showed signals of a 1,3,5,6-tetrahydroxyxanthone, a chelated hydroxyl proton 1-OH (δ 13.08), an *ortho*-coupling aromatic protons H-7 (δ 7.02, *d*, *J* = 9.0 Hz) and H-8 (δ 7.70, *d*, *J* = 9.0 Hz), and *meta*-coupling aromatic protons H-2 (δ 6.27, *d*, *J* = 2.1 Hz) and H-4 (δ 6.47, *d*, *J* = 2.1 Hz). The ^{1}H NMR spectrum further exhibited the resonances of an ABM pattern of H-2′ (δ 7.18, *d*, *J* = 1.8 Hz), H-5′ (δ 6.91, *d*, *J* = 8.1 Hz) and H-6′ (δ 7.03, *dd*, *J* = 8.1, 1.8 Hz). The remaining signals showed two oxygenated methines H-7′ (δ 5.22, *d*, *J* = 8.1 Hz) and H-8′ (δ 4.31, *m*), a hydroxymethylene H-9′ (δ 3.62, *dd*, *J* = 12.6, 3.6 Hz and δ 3.94, *dd*, *J* = 12.6, 2.4 Hz), and a methoxy group 3′-OCH$_3$ (δ 3.88, *s*). The cosy spectrum showed two oxygenated methines (H-7′ and H-8′) and a hydroxymethylene (H-9′) as a linear framework. The position of H-7′ was confirmed by the HMBC correlations of H-7′ to C-1′, C-2′, and C-6. The HMBC correlations of 3′-OCH$_3$ to C-3′ indicated the position of methoxy group at C-3′ (table 4.7).

   This phenylpropanoid moiety and the tetrahydroxyxanthone were combined to give a proposed xanthonolignoid structure of **OLA8** where H-7′ and H-8′ are *trans*-orientated. Subsequently, **OLA8** was identified as 5′-demethoxycadensin G (Sia, Bennett, Harrison & Sim, 1995).

ORD2 was obtained as a yellow solid, m.p. 228-230 °C. (236-238 ˚C, Kraus and Mengwasser, 2009). This compound exhibited UV (in MeOH) maximum absorption bands (log ε) at 243 (5.10), 259 (5.00), 316 (4.93), and 356 (3.48) nm. The IR (KBr) spectrum showed the absorption bands at 3306 cm^{-1} (a hydroxyl group) and 1605 cm^{-1} (a carbonyl group). The ^{1}H NMR spectral data (table 4.8) revealed the presence of a signal of a chelated hydroxyl proton 1-OH (δ 12.62, *brs*). The signals of an ABM system at δ 6.77 (*dd*, J = 8.0, 0.4 Hz), δ 7.70 (*t*, J = 8.4 Hz) and δ 7.01 (*d*, J = 8.4 Hz), were assigned for H-2, H-3, and H-4, respectively. In addition, the resonances of an ABX system of H-5, H-6, and H-8 were detected at δ 7.53 (*d*, J = 8.8 Hz), δ 7.44 (*dd*, J = 8.8, 3.2 Hz), and δ 7.61 (*d*, J = 3.2 Hz), respectively. Therefore, **ORD2** was characterized as 1,7-dihydroxyxanthone which was known as euxanthone (Fujita et al., 1992).

ORD3 was isolated as a yellow solid, m.p. 195-196 °C (196-197 ˚C, Na Pattalung, Thongtheeraparp, Wiriyachitra & Taylor, 1994). The UV spectrum in MeOH showed maximum absorption bands (log ε) at 242 (4.91), 258 (4.52), 320 (4.33), and 362 (4.17) nm. The IR (KBr) spectrum showed the absorption bands of stretching of hydroxyl (3529 cm^{-1}) and carbonyl (1611 cm^{-1}) groups. The ^{1}H NMR spectral data (table 4.8) exhibited *singlet* signals of a chelated phenolic hydroxyl proton 1-OH at δ 13.46, three isolated aromatic protons H-4 (δ 6.48), H-5 (δ 6.91), H-8 (δ 7.55), and a methoxy group 3′-OCH$_3$ (δ 4.04). In addition, the presence of a geranyl unit was observed from the characteristic signals of a *doublet* signal of benzylic methylene protons at δ 3.38 (J = 7.2 Hz), two set of *broad triplet* signals of olefinic methine protons at δ 5.31 and δ 5.08, two sets of *multiplet* signals of methylene protons at δ 1.97 and δ 1.88, and three *singlet* signals of vinylic methyl groups at δ 1.80, 1.60, and 1.55. According to these data **ORD3** was identified as 1,3,6-trihydroxy-7-methoxy-2-(3,7-dimethyl-2,6-octadienyl)xanthone or cowaxanthone (Likhitwitayawuid, Phadungcharoen, Mahidol & Ruchirawat, 1997).

OTA2 was obtained as a yellow solid. This compound exhibited UV (in MeOH) maximum absorption bands (log ε) at 204 (4.74), 258 (4.43), and 293 (4.14) nm. The IR (KBr) spectrum showed the absorption bands at 3193 cm^{-1} (a hydroxyl group) and 1681 cm^{-1} (a carbonyl group). The ^{1}H NMR spectral data (table 4.9) showed a *singlet* signal of a methoxy group 1-OCH$_3$ (3H, *s*). The signals of a *meta*-coupling at δ 7.56 (1H, *d*, *J* = 1.6 Hz) and 7.22 (1H, *d*, *J* = 1.6 Hz) were assigned to be H-2 and H-4, respectively. The remaining signals of an ABX pattern H-5 (δ 6.91, *d*, *J* = 8.4 Hz), H-6 (δ 7.59, *dd*, *J* = 8.4, 2.0 Hz), and H-8 (δ 7.55, *d*, *J* = 2.0 Hz) were displayed in the spectrum. The ^{13}C NMR spectral data and HMBC correlations (table 4.9) supported the assignment. Hence, **OTA2** was identified to be 3,7-dihydroxy-1-methoxyxanthone.
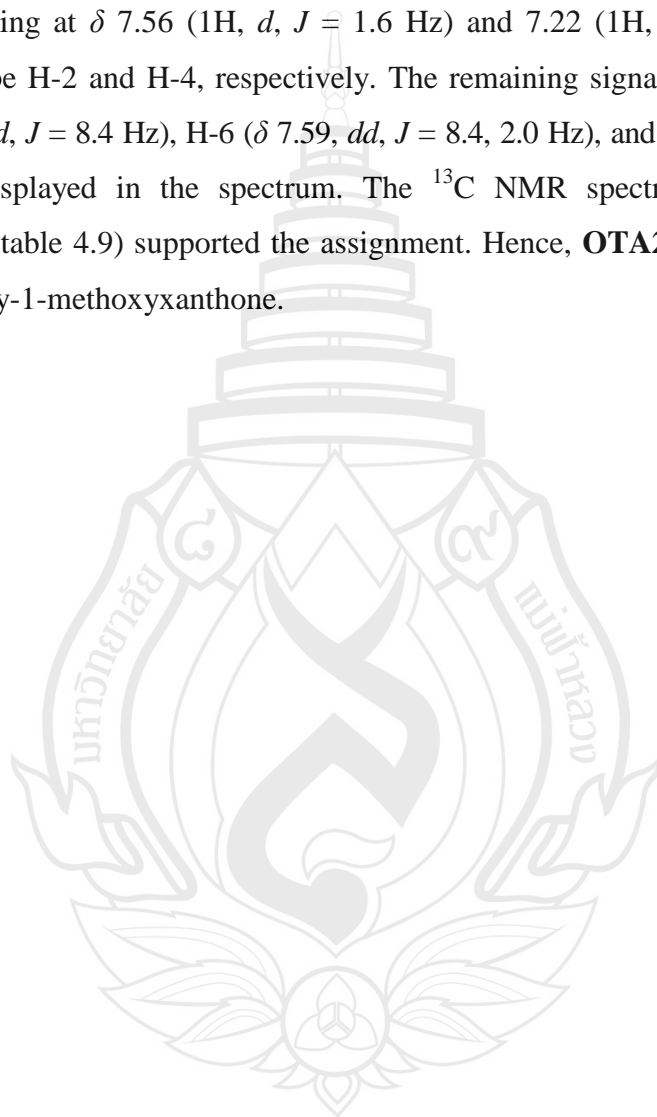
Table 4.7 ^{1}H NMR, ^{13}C NMR and HMBC spectral data of compound **OLA8**
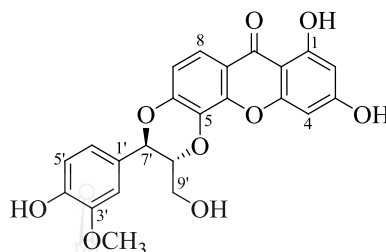
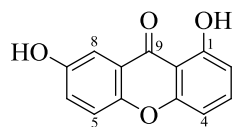

Position	^{1}H NMR (400 MHz, Acetone-d_6)	^{13}C NMR (100 MHz, Acetone-d_6)	HMBC
1	-	164.9 (C)	-
2	6.27 (1H, d, J = 2.1 Hz)	99.3 (CH)	C-1, C-3, C-4, C-9a
3	-	166.3 (C)	-
4	6.47 (1H, d, J = 2.1 Hz)	95.0 (CH)	C-2, C-3, C-4a, C-9, C-9a
4a	-	158.9 (C)	-
5	-	133.0 (C)	-
6	-	150.4 (C)	-
7	7.01 (1H, d, J = 9.0 Hz)	114.7 (CH)	C-5, C-6, C-8a
8	7.70 (1H, d, J = 9.0 Hz)	117.9 (CH)	C-6, C-9, C-10a
8a	-	115.8 (C)	-
9	-	180.9 (C)	-
9a	-	103.4 (C)	-
10a	-	147.2 (C)	-
1'	-	128.4 (C)	-
2'	7.18 (1H, d, J = 1.8 Hz)	112.2 (CH)	C-1', C-4', C-6', C-7'
3'	-	148.7 (C)	-
4'	-	148.5 (C)	-
5'	6.91 (1H, d, J = 8.1 Hz)	116.0 (CH)	C-1', C-3'
6'	7.03 (1H, dd, J = 8.1, 1.8 Hz)	121.9 (CH)	C-2', C-4', C-7'
7'	5.22 (1H, d, J = 8.1 Hz)	78.0 (CH)	C-1', C-2', C-6', C-8'
8'	4.32 (1H, m)	79.7 (CH)	-
9'	3.62 (1H, dd, J = 12.6, 3.6 Hz)	61.7 (CH$_2$)	C-7', C-8'
	3.94 (1H, dd, J = 12.6, 2.4 Hz)		
1-OH	13.08 (1H, s)	-	C-1, C-2, C-9a
3'-OCH$_3$	3.88 (3H, s)	56.5 (CH$_3$)	C-3'

Table 4.8 ^{1}H NMR and ^{13}C NMR spectral data of compounds **ORD2** and **ORD3**
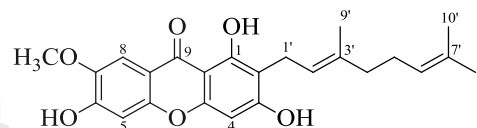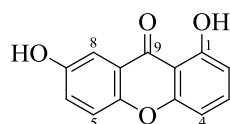
Position	ORD2		ORD3
	^{1}**H NMR** (400 MHz, Acetone-d_6)	^{13}**C NMR** (100 MHz, Acetone-d_6)	^{1}**H NMR** (400 MHz, Acetone-d_6)
1	-	162.7 (C)	-
2	6.77 (1H, *dd*, *J* = 8.4, 0.4 Hz)	109.2 (CH)	-
3	7.70 (1H, *t*, *J* = 8.4 Hz)	110.5 (CH)	-
4	7.01 (1H, *d*, *J* = 8.4 Hz)	107.9 (CH)	6.48 (1H, *s*)
4a	-	157.4 (C)	-
5	7.53 (1H, *d*, *J* = 8.8 Hz)	137.8 (CH)	6.91 (1H, *s*)
6	7.44 (1H, *dd*, *J* = 8.8, 3.2 Hz)	126.2 (CH)	-
7	-	151.1 (C)	-
8	7.61 (1H, *d*, *J* = 3.2 Hz)	121.9 (CH)	7.55 (1H, *s*)
8a	-	120.3 (C)	-
9	-	183.0 (C)	-
9a	-	113.2 (C)	-
10a	-	155.0 (C)	-
1'	-	-	3.38 (2H, *d*, *J* = 7.2 Hz)
2'	-	-	5.31 (1H, *m*)
4'	-	-	1.97 (2H, *m*)
5'	-	-	1.88 (2H, *m*)
6'	-	-	5.08 (1H, *m*)

Table 4.8 (continued)
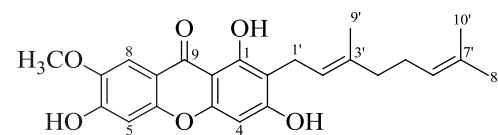
Position	ORD2		ORD3
	¹H NMR (400 MHz, Acetone-d_6)	**¹³C NMR** (100 MHz, Acetone-d_6)	**¹H NMR** (400 MHz, Acetone-d_6)
8'	1.60 (3H, *s*)	-	1.60 (3H, *s*)
9'	-	-	1.80 (3H, *s*)
10'	-	-	1.55 (3H, *s*)
1-OH	12.72 (1H, *br s*)	-	13.46 (1H, *br s*)
7- OCH₃	-	-	4.04 (3H, *s*)
7-OH	9.01 (1H, *br s*)	-	-

Table 4.9 ^{1}H NMR, ^{13}C NMR and HMBC spectral data of compound **OTA2**
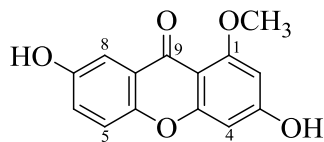
Position	^{1}H NMR (400 MHz, Acetone-d_6)	^{13}C NMR (100 MHz, Acetone-d_6)	HMBC
1	-	162.7	-
2	7.56 (1H, d, J = 1.6 Hz)	116.0	C-1, C-4, C-9a
3	-	164.1	-
4	7.22 (1H, d, J = 1.6 Hz)	115.6	C-2, C-3, C-4a, C-9a
4a	-	159.3	-
5	6.91 (1H, d, J = 8.4 Hz)	123.1	C-6, C-7, C-8a, C-10a
6	7.59 (1H, dd, J = 8.4, 2.0 Hz)	126.8	C-5, C-7, C-8, C-10a
7	-	152.1	-
8	7.55 (1H, d, J = 2.0 Hz)	114.8	C-6, C-7, C-9, C-10a
8a	-	125.0	-
9	-	179.9	-
9a	-	111.3	-
10a	-	148.2	-
1-OCH$_3$	3.90 (3H, s)	56.5	C-1
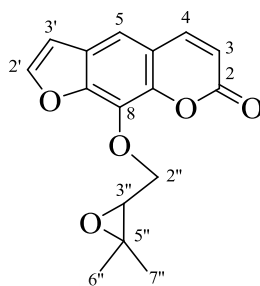
Figure 4.3 Structural Determination of Compound **ORA1**

ORA1 was obtained as a white solid, m.p. 102-107 °C (102-106 °C, Wang et al., 2008). The UV spectrum in MeOH showed maxima absorptions (log ε) at 217 (4.59), 247 (4.55), and 297 (4.24) nm, which was characteristic of coumarin. The IR (KBr) spectrum showed absorption bands of C=O stretching at 1728 cm^{-1} and C=C stretching at 1628 and 1588 cm^{-1}. The ^{1}H NMR spectral data (table 4.10) exhibited a pair of *cis*-coupled olefinic protons at H-3 (δ 6.39, 1H, *d*, *J* = 9.6 Hz) and H-4 (δ 7.79, 1H, *J* = *d*, 9.6 Hz) and an isolated aromatic proton H-5 (δ 7.42), which were the signals of a coumarin skeleton. Two *doublet* signals with a coupling constant of 2.4 Hz at δ 7.71 and 6.84 were assigned for H-2' and H-3', respectively. In addition, two tertiary-methyl protons H-6'' at δ 1.36 and H-7'' at δ 1.29 (each 3H, *s*), methylene protons H-2'' at δ 4.60 (2H, *m*), and a *singlet* proton H-3'' at δ 3.33 (1H, *m*) were displayed in the spectrum. The positions of H-4, H-5, H-3' and H-3'' were confirmed by HMBC correlations (table 4.10): H-4 to C-2, C-3, C-4a, C-5, C-8, C-8a; H-5 to C-4, C-7, C-8a, C-3'; H-3' to C-5, C-6, C-2'; H-3'' to C-2'', C-5'', C-6'', respectively. Based on the spectral data, the structure **ORA1** was determinated as heraclenin (Wang et al., 2008).

Table 4.10 ^{1}H NMR, ^{13}C NMR, and HMBC spectral data of compound **ORA1**
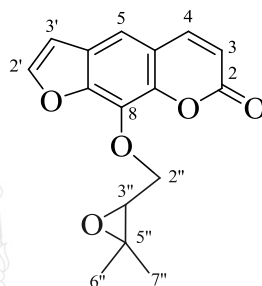
Position	^{1}H NMR (400 MHz, Acetone-d_6)	^{13}C NMR (100 MHz, Acetone-d_6)	HMBC
2	-	160.4 (C)	-
3	6.39 (1H, *d*, *J* = 9.6 Hz)	114.8 (CH)	C-2, C-4a,
4	7.79 (1H, *d*, *J* = 9.6 Hz)	144.3 (CH)	C-2, C-3, C-4a, C-5,C-8, C-8a
4a	-	116.5 (C)	-
5	7.42 (1H, *s*)	113.9 (CH)	C-4, C-7, C-8a, C-3'
6	-	126.0 (C)	-
7	-	148.3 (C)	-
8	-	143.5 (C)	-
8a	-	131.5 (C)	-
2'	7.71 (1H, *d*, *J* = 2.4 Hz)	146.8 (CH)	C-6, C-7, C-3'
3'	6.84 (1H, *d*, *J* = 2.4 Hz)	106.8 (CH)	C-5, C-6, C-2'
2''	4.60 (2H, *m*)	72.5 (CH$_2$)	C-8a, C-3'', C-5''
3''	3.33 (1H, *m*)	61.3 (CH)	C-2'', C-5'', C-6''
5''	-	58.2 (C)	-
6''	1.36 (3H, *s*)	24.6 (CH$_3$)	C-3'', C-5'', C-7''
7''	1.29 (3H, *s*)	18.9 (CH$_3$)	C-6''
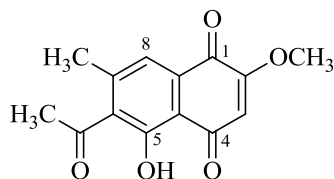
Figure 4.4 Structural Determination of Compound **ORD4**

      ORD4 was isolated as a yellow solid. The strong absorption bands (log ε) at 224 (4.51), 288 (4.13), and 422 (3.69) nm were detected on an UV spectrum in MeOH. The IR spectrum (KBr) showed maximum absorption bands at 3411 cm^{-1} (O-H stretching) and 1713 cm^{-1} (C=O stretching). The ^{1}H NMR spectral data (table 4.11) exhibited a *singlet* signal of an olefinic proton H-3 at δ 6.29, a *broad singlet* signal of a chelated hydroxy 5-OH at δ 13.01, a *singlet* signal of an aromatic proton H-8 at δ 7.46. The remaining signals are a *singlet* signal of a methoxy 2-OCH$_3$ at δ 3.97, a *singlet* signal of an acetyl 6-COC$\underline{H}_3$ at δ 2.53, and a *singlet* signal of a methyl 7-CH$_3$ at δ 2.34. These assignment were confirmed by HMBC correlations of 2-OCH$_3$ to C-2; H-3 to C-1, C-2, C-4, C-4a; 6-COC$\underline{H}_3$ to C-6, 6-$\underline{C}$OCH$_3$; 7-CH$_3$ to C-6, C-7, C-8, C-8a and H-8 to C-1, C-4a, C-6, 7-$\underline{C}$H$_3$, respectively. The ^{13}C NMR spectrum (table 4.11) showed fourteen carbons. **ORD4** was assigned to be 2-methoxystypandrone or orientalone (Nishina, Kubota & Osawa, 1993).

Table 4.11 ^{1}H NMR, ^{13}C NMR, and HMBC spectral data of compound **ORD4**
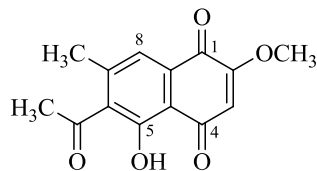
Position	^{1}H NMR (400 MHz, Acetone-d_6)	^{13}C NMR (100 MHz, Acetone-d_6)	HMBC
1	-	179.4 (C)	-
2	-	162.5 (C)	-
3	6.29 (1H, *s*)	110.2 (CH)	C-1, C-2, C-4, C-4a
4	-	191.9 (C)	-
4a	-	113.0 (C)	-
5	-	159.3 (C)	-
6	-	139.0 (C)	-
7	-	143.8 (C)	-
8	7.46 (2H, *s*)	121.6 (CH)	C-1, C-4a, C-6, 7-CH$_3$
8a	-	135.0 (C)	-
2-OCH$_3$	3.97 (3H, *s*)	57.3 (CH$_3$)	C-2
5-OH	13.02 (1H, *br s*)	-	-
6-<u>C</u>OCH$_3$	-	202.9 (C)	-
6-CO<u>C</u>H$_3$	2.53 (3H, *s*)	31.8 (CH$_3$)	C-6
7-CH$_3$	2.34 (3H, *s*)	19.7 (CH$_3$)	C-6, C-7, C-8, C-8a
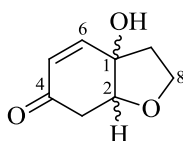
Figure 4.5 Structural Determination of Compound **OSA2**

      OSA2 was obtained as a yellow solid, $[\alpha]_D$ +174.28°, (+0.26°, Endo & Hikino, 1984). This compound exhibited UV (in MeOH) maximum absorption bands (log ε) at 206 (4.90), 225 (4.82), 275 (4.50), and 303 (4.40) nm. The IR (KBr) spectrum showed the absorption bands at 3418 cm^{-1} (a hydroxyl group) and 1668 cm^{-1} (a carbonyl group). The ^{1}H NMR spectral data (table 4.12) exhibited the signals of olefinic protons H-5 (δ 5.87, 1H, *d*, *J* = 10.0 Hz) and H-6 (δ 6.78, 1H, *dd*, *J* = 10.0, 2.0 Hz), and an oxymethine proton δ 4.14 (1H, *td*, *J* = 4.4, 2.0 Hz). Methylene proton H-3 (δ 2.69, 1H, *dd*, *J* = 16.4, 4.4 Hz and 2.73, 1H, *dd*, *J* = 16.4, 4.4 Hz), H-7 (δ 2.24, 2H, *m*), and H-8 (δ 3.79, 1H, *dd*, *J* = 15.2, 7.6 Hz and 3.94, 1H, *dd*, *J* = 15.2, 7.6 Hz) were displayed in spectrum. The olefinic proton H-6 was coupling with methine proton H-2 with a long range coupling (*J* = 2.0, 1.6 Hz). The ^{13}C NMR spectral data and HMBC correlations (table 4.12) supported the assignment. Hence, **OSA2** was identified to be rengyolone (Endo & Hikino, 1984).

Table 4.12 ^{1}H NMR, ^{13}C NMR, and HMBC spectral data of compound **OSA2**
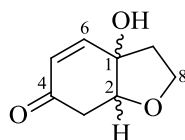
Position	^{1}H NMR (400 MHz, Acetone-d_6)	^{13}C NMR (100 MHz, Acetone-d_6)	HMBC
1	-	75.6 (C)	-
2	4.14 (1H, *td*, *J* = 4.4, 2.0 Hz)	82.0 (CH)	C-1, C-4, C-6
3	2.69 (1H, *dd*, *J* = 16.4, 4.4 Hz)	38.1 (CH$_2$)	C-1, C-2, C-4, C-5
	2.73 (1H, *dd*, *J* = 16.4, 4.4 Hz)		C-1, C-2, C-4
4	-	196.9 (C)	-
5	5.87 (1H, *d*, *J* = 10.0 Hz)	128.5 (CH)	C-1, C-4, C-7
6	6.78 (1H, *dd*, *J* = 10.0, 2.0 Hz)	149.7 (CH)	C-2, C-4, C-7
7	2.24 (2H, *m*)	40.4 (CH$_2$)	C-1, C-2, C-6, C-8
8	3.79 (1H, *dd*, *J* = 15.2, 7.6 Hz)	66.5 (CH$_2$)	C-1, C-2, C-7
	3.94 (1H, *dd*, *J* = 15.2, 7.6 Hz)		
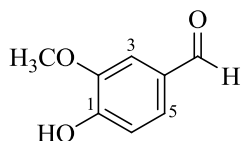
Figure 4.6 Structural Determination of Compound **OSA3**

       OSA3 was isolated as a yellow solid, m.p. 82-84 °C (83-85 °C, Lee, Lu, Kuo, Chen & Sun, 2004). The UV spectrum (in MeOH) showed strong absorption bands (log ε) at 205 (4.27), 214 (4.19), 256 (4.00), and 293 (3.58) nm. The IR (KBr) spectrum showed hydroxyl (3426 cm^{-1}) and carbonyl (1684 cm^{-1}) stretching groups. The ^{1}H NMR spectral data (table 4.13) exhibited two *singlet* signals at δ 3.98 (2-OCH$_3$, 3H) and δ 9.83 (4-C$\underline{H}$O, 1H). The remaining signals are the signals of aromatic protons H-3 at δ 7.44 (*d*, *J* = 1.8 Hz), H-5 at δ 7.43 (*dd*, *J* = 8.4, 1.8 Hz), and H-6 at δ 7.05 (*d*, *J* = 8.4 Hz). The ^{13}C NMR spectral data and the complete HMBC correlations supported the proposed structure as shown in table 4.13. Therefore, **OSA3** was identified as 4-hydroxy-3-methoxybenzaldehyde or vanillin (Lee et al., 2004).

Table 4.13 ^{1}H NMR, ^{13}C NMR, and HMBC spectral data of compound **OSA3**

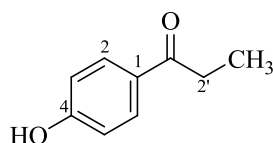| Position	^{1}H NMR (300 MHz, Acetone-d_6)	^{13}C NMR (75 MHz, Acetone-d_6)	HMBC
1	-	151.0 (C)	-
2	-	148.5 (C)	-
3	7.44 (1H, *d*, *J* = 1.8 Hz)	108.8 (CH)	C-1, C-5
4	-	130.0 (C)	-
5	7.43 (1H, *d*, *J* = 8.4, 1.8 Hz)	127.5 (CH)	C-1, C-3
6	7.05 (1H, *d*, *J* = 8.4 Hz)	114.4 (CH)	C-2, C-4
2-OCH$_3$	3.98 (3H, *s*)	148.5 (C)	C-2
4-CHO	9.83 (1H, *s*)	190.8 (CH)	C-3

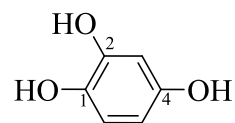**Figure 4.7** Structural Determination of Compound **OSA4**

OSA4 was isolated as a yellow solid, m.p. 148-150 °C (142 °C, González-Calderón et al., 2013). The strong absorption (log ε) at 205 (3.85), 216 (3.77), 260 (3.52), and 289 (3.37) nm were detected on UV spectrum in MeOH. The IR spectrum (KBr) showed maximum absorption bands at 3387 cm^{-1} (O-H stretching) and 1714 cm^{-1} (C=O stretching). The ^{1}H NMR spectral data (table 4.14) exhibited a series of AA'BB' system at δ 7.91 (2H, d, J = 8.8 Hz) and δ 6.92 (2H, d, J = 8.8 Hz) which were assigned to be H-2,6 and H-3,5, respectively. The remaining signals are a *quartet* signal of methylene proton H-2' at δ 3.35 (J = 7.2 Hz) and a *triplet* signal of a methyl 2'-CH$_3$ at δ 1.19 (J = 7.2 Hz). The ^{13}C NMR spectral data (table 4.14) showed nine carbons. These assignment were confirmed by HMBC correlations (table 4.14). **OSA4** was assigned to be 1-(4-hydroxyphenyl)propan-1-one (González-Calderón et al., 2013).

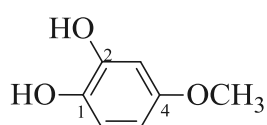**Table 4.14** ^{1}H NMR, ^{13}C NMR, and HMBC spectral data of compound **OSA4**

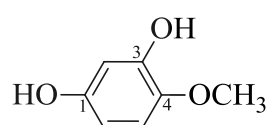| Position	^{1}H NMR (400 MHz, Acetone-d_6)	^{13}C NMR (100 MHz, Acetone-d_6)	HMBC
1	-	123.2	-
2,6	7.91 (2H, d, J = 8.8 Hz)	124.9	C-3, C-4, C-6, C-1'
3,5	6.92 (2H, d, J = 8.8 Hz)	114.9	C-1
4	-	166.5	-
1'	-	199.7	-
2'	3.35 (1H, q, J = 7.2 Hz)	32.9	C-1', 2'-CH$_3$
2'-CH$_3$	1.19 (3H, t, J = 7.2 Hz)	6.3	C-2'
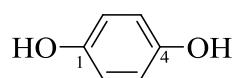
OLA7

1,4-dihydroxybenzene
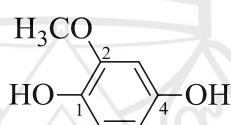
(hydroquinone)

OLA9

1,2,4-trihydroxybenzene

(hydroxyquinol)

4-methoxy-1,2-benzenediol

4-methoxy-1,3-benzenediol

2-methoxy-1,4-benzenediol

Possible Structures of **ORA2**

Figure 4.8 Structural Determination of Compounds **OLA7**, **OLA9**, and **ORA2**

OLA7 was obtained as a yellow solid. The UV spectrum in MeOH exhibited maximum absorption bands (log ε) at 204 (4.79) and 254 (4.70) nm. The IR spectrum (KBr) showed an absorption band at 3387 cm^{-1} (O-H stretching). The ^{1}H NMR spectral data (table 4.15) exhibited two *doublet* signals at δ7.91 (2H, *d*, *J* = 8.4 Hz, H-2,6) and δ 6.91 (2H, *d*, *J* = 8.4 Hz, H-3,5). The resulting structure was corresponded with ^{13}C NMR spectral data (table 4.15) and confirmed by HMBC correlations (table 4.15). According to these data **OLA7** was identified as 1,4-dihydroxybenzene (hydroquinone).

OLA9 was obtained as a yellow solid. The UV spectrum in MeOH exhibited maximum absorptions (log ε) at 208 (4.81), 217 (4.70), 258 (4.40), and 294 (4.13) nm. The IR spectrum (KBr) showed the stretching of a hydroxyl group (3365 cm^{-1}). The ^{1}H NMR spectral data (table 4.16) showed the resonances of an ABM pattern of aromatic protons H-3, H-5, and H-6 at δ 7.52 (1H, *d*, *J* = 2.0 Hz),7.47 (1H, *dd*, *J* = 8.0, 2.0 Hz), and 6.89 (1H, *d*, *J* = 8.0 Hz), respectively. The ^{13}C NMR spectral data (table 4.16) exhibited three methine carbons at δ 117.5 (C-3), 123.2 (C-5), 115.7 (C-6) and three oxygenated carbons at δ 150.7 (C-1), 145.4 (C-2), 167.6 (C-4). The elucidated structure was confirmed by HMBC correlations (table 4.16) of H-3 to C-1, C-2, C-4, C-5; H-5 to C-1, C-2, C-3, C-4, C-6; H-6 to C-1, C-2, C-3, C-4, C-5. According to the ^{13}C NMR and HMBC correlations, therefore, **OLA9** was identified to be 1,2,4-trihydroxybenzene or hydroxyquinol.

ORA2 was obtained as a yellow solid. The UV spectrum in MeOH exhibited maximum absorption bands (log ε) at 206 (4.03), 246 (3.93), 257 (3.72), and 289 (3.38) nm. The IR spectrum (KBr) showed an absorption band at 3301 cm^{-1} (hydroxyl group). The ^{1}H NMR spectral data (table 3) exhibited a *singlet* signal of a methoxy group at δ 3.90 (3H, *s*) and an ABX pattern at δ 7.56 (1H, *d*, *J* = 1.6 Hz), 7.59 (1H, *dd*, *J* = 8.4, 1.6 Hz), and 6.90 (1H, *d*, *J* = 8.0 Hz). According to these data **ORA2** can be predicted to be three possible structure, as shown in figure 4.9.

Table 4.15 ^{1}H NMR, ^{13}C NMR, and HMBC spectral data of compound **OLA7**

HO—⟨1⟩—⟨4⟩—OH
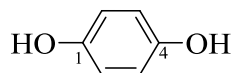
Position	^{1}H NMR(400 MHz, Acetone-d_6)	^{13}C NMR(100 MHz, Acetone-d_6)	HMBC
1	-	168.0	-
2,6	7.91 (2H, d, J = 8.4 Hz)	122.6	C-1, C-3,5, C-4
3,5	6.91 (2H, d, J = 8.4 Hz)	132.6	C-2,6, C-4
4	-	162.2	-

Table 4.16 ^{1}H NMR, ^{13}C NMR, and HMBC spectral data of compound **OLA9**

HO—⟨2⟩
HO—⟨1⟩—⟨4⟩—OH
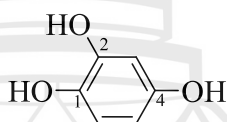
Position	^{1}H NMR(400 MHz, Acetone-d_6)	^{13}C NMR(100 MHz, Acetone-d_6)	HMBC
1	-	150.7	-
2	-	145.4	-
3	7.52 (1H, d, J = 2.0 Hz)	117.5	C-1, C-2, C-4, C-5
4	-	167.6	-
5	7.47 (1H, dd, J = 8.0, 2.0 Hz)	123.2	C-1, C-2, C-3, C-4, C-6
6	6.89 (1H, d, J = 8.0 Hz)	115.7	C-1, C-2, C-3, C-4, C-5

HO—⟨2⟩
HO—⟨1⟩—⟨4⟩—OCH₃   H₃CO—⟨2⟩
HO—⟨1⟩—⟨4⟩—OH   OH—⟨3⟩
HO—⟨1⟩—⟨4⟩—OCH₃
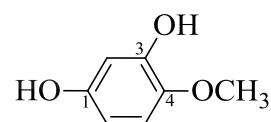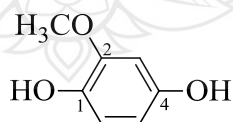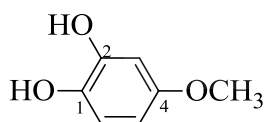
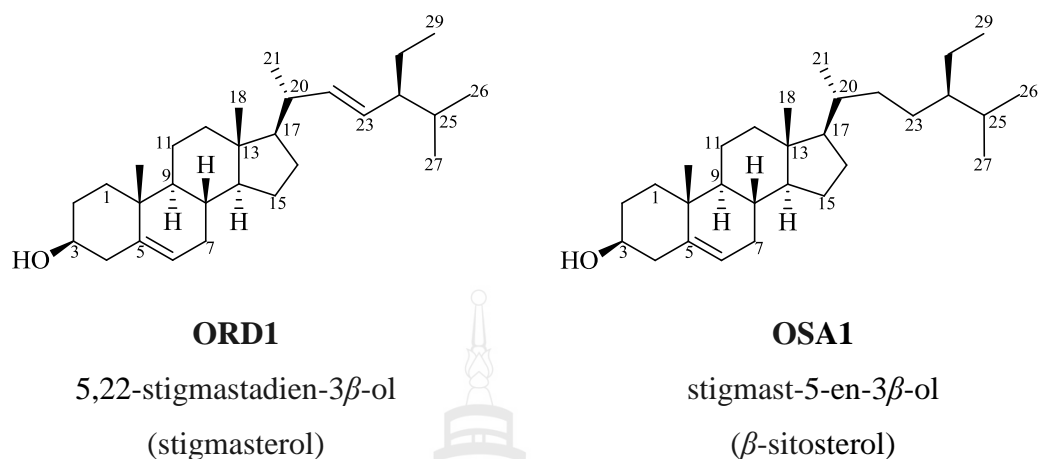**Figure 4.9** Possible Structures of **ORA2**

Figure 4.10 Structural Determination of Compounds **ORD1** and **OSA1**

ORD1 was isolated as a white solid, m.p. 162-164 °C (163-166 °C, Nyamoita, 2013). The ^{1}H NMR spectral data (table 4.17) showed the presence of three olefinic protons H-6 (δ 5.28, *d*, *J* = 4.8 Hz,),H-22 (δ 5.08, *m*),H-23 (δ 4.94, *m*), and an oxymethine proton H-3 (δ 3.46, *m*). Moreover, the signals of six methyl groups were shown at δ 1.02 (*br s*, 21-CH$_3$), δ 1.02 (*s*, 19-CH$_3$), δ 0.74×2 (*br s*, 27-CH$_3$, 29-CH$_3$), δ 0.74 (*s*, 26-CH$_3$), and δ 0.62 (*s*, 18-CH$_3$). The ^{1}H and ^{13}C NMR data were corresponded to the previous reported data (Forgo & Köver, 2004). The structure of **ORD1** was proposed to be 5,22-stigmastadien-3β-ol or stigmasterol.

OSA1 was obtained as a white solid, m.p. 136-138 °C (136-140 °C, Oja, Chen, Hajaligol & Chan, 2009). The ^{1}H NMR spectral data (table 4.17) exhibited an oxymethine proton H-3 (δ 3.53, *m*) and an olefinic proton H-6 (δ 5.36, *m*). The presence of six methyl groups were deduced by the signals at δ 0.63 (*s*, H-18), δ 0.81 (*d*, *J* = 6.5 Hz, H-27), δ 0.84 (*d*, *J* = 6.5 Hz, H-26), δ 0.85 (*t*, *J* = 8.0 Hz, H-29), δ 0.92 (*d*, *J* = 6.5 Hz, H-21), and δ 1.01 (*s*, H-19). The ^{1}H NMR spectral data of **OSA1** was identical with those of stigmast-5-en-3β**-**ol, which was known as β-sitosterol (Nguyen et al., 2004).

Table 4.17 ^{1}H NMR and ^{13}C NMR spectral data of compounds **ORD1** and **OSA1**

Position	ORD1		OSA1
	^{1}H NMR (300 MHz, CDCl$_3$)	^{13}C NMR (75 MHz, CDCl$_3$)	^{1}H NMR (300 MHz, CDCl$_3$)
1	1.81 (1H, *m*), 1.02 (1H, *m*)	37.3	1.08 (*m*), 1.84 (*m*)
2	1.83 (1H, *m*), 1.50 (1H, *m*)	28.9	1.59 (*m*), 1.96 (*m*)
3	3.46 (1H, *m*)	71.8	3.53 (1H, *m*)
4	2.19 (2H, *m*)	42.3	2.24 (1H, *m*), 2.31 (1H, *m*)
5	-	140.8	-
6	5.28 (1H, *d*, *J* = 4.8 Hz)	121.4	5.36 (1H, *m*)
7	1.94 (1H, *m*), 1.50 (1H, *m*)	31.9	1.98 (2H, *m*)
8	1.44 (1H, *m*)	31.9	1.50 (*m*)
9	0.89 (1H, *m*)	50.1	0.93 (*m*)
10	-	36.5	-
11	1.58 (1H, *m*)	24.4	1.02 (*m*), 1.57 (*m*)
12	1.19 (2H, *m*)	39.8	1.28 (*m*), 2.03 (*m*)
13	-	39.7	-
14	1.02 (1H, *m*)	56.9	1.02 (*m*)
15	1.50 (1H, *m*), 1.02 (1H, *m*)	24.3	1.08 (*m*), 1.15 (*m*)
16	1.13 (2H, *m*)	28.3	1.83 (*m*), 1.86 (*m*)

Table 4.17 (continued)
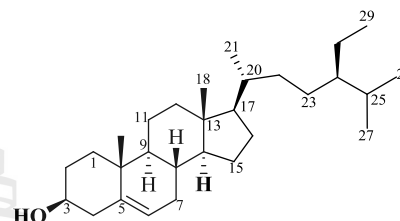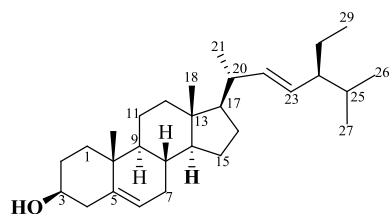
Position	ORD1		OSA1
	¹H NMR (300 MHz, CDCl₃)	¹³C NMR (75 MHz, CDCl₃)	¹H NMR (300 MHz, CDCl₃)
17	1.02 (1H, *m*)	56.1	1.15 (*m*)
18	0.62 (3H, *s*)	12.2	0.63 (3H, *s*)
19	1.02 (3H, *s*)	21.1	1.01 (3H, *s*)
20	2.17 (1H, *m*)	40.5	1.28 (m)
21	1.02 (3H, *br s*)	21.2	0.92 (3H, *d*, *J* = 6.5 Hz)
22	5.08 (1H, *m*)	138.3	1.00 (*s*), 1.29 (*m*)
23	4.94 (1H, *m*)	129.3	1.16 (2H, m)
24	1.46 (1H, *m*)	51.3	0.93 (m)
25	1.59 (1H, *m*)	31.9	1.66 (m)
26	0.74 (3H, *s*)	19.4	0.84 (3H, *d*, *J* = 6.5 Hz)
27	0.74 (3H, *br s*)	19.0	0.81 (3H, *d*, *J* =6.5 Hz)
28	1.43 (1H, *m*), 1.19 (1H, *m*)	25.4	1.25 (*br s*)
29	0.74 (3H, *br s*)	12.1	0.85 (3H, *t*, *J* = 8.0 Hz)

4.2 Evaluation of Antibacterial Activity

4.2.1 Antibacterial Activity of Crude Extracts

Crude extracts of *O. indicum* (LH, LD, LA, LM, RD, RA, SA, SM, TD, TA, and TM) were tested for antibacterial activity against gram-positive bacteria (*B. cereus* TISTR 687, MRSA-SK1, *S. aureus* TISTR 1466) and gram-negative bacteria (*E. coli* TISTR 780, *P. aurenginosa* TISTR 781, *S. typhimurium* TISTR 292) by Broth Microdilution Method (Clinical and Laboratory Standards Institute, 2002).

In screening results, all crude extracts exhibited the positive screening results which were able to inhibit the growth of gram-positive and gram-negative bacteria. Therefore, all crude extracts were selected for determining the minimum inhibition concentrations (MICs) values.

The MIC values of all crude extracts were summarized in table 4.18. The crude SA extract exhibited strong antibacterial activity against MRSA with MICs value of 80 μg/mL. Moreover, crude LA, SA, SM, TD, and TA extracts exhibited moderate antibacterial activity against gram-positive bacteria with MICs in range of 160-320 μg/mL. All crude extracts showed weak antibacterial activity against gram-negative bacteria with MICs values of 640-1,280 μg/mL. Hence, all crude extracts of *O. indicum* exhibited stronger antibacterial activity against gram-positive than gram-negative bacteria. Gram-negative bacteria having an outer polysaccharide membrane carrying the structural lipopolysaccharide components which were impermeable to lipophilic solutes. Gram-positive bacteria were more susceptible, perhaps as a consequence of the gram-negative outer membrane barrier (Kong, Chen, Xing & Park, 2010), a reason of antibacterial potency could be described to cell surface characteristics differences between gram-positive and gram-negative bacteria.

Table 4.18 MICs Values of Antibacterial Activity of *O. indicum* Crude Extracts

Crude	MIC (µg/mL)					
	Gram Positive			**Gram Negative**		
	B.C	**MRSA-SK1**	**S.A**	**E.C**	**S.T**	**Ps.A**
LH	640	1280	1280	640	1280	1280
LD	640	1280	1280	640	1280	1280
LA	320	160	160	640	1280	1280
LM	640	1280	1280	640	1280	1280
RD	640	1280	1280	1280	1280	1280
RA	640	1280	1280	640	1280	1280
SA	640	80	160	640	1280	640
SM	1280	320	640	640	1280	1280
TD	640	640	320	640	1280	1280
TA	160	320	320	640	1280	1280
TM	1280	1280	N/A	640	1280	1280
Vancomycin	1	1	2	-	-	-
Gentamicin	-	-	-	0.25	0.125	0.5

4.2.2 Antibacterial Activity of Pure Compounds

All isolated compounds obtained from crude extracts (LH, LD, LA, LM, RD, RA, SA, SM, TD, TA, and TM) were evaluated for their antibacterial activity against gram-positive bacteria (*B. cereus* TISTR 687, MRSA-SK1, *S. aureus* TISTR 1466) and gram-negative bacteria (*E. coli* TISTR 780, *P. aurenginosa* TISTR 781, *S. typhimurium* TISTR 292) by broth microdilution method (CLSI, 2002). All isolated compounds which showed the positive screening results were further selected to determine the minimum inhibition concentrations (MICs) values.

The MICs values of all isolated compounds were summarized in table 4.19. Compound **OLA3** exhibited significant antibacterial activity against MRSA with an MIC value of 32 μg/mL, whereas xanthonolignoid **OLA8** exhibited stronger activity against *B. cereus* with an MIC value of 16 μg/mL according to the other xanthonolignoid, such as cadensin D from *Hypericum riparium* showed antibacterial activity against both of *E. coli* and *Enteroccocus faecalis* with MIC value of 125 μg/mL (Tala et al., 2013). In addition, other isolated compounds showed weak antibacterial activity against gram-positive and gram-negative bacteria with MICs range of 64-128 μg/mL. The resulting antibacterial activity was corresponded with antibacterial activity against gram-positive and gram-negative bacteria of the crude extracts as shown in table 4.18.

Table 4.19 MICs Values of Antibacterial Activity of *O. indicum* Isolated Compounds

Isolated Copound	MIC (µg/mL)					
	Gram Positive			Gram Negative		
	B.C	MRSA-SK1	S.A	E.C	S.T	Ps.A
OLA1	128	128	128	128	128	128
OLA2	128	128	128	128	128	128
OLA3	64	32	128	128	128	128
OLA5	128	128	128	128	128	128
OLA7	128	>128	>128	128	128	128
OLA8	16	128	64	128	128	128
OLA9	128	>128	>128	128	>128	128
OLA10	128	128	128	128	128	128
ORD2	128	128	128	128	128	128
ORD3	64	64	128	64	128	128
ORD4	128	128	128	128	128	128
ORA1	128	>128	>128	128	128	128
ORA2	128	>128	>128	128	128	128
OSA2	128	128	128	128	128	128
OSA3	128	>128	>128	>128	128	128
OSA4	128	>128	>128	>128	128	128
OSA5	64	64	128	64	128	128
OTA1	128	128	128	128	128	128
OTA2	128	128	128	128	128	128
Vancomycin	1	1	2	-	-	-
Gentamicin	-	-	-	0.25	0.125	0.5

4.3 Evaluation of Antioxidation Activity

Antioxidation activity evaluation of crude extracts and isolated compounds from *O. indicum* were studied on the basis of scavenging activity of the stable (DPPH) free radical by FIA method. The DPPH assay is one of the methods used for antioxidant testing on free radical terminator because its odd electron can be used as a convenient tool for the antioxidant assay. The DPPH free radical is dark violet solid, its solubility is not great, alcoholic solution having concentrations of approximately 5×10^{-4} are nevertheless densely colored. Its solution shows a strong absorption band at λ 520 nm (in ethanol). The capacity of the substances to donate electrons can be estimated from the degree of loss color (Blois, 1958). Coexistence of an antioxidant compound (AH) and free radical (DPPH$^{\bullet}$) leads to the disappearance of DPPH free radical and the appearance the free radical (A$^{\bullet}$) as shown in figure 4.11.
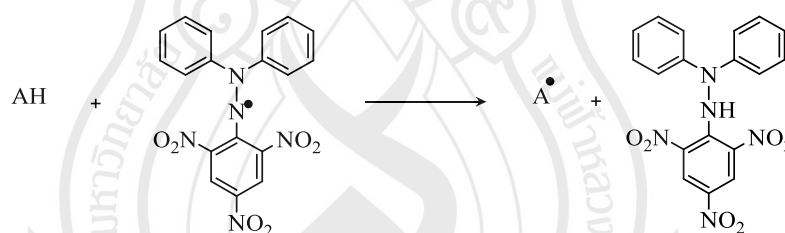

Figure 4.11 DPPH Free Radical and the Appearance of the Free Radical

4.3.1 Screening on the Antioxidation Activity and Evaluation of 50% Inhibition Concentration (IC$_{50}$) of Crude Extracts of *O. indicum*
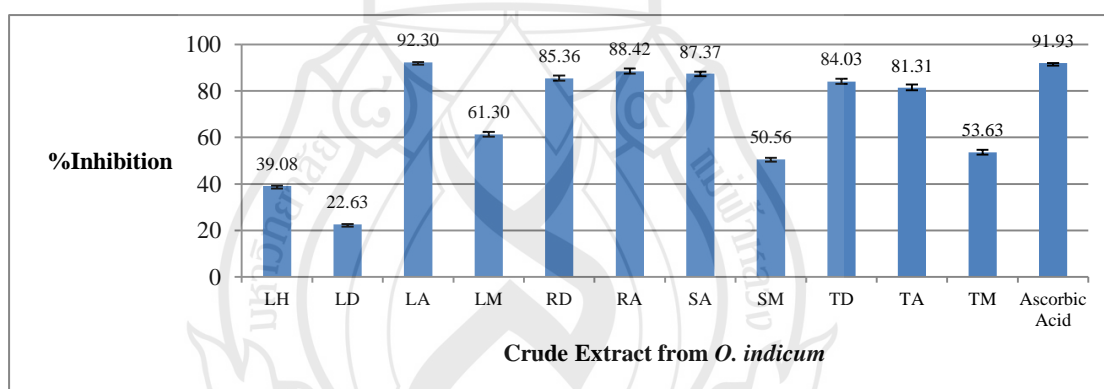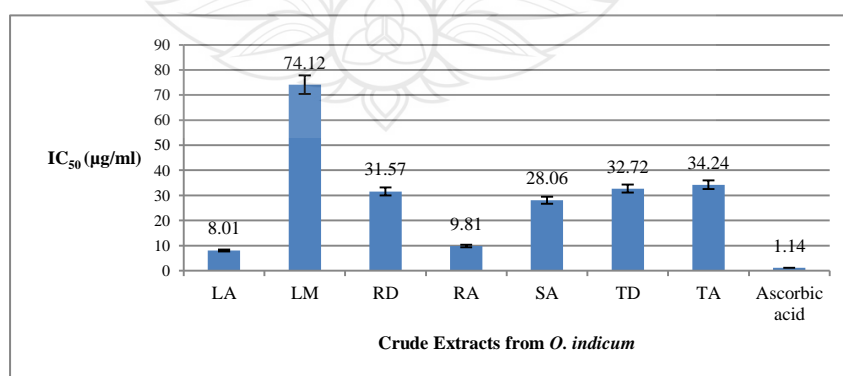
Screening and IC$_{50}$ evaluation of the crude extracts were tested for antioxidation property, which the concentration of crude extracts at 6.1 mg/mL were used. The activity was determined by FIA method based on the decrease of absorbance of the DPPH solution at 520 nm.

The results of antioxidation activity screening of crude extracts exhibited in table 4.20 and figure 4.12. The acetone extract of leaves was the most able to scavenge the DPPH radical (92.30% inhibition) followed by crude RA, SA, RD, TD and TA extracts with percentage inhibition of 88.42, 87.37, 85.36, 84.03, and 81.31, respectively. The ascorbic acid exhibited 91.93% inhibition. The crude LM, TM, and SM extracts exhibited percentage of scavenge in range 50-60% (61.28, 53.63, and 50.56% inhibition, respectively). The other crude extracts (LH and LD) showed percentage of inhibition less than 50%.

Crude extracts, which showed inhibited percentage of inhibition more than 50%, were evaluated IC$_{50}$ values, as shown in table 4.20 The various concentration (6.10, 3.05, 1.53. 0.76, and 0.38 µg/mL) of crude LA, RA, SA, RD, TD, TA, and LM extracts were plotted againt % inhibition. Their crude extracts exhibited IC$_{50}$ values of 8.01 ± 0.29, 9.81 ± 0.09, 28.06 ± 1.66, 31.57 ± 1.08, 32.72 ± 0.41, 34.24 ± 1.77, and 74.12 ± 0.91 µg/mL, respectively (table 4.20 and figure 4.13). Crude LA and RA extracts exhibited strong antioxidative activity than that of ascorbic acid (IC$_{50}$ value of 1.14 ± 0.01 µg/mL) whereas crude SA, RD, TD, and TA extracts showed moderate antioxidative activity. The results inferred that acetone were suitable solvent to extract the antioxidant compounds from *O. indicum*. The crude extracts showed difference antioxidative activity may be because the extract contained a mixture of phenolic compounds at different levels according to the polarity of solvent used in the extraction process (Zarena & Sankar, 2009).

Table 4.20 The % Inhibition and IC$_{50}$ Values of Crude Extracts from *O. indicum*

Crude Extract	Antioxidation Activity	
	% Inhibition ± SD	IC$_{50}$ ± SD (μg/mL)
LH	39.08 ± 0.18	N/A
LD	22.63 ± 0.09	N/A
LA	92.30 ± 0.03	8.01 ± 0.29
LM	61.30 ± 1.04	74.12 ± 0.91
RD	85.36 ± 1.27	31.57 ± 1.08
RA	88.42 ± 1.15	9.81 ± 0.09
SA	87.37 ± 0.93	28.06 ± 1.66
SM	50.56 ± 0.64	N/A
TD	84.03 ± 1.22	32.72 ± 0.41
TA	81.31 ± 1.43	34.24 ± 1.77
TM	53.63 ± 1.01	N/A
Ascorbic Acid	91.93 ± 0.04	1.14 ± 0.01

Figure 4.12 Inhibition Percentage of Crude Extracts from *O. indicum*

Figure 4.13 IC$_{50}$ Values of Crude Extracts from *O. indicum*

4.3.2   Screening on Antioxidation Activity and Evaluation of 50% Inhibition Concentration (IC_{50}) of Isolated Compounds of *O. indicum*

The isolated compounds of *O. indicum* were evaluated antioxidation activity using FIA method following the decrease of absorbance of the DPPH solution at 520 nm. The concentration of isolated compounds were used at 3.05 mM.

Screening on antioxidation activity of isolated compounds exhibited the % inhibition, as shown in table 4.21 and figure 4.14. Compounds **OLA5**, **OLA10**, and **OTA1** exhibited high efficacy of the DPPH scavenging radical with 84.78%, 73.91%, and 69.49% inhibition, respectively. Compounds **OLA1**, **OLA2**, **OLA3**, **OLA7**, **OLA8**, **OLA9**, **OSA2**, **ORD1**, **ORD2**, **ORD3**, **ORD4**, **ORA1**, **ORA2**, **OSA1**, **OSA2**, **OSA3**, **OSA4**, **OSA5**, and **OTA2** showed the percentage of inhibition less than 50%.

The results of antioxidation activity of isolated compounds **OLA5**, **OLA10**, and **OTA1** were expressed at IC_{50} values of 11.88 ± 0.06, 33.45 ± 1.45, and 54.76 ± 1.56 μM, respectively (table 4.21 and figure 4.15) whereas ascorbic acid showed IC_{50} value of 6.45 ± 0.04 μM. **OLA5** and **OLA10** exhibited strong and moderate antioxidative activity with IC_{50} values of 11.88 and 33.45 ± 1.45 μM, respectively.

From the results, **OLA5**, **OLA10**, and **OTA1** are flavonoid compounds which showed the percentage of inhibition more than 50% and exhibited strong to moderate antioxidation activity. As a result of antioxidation activity is attributed to their hydrogen-donating ability. Extremely, the phenolic part of flavonoids serve as a source of a readily available H atoms which the subsequent radicals produced can be delocalized over the flavonoid structure. Free radical scavenging capacity is primarily attributed to high reactivities of hydroxyl substituents that participate in the reaction (Heim et al., 2002). Also, the DPPH scavenging activity was related to the number of the active group, as the compounds have more than one active group, they become more activite (Bendary, Francis, Ali, Sarwat & Hady, 2013). According to these data, **OLA5** possessed more hydroxyl groups than other flavonoids. Therefore, **OLA5** showed strong antioxidation activity.

Table 4.21 The % Inhibition and IC$_{50}$ Values of Crude Extracts from *O. indicum*

Isolated Compound	Antioxidation Activity	
	% Inhibition ± SD	IC$_{50}$ ± SD (µM)
OLA1	8.27 ± 0.23	N/A
OLA2	7.68 ± 0.09	N/A
OLA3	7.39 ± 0.05	N/A
OLA5	84.78 ± 1.14	11.88 ± 0.06
OLA7	7.06 ± 0.15	N/A
OLA8	8.27 ± 0.97	N/A
OLA9	8.93 ± 0.34	N/A
OLA10	73.91 ± 1.24	33.45 ± 1.45
ORD1	6.96 ± 0.07	N/A
ORD2	9.11 ± 0.86	N/A
ORD3	12.85 ± 1.22	N/A
ORD4	7.73 ± 0.49	N/A
ORA1	8.86 ± 0.08	N/A
ORA2	8.09 ± 0.10	N/A
OSA1	6.07 ± 0.02	N/A
OSA2	7.58 ± 0.11	N/A
OSA3	7.01 ± 0.09	N/A
OSA4	8.16 ± 0.21	N/A
OSA5	7.98 ± 0.16	N/A
OTA1	69.49 ± 1.38	54.76 ± 1.56
OTA2	8.60 ± 0.50	N/A
Ascorbic Acid	91.93 ± 0.05	6.45 ± 0.04
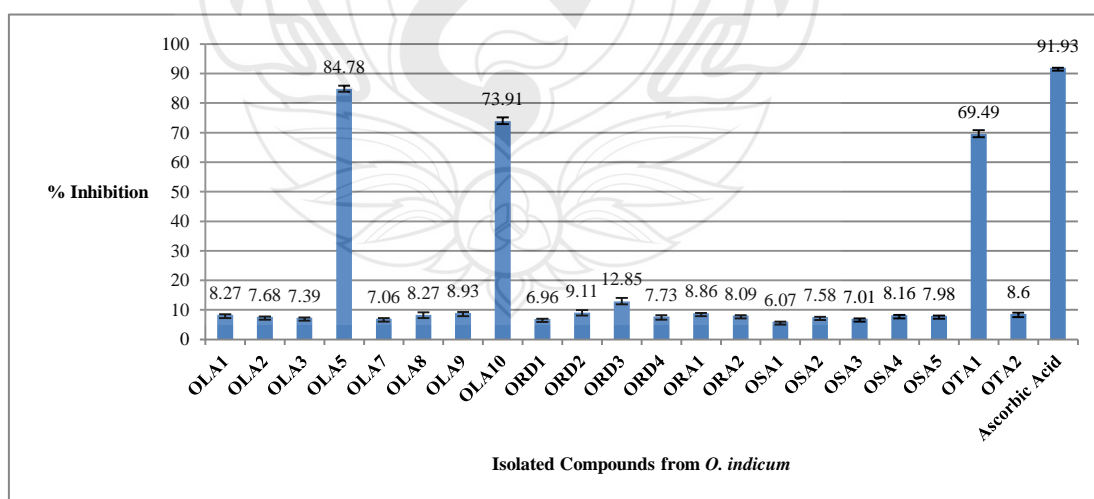
Figure 4.14 Inhibition Percentage of Isolated Compounds from *O. indicum*
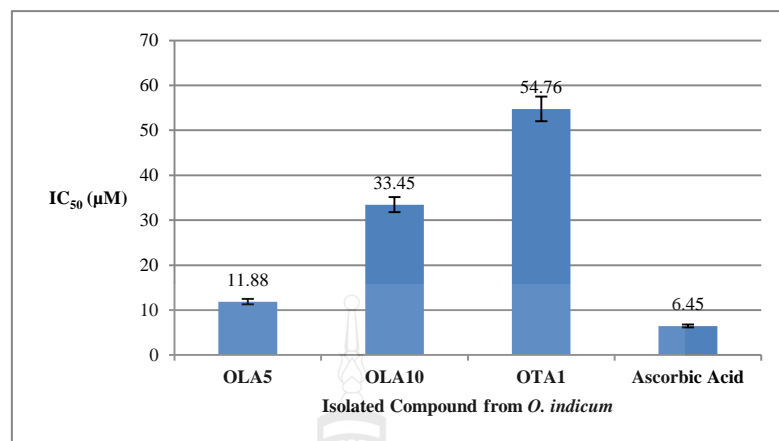
Figure 4.15 IC_{50} Values of Isolated Compounds from *O. indicum*

4.4 Structure Relationship of Isolated Compounds from

Oroxylum indicum

Chromatographic separation of the extracts from the leaves, roots, stems, and twigs of *O. indicum* revealed the presence of flavones and xanthones which were two major components in this plant. Secondary metabolites of *O. indicum* based on the intermediates of the shikimate pathway. The resulting hydroxycinnamic acids and esters are amplified in several cascades by a combination of reductases, oxygenases, and transferases to result in an organ and developmentally specific pattern of metabolites, characteristic for each plant species (Vogt, 2010). The biosynthetic pathway (figure 4.16) are described for production of flavones and xanthones. Flavonoid and xanthone compounds were possibly obtained from the precursor (**OSA5** and 1,3,7-trihydroxyxanthone) by reduction, hydroxylation, and methylation processes as shown in figure 4.17 and 4.18.
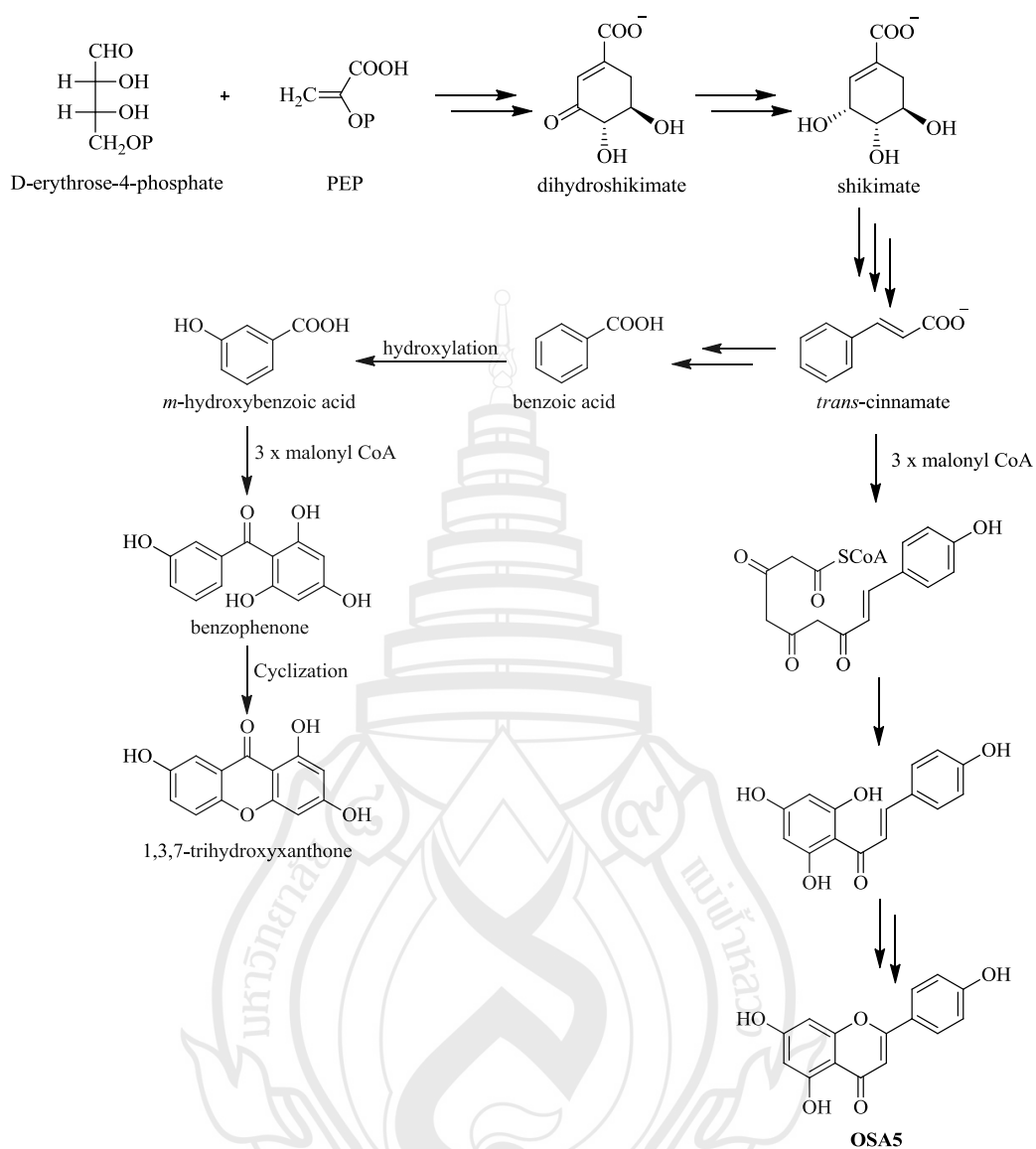
Figure 4.16 Precursor of Flavonoid and Xanthone Compounds via Shikimate Pathway
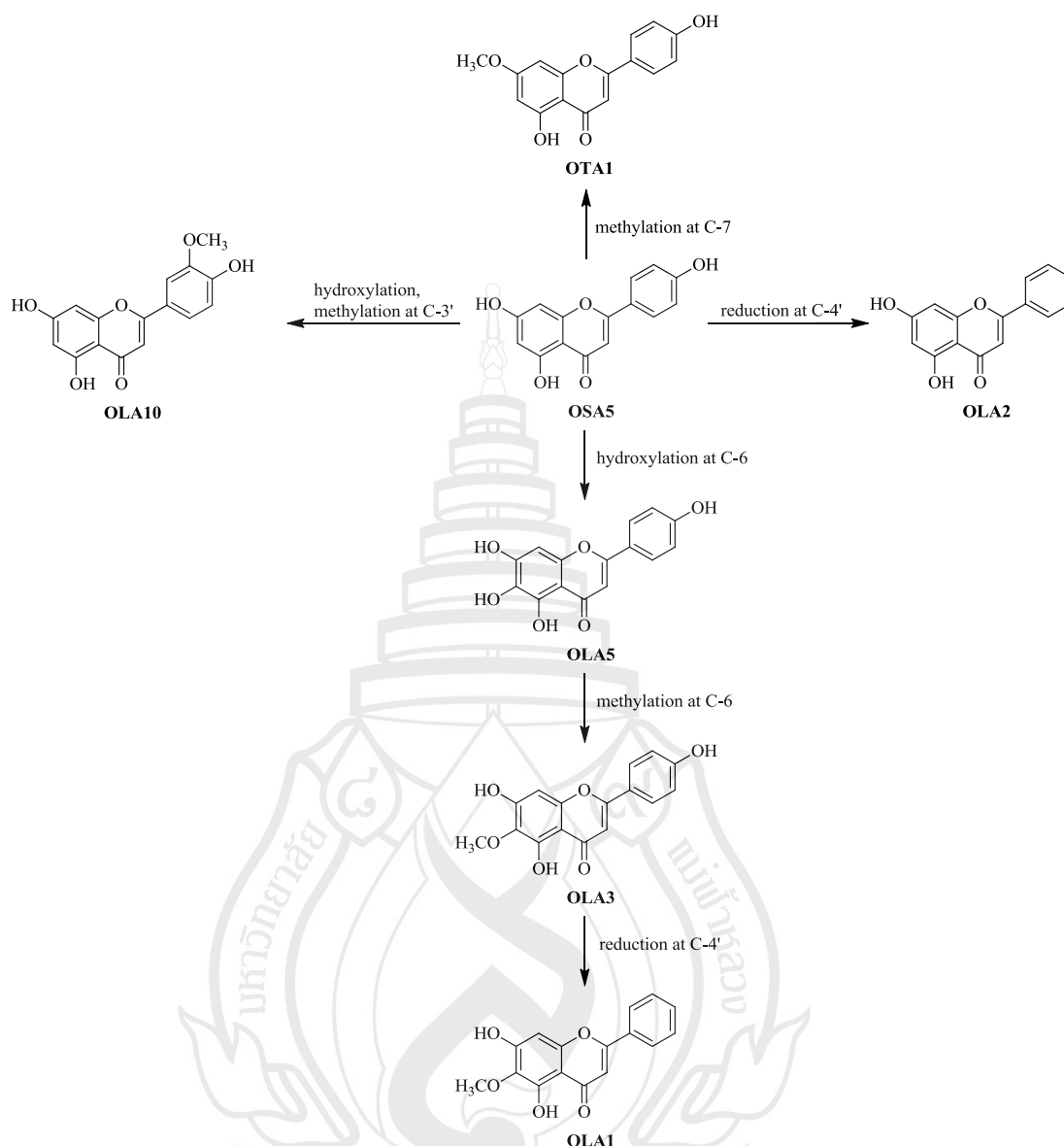
Figure 4.17 Structure Relationship of Flavonoid Compounds from *O. indicum*

The proposed biosynthetic pathway of flavonoid derivatives of *O. indicum* showed in figure 4.17. **OSA5** was proposed to be a precursor of flavonoid derivatives (**OLA1**, **OLA2**, **OLA3**, **OLA5**, **OLA10**, and **OTA1**). Methylation of **OSA5** at C-7 gave **OTA1** whereas reduction of **OSA5** at C-4' afforded **OLA2**. **OLA10** was obtained by hydroxylation followed by methylation at C-3' of **OSA5**. Hydroxylation of **OSA5** at C-6 gave **OLA5**, afterwards methylation of **OLA5** at C-6 yielded **OLA3**. **OLA1** was obtained from **OLA3** by reduction at C-4'.
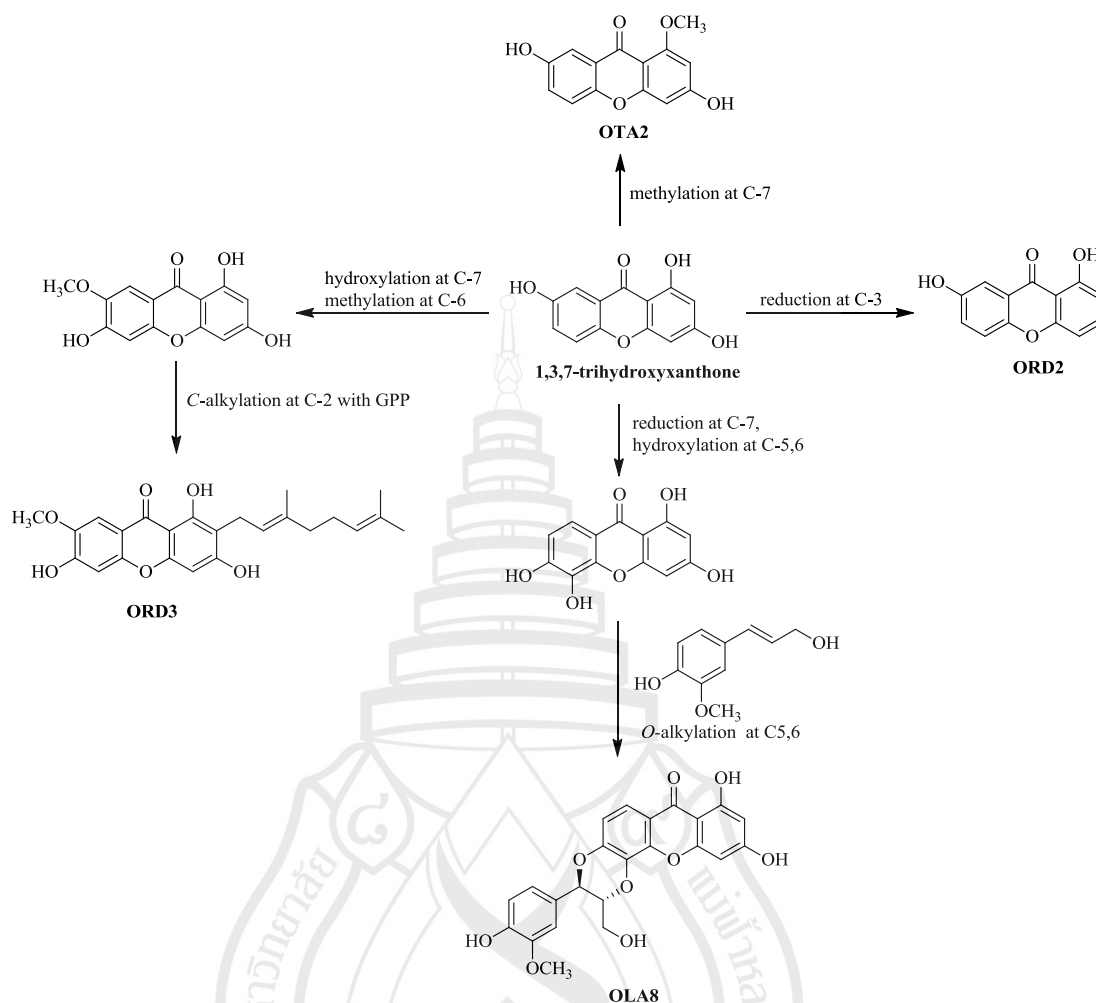
Figure 4.18 Structure Relationship of Xanthone Compounds from *O. indicum*

Xanthone derivatives of *O. indicum* were proposed by biosynthetic pathway as shown in figure 4.18. 1,3,7-trihydroxyxanthone act as a precursor of xanthone derivatives (**OLA8**, **ORD2**, **ORD3**, and **OTA2**). **OTA2** was obtained from a precursor by methylation at C-7. Reduction of a precursor at C-3 afforded **ORD2**. Hydroxylation and methylation of a precursor at C-7 and C-6, respectively, afterwards it was *C*-alkylated with GPP at C-2 gave **ORD3**. Reduction and hydroxylation of a precursor at C-7, C-5, and C-6, respectively, after that *O*-alkylation with coniferol at C-5 and C-6 afforded **OLA8**.

CHAPTER 5

CONCLUSIONS

In conclusion, the phytochemical study of *O. indicum* of the leaves, roots, stems, and twigs had led to the isolation of twenty one known compounds. There are **OLA1** (oroxylin A), **OLA2** (chrysin), **OLA3** (hispidulin), **OLA5** (scutellarein), **OLA7** (hydroquinone), **OLA8** (5'-demethoxycadensin G), **OLA9** (hydroxyquinol), **OLA10** (chrysoeriol), **ORD1** (stigmasterol), **ORD2** (euxanthone), **ORD3** (cowaxanthone), **ORD4** (orientalone), **ORA1** (heraclenin), **OSA1** (*β*-sitosterol), **OSA2** (rengyolone), **OSA3** (vanillin), **OSA4** (1-(4-hydroxyphenyl)propan-1-one), **OSA5** (apigenin), **OTA1** (genkwanin), **OTA2** (3,7-dihydroxy-1-methoxyxanthone), and three possible structures of **ORA2** (2-methoxy-1,4-benzenediol or 4-methoxy-1,2-benzenediol or 4-methoxy-1,3-benzenediol).
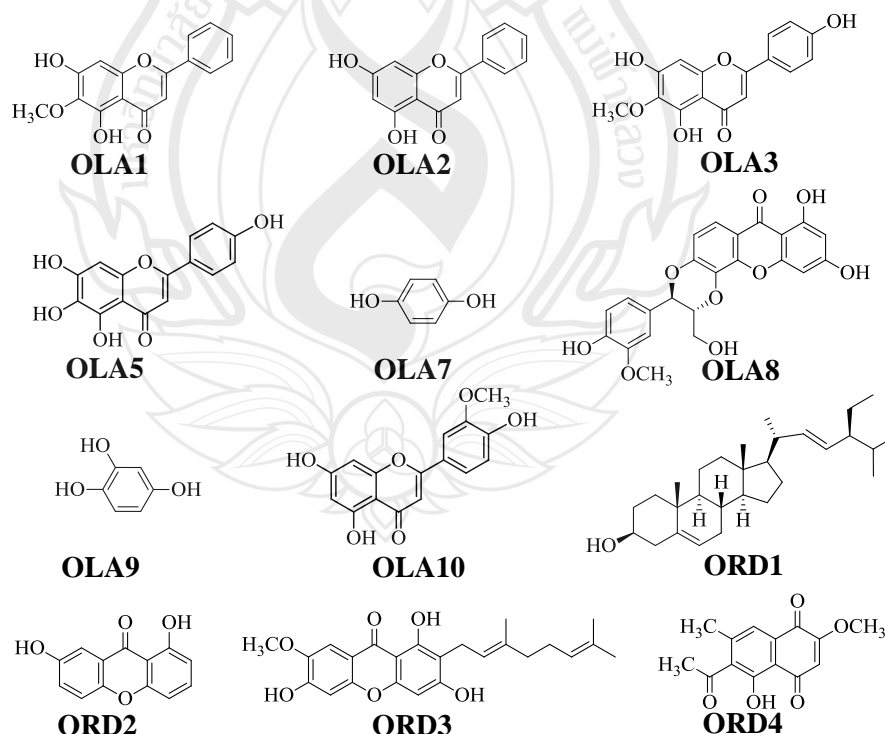

Figure 5.1 Structures of Isolated Compounds from *O. indicum*

ORA1　　**OSA1**　　**OSA2**

OSA3　　**OSA4**　　**OSA5**

OTA1　　**OTA2**

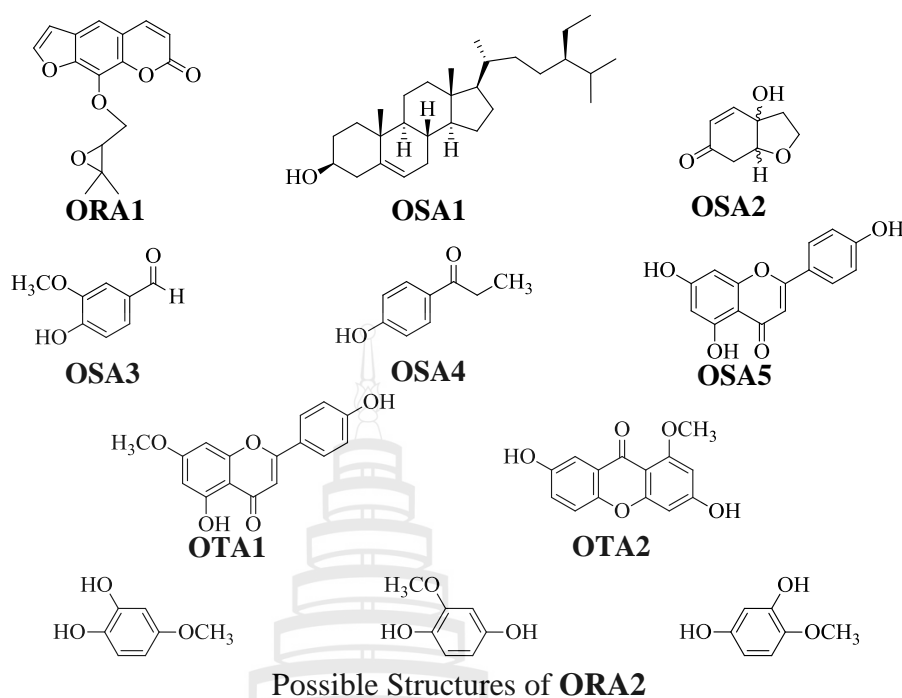Possible Structures of **ORA2**

Figure 5.1 (continued)

The biological activities of the crude extracts and some isolated compounds were evaluated for their antibacterial and antioxidation activities. The acetone extract from the leaves and the roots were exhibited strong radical scavenging activity with IC_{50} of 8.01 ± 0.29 and 9.81 ± 0.09 µg/mL. **OLA5** and **OLA10** exhibited strong and moderate antioxidative activity with IC_{50} values of 11.88 ± 0.06 and 33.45 ± 1.45 µM, respectively. In addition, all crude extracts exhibited weak to moderate antibacterial activities against gram-positive and gram-negative bacteria. **OLA3** was found to possess moderate activity against MRSA-SK1 with an MIC value of 32 µg/mL, whereas **OLA8** exhibited strong activity against *B. cereus* with an MIC value of 16 µg/mL.

In the future, the acetone extract and active compounds of *O. indicum* should be studied extensively in animal models for antitumor-promoting, immunomodulatory and chronic toxic effects because there have been no reports on these aspects in animal models. Some active compounds might be further studied in the field of cosmetic, pharmacy or agriculture. The results will contribute significantly to scientific basic of traditional medicine. Therefore, the isolation of chemical constituents and evaluation of biological activities of *O. indicum* is of great importance because of their role in drug development and in management of many chronic diseases.

REFERENCES

REFERENCES

Al-Bakri, A. G. & Afifi, F. U. (2007). Evaluation of antimicrobial activity of selected plant extracts by rapid XTT colorimetry and bacterial enumeration. *J Microbiol Methods*, *68*, 19–25.

Ali, M. R., Houghton, P. J., Raman, A. & Hoult, J. R. S. (1998). Antimicrobial and antiinflammatory activities of extracts and constituents of *Oroxylum indicum* (L.) Vent. *Phytomedicine*, *5*, 375–381.

Aliyu, A. B., Ibrahim, M. A., Musa, A. M., Ibrahim, H., Abdulkadir, I. E. & Oyewale, A. O. (2009). Evaluation of antioxidant activity of leave extract of *Bauhinia rufescens* Lam. (Caesalpiniaceae). *J Med Plants Res*, *3*, 563-567.

Anushia, C., Sampathkumar, P. & Ramkumar, L. (2009). Antibacterial and antioxidant activities in *Cassia auriculata*. *Proteus*, *3*, 127-130.

Ayatollahi, S. A., Shojaiia, A., Kobarfard, F., Mohammadzadehd, M. & Choudharye, M. I. (2009). Two Flavones from *Salvia leriaefolia*. *Iran J Pharm Res*, *8*(3),179–184.

Babu, T. H., Manjulatha, K., Kumar, S. G., Hymavathi, A., Tiwari, A. K., Purohit, M., Rao, M. J. & Babu, S. K. (2010). Gastroprotective flavonoid constituents from *Oroxylum indicum* Vent. *Bioorg Med Chem Lett*, *20*, 117–120.

Bendary, E., Francis, R. R., Ali, H. M. G., Sarwat, M. I. & Hady, S. E. (2013). Antioxidant and structure–activity relationships (SARs) of some phenolic and anilines compounds. *Ann Agric Sci*, *58*, 173–181.

Blois, M. S. (1958). Antioxidant determinations by the use of a stable free radical. Nature, *181*, 1199-1200.

Bose, P. K. & Battachaya, S. N. (1938). Natural flavones II colouring matters of the bark of *Oroxylum indicum* Vent. *J Indian Chem Soc*, *15*, 311-16.

Brahma, B., Prasad, B. S., Verma, K. A. & Rosangkima, G. (2011). Study on the antitumor efficacy of some select medicinal plants of assam against murine ascites Dalton's lymphoma. *Pharmacologyonline*, *3*, 155-168.

Chen, L.-J., Games, D. E. & Jones, J. (2003). Isolation and identification of four flavonoid constituents from the seeds of *Oroxylum indicum* by high-speed counter-current chromatography. *J Chromatogr A*, *988*, 95–105.

Chen, V., Staub, R. E., Baggett, S., Chimmani, R., Tagliaferri, M., Cohen, I., & Shtivelman, E. (2012). Identification and analysis of the active phytochemicals from the anti-cancer botanical extract Bezielle. *PloS One*, *7*.

Clinical and Laboratory Standards Institute. (2002). *Reference method for dilution antimicrobial susceptibility test for bacteria that grow aerobically. approved Standard M7-A4*. Wayne, PA, USA: Clinical and Laboratory Standards Institute.

Costa-Lotufo, L. V., Khan, M. T. H., Ather, A., Wilke, D. V., Jimenez, P. C., Pessoa, C., de Moraes, M. E. A. & de Moraes, M. O. (2005). Studies of the anticancer potential of plants used in Bangladeshi folk medicine. *J Ethnopharmacol*, *99*, 21–30.

Das, S. & Choudhury, M. D. (2010). Antimicrobial activity of stem bark extracts from the plant *Oroxylum indicum* Vent. Assam University Journal of Science & Technology: *Biological and Environmental Sciences*, *5*, 95-99.

Dey, A. K., Mukherjee, A., Das, P. C. & Chatterjee, A. (1978). Occurrence of aloe-emodin in the leaves of *Oroxylum indicum* Vent. *Indian J Chem*, *16*B, 1042.

Dharmananda, S. (2006a). *Oroxylum indicum* fruits. Retrieved May, 2006, from http://www.itmonline.org/arts/oroxylum.htm

Dharmananda, S. (2006b). *Oroxylum indicum* seeds. Retrieved May, 2006, from http://www.itmonline.org/arts/oroxylum.htm

Dinda, B., Mohanta, B. C., Arima, S., Sato, N. & Harigaya, Y. (2007). Flavonoids from the stem-bark of *Oroxylum indicum*. *Korean Society of Pharmacognosy*, *13*(3), 190-194.

Dris, R. & Jain, S. M. (2004). *Production practices and quality assessment of food crops*. Kluwer Academic, 4.n.p.: N.P.

Endo, K. & Hikino, H. (1984). Structures of rengyol, rengyoxide, and rengyolone, new cyclohexylethane derivatives from *Forsythia suspensa* fruits. *Can J Chemistry*, *62*(10), 2011-2014.

Forgo, P. & Köver, K. E. (2004). Gradient enhanced selective experiments in the ^{1}H NMR chemical shift assignment of the skeleton and side-chain resonances of stigmasterol, a phytosterol derivative. *Steroids*, *69*, 43-50.

Fujita, T., Liu, D. Y., Ueda, S., Takeda, Y. (1992). Xanthones from *Polygala tenuifolia*. *Phytochemistry*, *31*, 3997-4000.

Gaitonde, R. V. & Sapre, S. P. (1989). Colorimetric method for the estimation of *p*-coumaric acid from the bark of *Oroxylum indicum* Vent. *Current Science*, *58*(16), 929-930.

Gardner, S., Sidisunthorn, P. & Anusarnsunthorn, V. (2000). *A field guide to forest trees of northern Thailand*. Chiang Mai: Chiang Mai University.

Garg, J. M. (2010). *Oroxylum indicum* flowers. Retrieved March 13, 2010, from http://en.wikipedia.org/wiki/Oroxylum_indicum

González-Calderón, D., González-González, C. A., Fuentes-Benítez, A., Cuevas-Yáñez, E., Corona-Becerril, D. & González-Romero, C. (2013). Cerium(IV) sulfate tetrahydrate: a catalytic and highly chemoselective deprotection of THP, MOM, and BOM ethers. *Tetrahedron Lett*, *54*, 7164–7166.

Gupta, C. R., Sharma, V., Sharma, N., Kumar, N. & Singh, B. (2008). *In vitro* Antioxidant activity from leaves of *Oroxylum indicum* (L.) Vent.-a north Indian highly threatened and vulnerable medicinal plant. *Research Article*, *1*(1), 65-72.

Heim, K. E., Tagliaferro, A. R. & Bobilya, D. J. (2002). Flavonoid antioxidants: chemistry, metabolism and structure-activity relationships. *J Nutr Biochem*, *13*, 572–584.

Harminder, S. V. & Chaudhary, A. K. (2009). A Review on The taxonomy, ethnobotany, chemistry and pharmacology of *Oroxylum indicum* Vent. *Indian J Pharm Sci*, *73*(5), 483-490.

Igbinosa, O. O., Igbinosa, E. O. & Aiyegoro, O. A. (2009). Antimicrobial activity and phytochemical screening of stem bark extracts from *Jatropha curcas* (Linn). *Afr J Pharm Pharmaco*, *3*, 058-062.

Islam, M. K., Eti, I. Z. & Chowdhury, J. A. (2010). Phytochemical and antimicrobial analysis on the extracte of *Oroxylum indicum* Linn. stem-bark. *Iran J Pharmacol Ther Ijpt*, *9*, 25-28.

Iwu, M. W., Ducan, A. R. & Okungi, C. O. (1999). New antimicrobials of plant orgin. *In Janik J*, ASHS press., 457-462.

Jeong, G.-S., Lee, S.-H., Jeong, S.-N., Kim, Y.-C. & Kim, E.-C. (2009). Anti-inflammatory effects of apigenin on nicotine- and lipopolysaccharide-stimulated human periodontal ligament cells via heme oxygenase-1. *Int Immunopharmacol*, *9*, 1374-1380.

Jorgensen, J. H. & Ferraro, M. J. (2009). Antimicrobial susceptibility testing: a review of general principles and contemporary practices. *Clin Infect Dis*, *49*, 1749–1755.

Joshi, S., Mishra, D., Khetwal, K.S. & Bisht, G. (2012). Antimicrobial evaluation of *Buddleja asiatica* Lour. leaves and flowers extract. *Res J Phytochem*, *6*, 92–95.

Kalaivani, T. & Mathew, L. (2009). Phytochemistry and free radical scavenging activities of *Oroxylum indicum*. *Environ We Int J Sci Tech*, *4*, 45-52.

Khandhar, M., Shah, M., Santani, D. & Jain, S. (2006). Antiulcer activity of the root bark of *Oroxylum indicum* against experimental gastric ulcers. *Pharm Biol*, *44*(5), 363-370.

Kizu, H., Habe, S., Ishida, M. & Tomimori, T. (1994). Studies on the nepalese crude drugs XVII. on the naphthalene related compounds from the root bark of *Oroxylum indicum* Vent. *Yakugaku Zasshi*, *114*(7), 492-513.

Kong, M., Chen, X. G., Xing, K. & Park, H. J. (2010). Antimicrobial properties of chitosan and mode of action: a state of the art review. *Int J Food Microbiol*, *144*, 51–63.

Kraus, G. A. & Mengwasser, J. (2009). Quinones as key intermediates in natural products synthesis. syntheses of bioactive xanthones from *Hypericum perforatum*. *Molecules*, *14*, 2857–2861.

Krüger, A. & Ganzera, M. (2012). *Oroxylum indicum* seeds-analysis of flavonoids by HPLC-MS. *J Pharmaceut Biomed*, *70*, 553-556.

Kumar, R. A., Rajkumar, V., Guha, G. & Mathew, L. (2010). Therapeutic potentials of *Oroxylum indicum* bark extracts. *Chin J Nat Med*, *8*, 121–126.

Kumar, N. R. D., George, C. V., Suresh, K. P. & Kumar, A. R. (2012). Cytotoxicity, apoptosis induction and anti-metastatic potential of *Oroxylum indicum* in human breast cancer cells. *Research Communication*, *13*, 2729-2734.

Laupattarakasem, P., Houghton, P., Hoult, J. R. & Itharat, A. (2003). An evaluation of the activity related to inflammation of four plants used in Thailand to treat arthritis. *J Ethnopharmacol*, *85*, 207–215.

Le, T. D. H. & Nguyen, X. T. (2005). Influence of flavonoids from *Oroxylum indicum* Vent. towards α-chymotrypsin in relation to inflammation. *Tap Chi Duoc Hoc*, *45*(8), 23-26.

Lee, C. K., Lu, C. K., Kuo, Y. H., Chen, J. Z. & Sun, G. Z. (2004). New prenylated flavones from the roots of *Ficus beecheyana*. *J Chin Chem Soc*, *51*, 437-442.

Likhitwitayawuid, K., Phadungcharoen, T., Mahidol, C. & Ruchirawat, S. (1997). 7-*O*-methylgarcinone E from *Garcinia cowa*. *Phytochemistry*, *45*(6), 1299-1301.

Lin, Y. & Kong, L. (2006). Studies on the chemical constituents of *Desmodium styracifolium* (Osbeck) Merr. [J]. *Asian J Trad Med*, *1*(1), 34.

Luitel, H. N., Rajbhandari, M., Kalauni, S. K., Awale, S., Masuda, K. & Gewali, M. B. (2010). Chemical constituents from *Oroxylum indicum* (L.) Kurz of Nepalese origin. *Scientific World*, *8*, 66-68.

Magalhães, L. M., Santos, M., Segundo, M. A., Reis, S. & Lima, J. L. F. C. (2009). Flow injection based methods for fast screening of antioxidant capacity. *Talanta*, *77*, 1559–1566.

Maungjunburee, S. & Mahabusarakam, W. (2010). Flavonoids from the stem bark of *Oroxylum indicum* (L.) Benth. ex Kurz. *Proceedings of the 7th IMT-GT UNINET and the 3rd International PSU-UNS Conferences on Bioscience*, 136-140.

Merina, N., Chandra, J. K. & Jibon, K. (2012). Medicinal plants with potential anticancer activities: a review. *International Research Journal of Pharmacy*, *3*, 26-30.

Middleton, E., Kandaswami, C. & Theoharides, T. C. (2000). The effects of plant flavonoids on mammalian cells: implications for inflammation, heart disease, and cancer. *Pharmacol Rev*, *52*, 673 –751.

Mouffok, S., Haba, H., Lavaud, C., Long, C. & Benkhaled, M. (2012). Chemical constituents of *Centaurea omphalotricha* Coss. & Durieu ex Batt. & Trab. *Record of Natural Product*, *6*(3), 292-295.

Mrazek, N., Watla-iad, K., Deachathai, S. & Suteerapataranon, S. (2012). Rapid antioxidant capacity screening in herbal extracts using a simple flow injection-spectrophotometric system. *Food Chem*, *132*, 544–548.

Muthumani, P., Meera, R., Devi, P., Mohamed-Sheik-Arabath, S. A., Seshu-Kumar-Koduri, L. V. & Manavarthi, S. (2010). Chemical investigation of *Toddalia asiatica* Linn, and *Cardiospermum halicacabum* Linn. *International Journal of Drug Formulation & Research*, *1*, 224-239

Na Pattalung, P., Thongtheeraparp, W., Wiriyachitra, P. & Taylor, W. C. (1994). Xanthones of *Garcinia cowa*. *Planta Med*, *60*, 365–368.

Nair, A. G. R. & Joshi, B. S. (1979). Oroxindin-A new flavone glucuronide from *Oroxylum indicum* Vent. *Proceedings of the Indian Academy of Sciences-Chemical Sciences*, *88*(5), 323-327.

Nakahara, K., Onishi-Kameyama, M., Ono, H., Yoshida, M. & Trakoontivakorn, G. (2001). Antimutagenic activity against Trp-P-1 of the edible Thai plant, *Oroxylum indicum* Vent. *Biosci Biotechnol Biochem*, *65*, 2358–2360.

Nguyen, A. T., Malonne, H., Duez, P., Vanhaelen-Fastre, R., Vanhaelen, M. & Fontaine, J. (2004). Cytotoxic constituents from *Plumbago zeylanica*. *Fitoterapia*, *75*, 500-504.

Nguyen, M. T. T., Nguyen, N. T., Nguyen, H. X., Huynh, T. N. N. & Min, B. S. (2012). Screening of α-glucosidase inhibitory activity of vietnamese medicinal plants: Isolation of active principles from *Oroxylum indicum*. *Natural Product Sciences*, *18*(1), 47-51.

Nishina, A., Kubota, K. & Osawa, T. (1993). Antimicrobial components, trachrysone and 2-methoxystypandrone, in *Rumex japonicus* Houtt. *J Agric Food Chem*, *41*, 1772–1775.

Nyamoita, M.G. (2013). Toxicity of individual and blends of pure phytoecdysteroids isolated from *Vitex Schiliebenii* and *Vitex Payos* against *Anopheles Gambiae* S.S. Larvae. *World J Org Chem, 1*, 1–5.

Oja, V., Chen, X., Hajaligol, M. R., & Chan, W. G. (2009). Sublimation thermodynamic parameters for cholesterol, ergosterol, *β*-sitosterol, and stigmasterol. *J Chem Eng*, *54*, 730–734.

Oliveira, B. H., Nakashima, T., Filho, J. D. S. & Frehse, F. L. (2001). HPLC analysis of flavonoids in *Eupatorium littorale*. *Journal of the Brazilian Chemical Society*, *12*(2), 243-246.

Osawa, T. (1999). Protective role of dietary polyphenols in oxidative stress. *Mech Ageing Dev*, *111*, 133–139.

Rajkumar, V., Guha, G. & Kumar, R. A. (2012). Isolation and bioactivity evaluation of two metabolites from the methanolic extract of *Oroxylum indicum* stem bark. *Asian Pac J Trop Biomed*, *2*, S7–S11.

Roy, M. K., Nakahara, K., Na Thalang, V., Trakoontivakorn, G., Takenaka, M., Isobe, S. & Tsushida, T. (2007). Baicalein, a flavonoid extracted from a methanolic extract of *Oroxylum indicum* inhibits proliferation of a cancer cell line in vitro via induction of apoptosis. *Pharmazie*, *62*(2), 149-53.

Sastry, S. V. A., Sastry, G. V., Mallikarjun, P. & Srinivas, K. (2011). Chemical and pharmacological evaluation of aqueous extract of root bark of "*Oroxylum indicum*" Vent. *International Journal of Pharmacy & Technology*, *3*, 1796-1806.

Scartezzini, P. & Speroni, E. (2000). Review on some plants of Indian traditional medicine with antioxidant activity. *J Ethnopharmacol*, *71*, 23–43.

Shah, R. C., Mehta, C. R. & Wheeler, T. S. (1935). Constitution of oroxylin. *Current Science*, *4*, 406.

Sia, G.-L., Bennett, G. J., Harrison, L. J. & Sim, K.-Y. (1995). Minor xanthones from the bark of *cratoxylum cochinchinense*. *Phytochemistry*, *38*, 1521–1528.

Siriwatanametanon, N., Fiebich, B. L., Efferth, T., Prieto, J. M. & Heinrich, M. (2010). Traditionally used Thai medicinal plants: *In vitro* anti-inflammatory, anticancer and antioxidant activities. *J Ethnopharmacol*, *130*, 196–207.

Tala, F. M., Tchakam, D. P., Wabo, K. H., Talontsi, M. F., Tane, P., Kuiate, R. J., Tapondjou, A. L. & Laatsch, H. (2013). Chemical constituents, antimicrobial and cytotoxic activities of *Hypericum riparium* (Guttiferae). *Rec Nat Prod*, *7*(1), 65-68.

Tenpe, C. R., Aman, U., Sushil, B. & Yeole, P. G. (2009). *In vitro* antioxidant and preliminary hepatoprotective activity of *Oroxylum indicum* Vent leaf extracts. *Pharmacologyonline*, *1*, 35-43.

Tepsuwan, A., Furihata, C., Rojanapo, W. & Matsushima, T. (1992). Genotoxicity and cell proliferative activity of a nitrosated *Oroxylum indicum* Vent fraction in the pyloric mucosa of rat stomach. *Mutat Res*, *281*(1), 55-61.

Teshima, K.-I., Kaneko, T., Ohtani, K., Kasai, R., Lhieochaiphant, S. & Yamasaki, K. (1996). Phenylethanoids and cyclohexylethanoids from *Oroxylum indicum*. *Natural Medicines*, *50*(4), 307.

Tomimori, T., Imoto, Y., Ishida, M., Kizu, H. & Namba, T. (1988). Studies on the Nepalese crude drugs (VIII). on the flavonoid constituents of the seed of *Oroxylum indicum* Vent. *Shoyakugaku Zasshi*, *42*, 98-101.

Uddin, K., Sayeed, A., Islam, A., Rahman, A. A., Ali, A., Astaq, G. R. M., Khan, A. M. & Sadik, M. G. (2003). Purification, characterization and cytotoxic activity of two flavonoids from *Oroxylum indicum* Vent. (Bignoniaceae). *Asian J Plant Sci*, *2*, 515–518.

Ukeda, H., Adachi, Y. & Sawamura, M. (2002). Flow injection analysis of DPPH radical based on electron spin resonance. *Talanta*, *58*, 1279–1283.

Upaganlawar, A. B. & Tenpe, C. R. (2007). *In vitro* antioxidant activity of leaves of *Oroxylum indicum* Vent. *Biomed*, *2*(3), 300-304.

Vasanth, S., Natarajan, M., Sundaresan, R., Rao, R. B. & Kundu, A. B. (1991). Ellagic acid from *Oroxylum indicum* Vent. *Indian Drugs*, *28*(11), 507.

Vinod, N. & Kamlesh, N. K. (2009). Comparative antimicrobial study of ethanolic and aqueous extracts of root bark of *Oroxylum indicum* (L.) Benth & Xkurz. *Journal of Pharmacy Research*, *2*(5), 967-969.

Vogt, T. (2010). Phenylpropanoid biosynthesis. *Mol Plant*, *3*, 2–20.

Vrajesh, P. (2009). *Oroxylum indicum* leaves. Retrieved March 2, 2009, from http://myhandycam.blogspot.com/2009_02_08_archive.html

Wang, X.-B., Li, G.-H., Li, L., Zheng, L.-J., Huang, R. & Zhang, K.-Q. (2008). Nematicidal coumarins from *Heracleum candicans* Wall. *Nat Prod Res*, *22*, 666–671.

World Health Organization. (2011). *Noncommunicable diseases country profiles 2011*. Geneva, Switzerland: World Health Organization.

Yadav, S. K. & Kalidhar, S. B. (1994). Alquinone: an anthraquinone from *Cassia alata*. *Planta Med*, *60*(6), 601.

Yan, R., Cao, Y., Chen, C., Dai, H., Yu, S., Wei, J., Li, H. & Yang, B. (2011). Antioxidant flavonoids from the seed of *Oroxylum indicum*. *Fitoterapia*, *82*, 841–848.

Yuan, Y., Hou, W., Tang, M., Luo, H., Chen, L.-J., Guan, Y. H. & Sutherland, I. A. (2008). Separation of flavonoids from the leaves of *Oroxylum indicum* by HSCCC. *Chromatographia*, *68*, 885–892.

Zarena, A. S. & Sankar, K. U. (2009). A study of antioxidant properties from *Garcinia mangostana* L. pericarp extract. *Acta Sci Pol*, *8*(1), 23-34.

Zaveri, M., Gohil, P. & Jain, S. (2006). Immunostimulant activity of *n*-butanol fraction of root bark of *Oroxylum indicum*, Vent. *J Immunotoxicol*, *3*(2), 83-99.
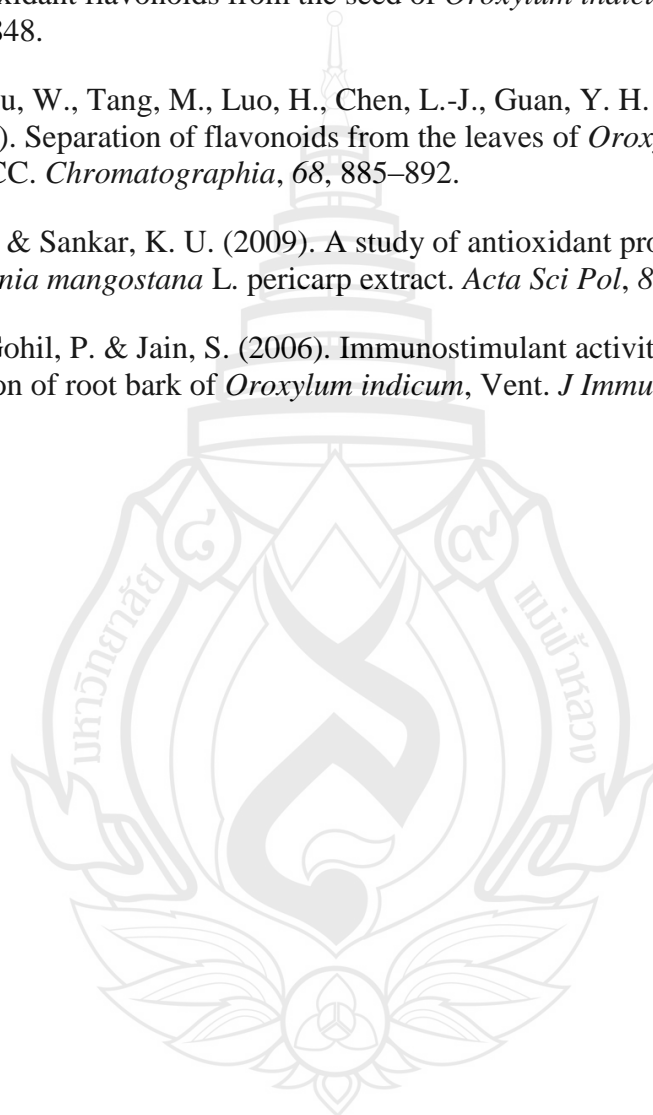
APPENDIX

APPENDIX

Chemicals and Biological Materials Preparation Methods

Preparation of bacterial

1. Streak culture from stock culture into MHA plate

2. Incubated at 35 °C, 18-24 h

3. Collected 3-5 single colonies to 1 mL of 0.85% NSS in sterile tube

4. Compare turbidity with 0.5 McFarland standard and adjust with 0.85% NSS

Preparation of Media

Mueller-Hinton agar (MHA), Difco

1 liter of media including	Beef extract powder	2.0	g
	Acid digest of casein	17.5	g
	Soluble starch	1.5	g
	Agar	17.5	g

Mueller-Hinton agar (MHB), Difco

1 liter of media including	Beef extract powder	2.0	g
	Acid digest of casein	17.5	g
	Soluble starch	1.5	g

Nutrient agar (NA), Difco

1 liter of media including	Beef extract	3.0	g
	Peptone	5.0	g
	Agar	15.0	g

Nutrient broth (NB), Difco

1 liter of media including	Beef extract	3.0	g
	Peptone	5.0	g

Preparation of standard drug

Prepared stock solution of vancomycin, gentamicin (concentration of 16 mg/mL)

- Dissolve 0.016 g of standard drug in sterile water 1 mL

- Store at in -20 °C

Preparation of 0.85% Normal saline solution (NSS)

NaCl   8.5 g

Distilled water   1 liter

Dissolve NaCl in water, heating if necessary. May be sterilized by autoclaving or membrane filtration. Store at ambient temperature for up to 6 months with caps tightened to prevent evaporation.

Turbidity standards (McFarland)

McFarland 0.5 turbidity standards are available from various manufacturers. Alternately, the 0.5 McFarland may be prepared by adding 0.5 mL of a 1.175% (w/v) barium chloride dihydrate ($BaCl_2 \cdot 2H_2O$) solution to 99.5 mL of 1% (v/v) sulfuric acid. The turbidity standard is then aliquoted into test tubes identical to those used to prepare the inoculum suspension. Seal the McFarland standard tubes with wax, parafilm, or some other means to prevent evaporation. McFarland standards may be stored for up to 6 months in the dark at room temperature (22 to 25 °C). Discard after 6 months or sooner if any volume is lost. Before each use, shake well, mixing the fine white precipitate of barium sulfate in the tube. The accuracy of the density of a prepared McFarland standard should be checked by using a spectrophotometer with a cm^{-1} light path; for the 0.5 McFarland standard, the absorbance at a wavelength of 625 nm should be 0.08 to 0.1. Alternately, the accuracy of the McFarland standard may be verified by adjusting a suspension of a control strain (e.g., *E. coli*) to the same turbidity, preparing serial 10-fold dilutions, and then performing plate counts. The adjusted suspension should give a count of 108 colony forming units/mL.

CURRICULUM VITAE

CURRICULUM VITAE

NAME   Miss. Kulsiri Yossathera

DATE OF BIRTH   29 March 1989

ADDRESS   524 Moo.24 Muang Chiang Rai 57000

EDUCATIONAL BACKGROUND

2010   Bachelor of Applied Thai Traditional Medicine

                              Thammasat University, Pathum Thani, Thailand

PUBLICATIONS

Maneerat, W., Phakhodee, W., Ritthiwigrom, T., Cheenpracha, S., Promgool, T., Yossathera, K., Deachathai, S. & Laphookhieo, S. (2012). Antibacterial carbazole alkaloids from *Clausena harmandiana* twigs. *Fitoterapia*, *83*, 1110-1114.

Maneerat, W., Ritthiwigrom, T., Cheenpracha, S., Promgool, T., Yossathera, K., Deachathai, S., Phakhodee, W. & Laphookhieo, S. (2012). Bioactive carbazole alkaloids from *Clausena wallichii* roots. *J Nat Prod*, *75*, 741-746.

Sripisut, T., Ritthiwigrom, T., Promgool, T., Yossathera, K., Deachathai, S., Phakhodee, W., Cheenpracha, S. & Laphookhieo, S. (2012). Glycopentaphyllone: The first isolation of hydroperoxyquinolone from the fruits of *Glycosmis pentaphylla*. *Phytochem Lett*, *5*, 379–381.

Tantapakul, C., Phakhodee, W., Ritthiwigrom, T., Yossathera, K., Deachathai, S. & Laphookhieo, S. (2012). Antibacterial compounds from *Zanthoxylum rhetsa*. *Arch Pharm Res*, *35*, 1139–1142.

Yossathera, K., Suteerapataranon, S. & Deachathai, S. (2014). Phytochemistry and bioactivities evaluation of *Oroxylum indicum* (L.) Vent. *Pure and Applied Chemistry Conference 2014 (PACCON2014)*, 258-260.

Yossathera, K., Tayana, N., Promgool, T., Suteerapataranon, S. & Deachathai, S. (2014). Antioxidation activity of compounds from medicinal plants. *1ˢᵗ Joint ACS AGFD- ACS ICSCT Symposium*, 146-150.

Yossathera, K., Sriprang, S., Suteerapataranon, S. & Deachathai, S. (2014). Antibacterial and antioxidative compounds from *Oroxylum indicum* (L.) Vent. *Chem Nat Comps*, submitted.

PRESENTATIONS

Kulsiri Yossathera, Siripat Suteerapataranon, Suwanna Deachathai, Antibacterial and Antioxidation Activities of Extracts and Chemical Constituents of *Oroxylum indicum* (L.) Vent., 15th Asian Chemical Congress 2013 (15th ACC), Resort World Sentosa, Singapore, 19-23 August 2013.
(poster presentation)

Kulsiri Yossathera, Siripat Suteerapataranon, Suwanna Deachathai, Phytochemistry and Bioactivities Evaluation of *Oroxylum indicum* (L.) Vent., Pure and Applied Chemistry Conference 2014 (PACCON2014), Centara Convention Centre, Khon Khaen, Thailand, 8-10 January 2014.
(oral presentation)

Kulsiri Yossathera, Ngampuk Tayana, Trinop Promgool, Siripat Suteerapataranon and Suwanna Deachathai, Antioxidation Activity of compounds from Medicinal Plant, 1st Joint ACS AGFD-ACS ICST Symposium on Agricultural and Food Chemistry, Montien Riverside Hotel, Bangkok, Thailand, 4-5 March 2014.
(poster presentation)